الآيــــــــــــــــــة

بسم الله الرحمن الرحيم

قال تعالى:

وَهُوَ الَّذِي يُرْسِلُ الرِّيَاحَ بُشْرًا بَيْنَ يَدَيْ رَحْمَتِهِ ۖ حَتَّىٰ إِذَا أَقَلَّتْ سَحَابًا ثِقَالًا سُقْنَاهُ لِبَلَدٍ مَّيِّتٍ فَأَنزَلْنَا بِهِ الْمَاءَ فَأَخْرَجْنَا بِهِ مِن كُلِّ الثَّمَرَاتِ ۚ كَذَٰلِكَ نُخْرِجُ الْمَوْتَىٰ لَعَلَّكُمْ تَذَكَّرُونَ

الاعراف 57

DEDICATION

To our Dear . . .

Father, Mother, Brothers and sisters.

To our all . . .

Family, Friends and Colleagues . . .

To those . . .

Who taught us letters of gold and words of jewel to our honored teachers.

Your sincerely;;;

Mohammad .. Zakaria .. Mohamed

ACKNOLEDGMENT

First of all thank Allah; who provides us with health and ability to fulfill this work. Words can't express the especial appreciation and the deepest gratitude that we feel for our supervisor, Mr. Al Siddig Abdelazim Babiker for his kind encouragement, close and valuable supervision as well as his precious advices.

We deeply grateful to Energy Research Center Staff and thanks extends to the staff of engineering faculty especially to the School of Mechanical Engineering lecturers.

Last But not least; we give our great gratitude for our family for their help, advice and continuous support.

ABSTRACT

In this project a wind pump system was designed, modeled and simulated to serve the goal of supporting water harvesting in many of rural areas rather than the efficiency of the system, which in this case the location were selected to be TOKER city where the condition are 3.5*m/s* wind velocity at 10*m* height and total head of 15*m* . In our design, horizontal axis windmill with 12 blades is used. Each blade has a radius of 1.352 *m* giving a total surface area of 0.29 m^2 and this gives a solidity of 0.6. The torque output of the windmill is 16.21 *Nm* and this is sufficient to sustain the desired Flow rate of (0.1736×10^{-3}) m^3 per second with a maximum head of 15*m*. The modeling, analysis and simulation were conducted using Solid Works version 14 on static loads bases.

المستخلــــــص

في هذا المشروع تم تصميم ونمذجة توربينة رياح من نوع المحور الافقي لضخ المياه الجوفيه بهدف دعم حصاد المياه بمدينة طوكر.صممت المنظومة على متوسط سرعة رياح يعادل 3.5 متر / الثانية ، ارتفاع 10 امتار من السطح و عمق كلي يعادل 15 متر. تم تصميم المنظومة بحيث تكون بها 12 ريشة مساحة الواحدة منها تعادل 0.29 متر مربع بنسبة تصميت (solidity) 0.6 ، ونصف قطر 1.350 متر لتنتج عزم مقداره 16.21 نيوتن متر لضخ المياه بمعدل $0.1736 * 10^{-3}$ متر مكعب / الثانية. حيث تم التحليل الإستاتيكي ، النمزجة و المحاكاة بإستخدام برنامج (Solidworks) النسخة الرابعة عشر.

TABLE OF CONTENTS

List of Tables

List of Figures

List of Symbols

C_p	Power coefficient
P_h	Hydraulic power
ρ	The density of the water
g	The acceleration Due to gravity
Q	The flow rate of water
H	The total Head of the water to be lifted
H_s	The elevation of the water to be lifted
H_f	The loss due to friction in the pipe
H_d	Stroke length
P_{Wind}	Power contained in the wind resource
v	Wind speed
A	Area of the rotor
R	Radius
n	Number of blades
As	Swept area of the rotor
A_b	Area of the blade
σ	Solidity
C_{tip}	width of the plate at the tip
C_{root}	width of the plate at the root
D	Diameter
V_{start}	Start speed

V_{stop}	Stop speed
η_{vol}	The volumetric efficiency
V_s	Stroke volume
λ_d	Design tip speed ratio
i	Transmission ratio
ρ	Air density
$C_p\eta$	overall power coefficient
T_e	The equivalent twisting moment
M	Maximum bending moment
T	Torque
τ	The allowable shear stress
d	The diameter of the shaft
M_e	Equivalent bending moment
σ	Tensile Strength
σ_u	Ultimate Tensile Strength
λ_{opt}	Optimal tip speed ratio
ω	Rotation speed of the rotor
f	Pump frequency
h_{pump}	Pump stroke length
P_{Mech}	Mechanical power
ω_{max}	Maximum Rotation speed of the rotor
λ_d	Design tip speed ratio

V_{rated} Rated wind speed

A_p Area of the pump piston

F_{st} Static force

F_{Pr} Maximum load on the pump rod

$\frac{A_p}{A_{rm}}$ Ratio of the area of the pump piston to the area of the raising main

K Over shot factor

s Pump stroke.

Chapter One

Introduction

CHAPTER ONE

INTRODUCTION

1.1 Introduction

The vacillating cost of fossil fuels, limited supply and side effects of using fossil fuels (pollution and global worming) lead to develop an alternative sources of energy that are cheaper, renewable and environmental friendly. The major resource in this category is wind energy.

The ancient Egyptian used wind power to propel boats 5000 years ago. It's uncertain when the first used on land to power rotating machinery but it's estimated to be 2000 years ago. Historical records showed that defiantly existed in 200 BC in the area now known as eastern Iran and western Afghanistan.

About 1000 years ago horizontal axis sail windmills were being used around the Mediterranean, by the 12th century windmills had reached Northern Europe they became an important part of the industry of both Britain and Netherland in the centuries that followed. In Britain the mostly used for milling grains and the Netherland many were used for dewatering polder land.

In the 19th Century, wind energy developed in the United States where horizontal axis windmills were used for farms, ranches and to generate electricity. This is where the first multi-blade was developed for irrigation purposes.

The wind power technology has evolved greatly and this has been motivated by the incredible benefits resulting from wind energy. Very efficient and technologically up-to- date designs have been developed and are used especially in arid and semi-arid areas to pump water for domestic and irrigation purposes. Viability of windmills is however practical only in areas with free flow of air and therefore site selection is very critical in the initial design process.

The power generated from the wind can be supplied directly to the national grid system or used to drive other mechanical devices such as windmills and grinders. This has greatly reduced the levels of pollution resulting from the use of fossil fuels. This project is mainly based on the design of a windmill for water pumping.

1.2 Problem Statement:

Now a day's power is a major problem that put the whole world in tension, as alternatives, research's has been conducted on the field of green energy. Solar, wind and water energy was the main scope of those researches.

In Sudan as a local situation water harvesting is major issue in many of the rural areas, the methods used to harvest water is either costly, polluting and there is a scarcity of it (diesel engine pump) and require much efforts (wells and bucket, crossing distance, etc.). While Sudan has enough underground water stored but it needs power to be collected, the running cost of power production is high.

1.3 Project Significant:

Most of the method used to supply water from either water surfaces or wells are mainly depend on using fusel fuel to drive a pumps which is very costly and environmental polluting. On the other hand, on some of rural area's hand pumps are used to left water from wells which need efforts.

Therefore this project will design a windmill which will reduce the cost of power production by using wind energy and convert it to useful mechanical energy to lift the underground water for either irrigation or domestic use. On the other hand the windmill is environment friendly and require no efforts to lift the water.

1.4 Objectives:

The main objective is to design a horizontal multi-blade wind mill for pumping water that in rural areas, the specific objective is the modeling and simulation of the windmill.

1.5 Scope of Design

The design of a windmill is a very wide subject and therefore the type of the system will be used is an American multi-blades wind mill which design will be limited to TOKER city – Eastern Sudan.

The assumptions of the design are:

- The wind mill will be placed at a 10 *m* Height.
- The average wind speed will be taken as 3.5 *m/s*.
- The water requirement was assumed to be 15 m^3/Day.
- The average total head of 15 m Height.

The modeling analysis and simulation will be carried out using solid works version 14.

1.6 Project Layout

The project report consists of five in which chapter one contains an introduction about the wind energy, the problem statement and scope of the project. Chapter two contains the information about the utilization of energy per unit capita and population growth and their effects on energy consumption, information about the renewable energy as substituent to the current power resources.

Chapter two also contains the information about wind energy development with their advantages and disadvantages and the current application of the wind system. The ability to apply wind power harvesting system in Sudan were demonstrated, the theory of working principle, categories and some types of the windmills were also demonstrated.

Chapter three consisted of the project methodology including the flow chart of the work since identifying the problem until the project is concluded and recommendations were made.

Chapter four include all the calculation made to finish the design combined with the analysis results and discussion. Conclusion and recommendations were made and it's included in chapter five

Chapter Two

Literature Review

CHAPTER TWO

LITERATURE REVIEW

2.1 Introduction

Energy is usually defined as the ability to do work. This is an anthropocentric and utilitarian perspective of energy; however, it is a useful definition for engineering where the aim of machines is to convert energy to work. As a more general description, energy is a fundamental entity whose availability and flow are required for all phenomena, natural or artificial.

An understanding of how energy is generated and measured is central to our decisions concerning the use and conservation of energy. Large-scale production of energy evolved over centuries but grew radically in the last 400 years and especially since the Industrial Revolution. A century of development and commercialization of electric power technology has ensured an easy supply, and continuous measurement.

Energy is derived in usable forms from numerous sources, such as flowing water, fossil fuels (e.g., coal and natural gas), uranium, and the sun. Electricity is a widely used form of energy. Any of these sources can be used to generate electricity. Liquid fuels such as gasoline and diesel derived from fossil fuels are a widely used source of energy. These fuels form the basis of our easy transportation. A complete understanding of the complexities of the energy systems within the natural environment requires knowledge of some basic physics and chemistry.

2.2 Background of utilization of energy per capita

Energy can be utilized but not consumed; it is a law of nature that energy is conserved. Instead of consuming it, we degrade or randomize energy, all energy we use is degraded into heat and eventually radiated out into space.

The energy utilization rate throughout the ages can only be estimated in a rough manner. In early times, man was totally non-technological, not even using fire. He used energy only as food, probably at a rate somewhat below the modern average of 2000 kilocalories per day, equivalent to 100 W. Later, with the discovery of fire and an improved diet involving cooked foods, the energy utilization rate may have risen to some 300 W/capita.

In the primitive agricultural Mesopotamia, around 4000 B.C., energy derived from animals was used for several purposes, especially for transportation and for pumping water in irrigation projects. Solar energy was employed for drying cereals and building materials such as bricks. Per capita energy utilization may have been as high as 800 W.

The idea of harnessing wind, water and fire to produce useful work is ancient. Wind energy has been in use to drive sailboats since at least 3000B.C. and windmills were described by Hero of Alexandria around 100 A.D. Extensive use of windmills started in Persia around 300 A.D. and, only much later, spread to China and Europe.

In spite of the availability of the technology, the ancients limited themselves to the use of human or animal muscle power. Lionel Casson (1981), a professor of ancient history at New York University, argues that this was due to cultural rather than economic constraints and that only at the beginning of the Middle Ages did the use of other energy sources become "fashionable." Indeed, the second millennium saw an explosion of mechanical devices starting with windmills and waterwheels.

The energy utilization rate in Europe was likely 2000 calories per capita around 1200 A.D. when there was widespread adoption of advanced agriculture, the use of fireplaces to heat homes, the burning of ceramics and bricks, and the use of wind and water. Since the popular acceptance of such activities, energy utilization has increased rapidly.

Figure 2.2 illustrates (a wild estimate) the number of kilowatts utilized per capita as a function of the date. It may be conclude that the annual rate of increase of the per capita energy utilization rate behaved as indicated in Figure 2.2, although the precision of these results is doubtful, it is almost certain that the general trend is correct for most of our history the growth of the per capita energy utilization rate was steady and quite modest. However, with the start of the industrial revolution at the beginning of the 19th century, this growth accelerated dramatically and has now reached a worrisome level.

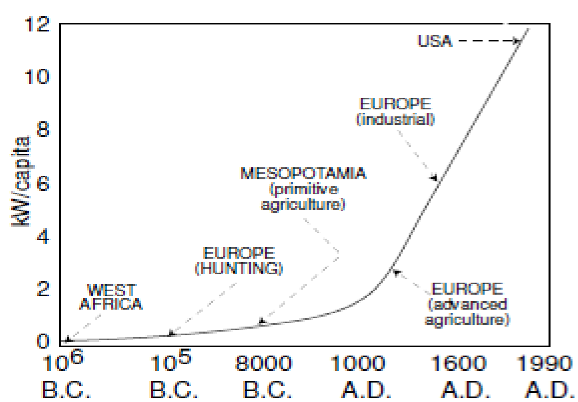

Fig 2.1: A very rough plot of the historical increase in per Capita energy utilization rate

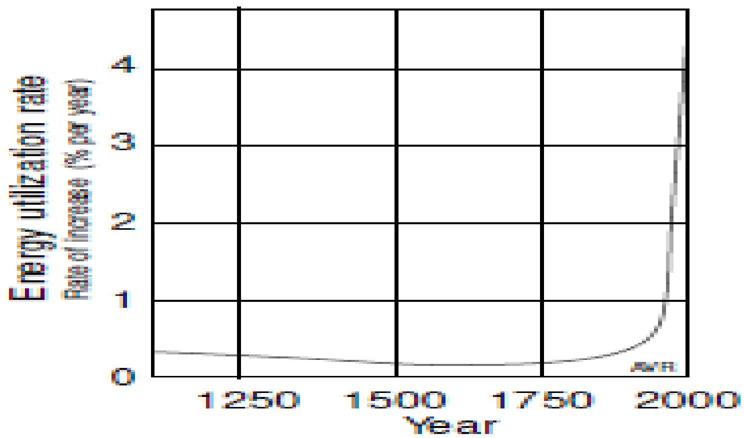

Fig 2.2: The Annual rate of increase of per capita energy utilization

One driving force behind the increasing worldwide per capita energy utilization was the low cost of oil before 1973 when the price of oil was substantially lower than what it is currently. Perez Alfonso, the Venezuelan Minister of Oil in 1946, was among those who recognized that this would lead to future difficulties. He was instrumental in creating OPEC in 1954, not as a cartel to squeeze out higher profits but to "reduce the predatory oil consumption to guarantee humanity enough time to develop an economy based on renewable energy sources." Alfonso also foresaw the ecological benefits stemming from a more rational use of oil.

OPEC drove the oil prices high enough to profoundly alter the world economy. The result was that the overall energy utilization rate slowed its increase. Owing to the time delay between the price increase and the subsequent response from the system, several years elapsed before a new equilibrium was established in the oil markets. The result was a major overshooting of the oil producing capacity of OPEC and the softening of prices that we witnessed up to the 1991 Iraqi crisis.

The recent effort of less developed countries (LDCs) to catch up with developed ones has been an important factor in the increase in energy demand. Figure 2.3 shows the uneven distribution of energy utilization rate throughout the world.72% percent of the world population uses less than2 kW/capita whereas 6% of the population uses more than 7 kW/ capita.

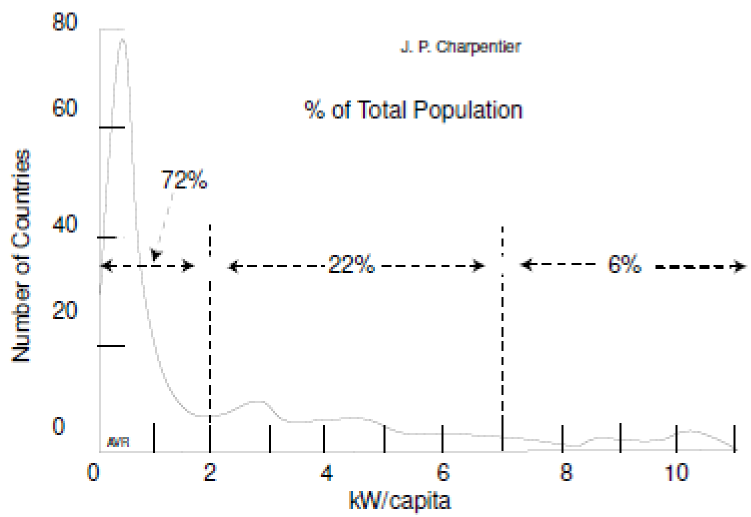

Fig 2.3: illustration of per capita energy utilization through countries

There is a reasonable correlation between the total energy utilization rate of a country and its corresponding annual gross national product. About 2.2W are used per dollar of yearly GNP. Thus, to generate each dollar, 69 MJ are needed. These figures, which are based on 1980 dollars, vary with time, in part owing to the devaluation of the currency, but also due to changing economic circumstances. It fact, it has been demonstrated that during an energy crisis, the number of mega joules per dollar decreases, while the opposite trend occurs during financial crises.

Further industrialization of developed countries may not necessarily translate into an increase of the per capita energy utilization rate -the trend toward higher efficiency in energy use may have a compensating effect.

However, in the USA, the present decline in energy utilization is due mainly to a change in the nature of industrial production. Energy intensive primary industries (such as steel production) are phasing out owing to foreign competition, while sophisticated secondary industries (such as electronics and genetic engineering) are growing.

Technological innovation has resulted in more efficient use of energy. Examples of this include better insulation in houses and better mileage in cars. Alternate energy sources have, in a small measure, alleviated the demand on fossil fuels. Such is the case of using ethanol from sugar cane for the propulsion of automobiles. It is possible that the development of fusion reactors will, one day, bring back the times of abundant energy. Introduction of a more efficient device does not immediately result in energy economy because it takes a considerable time for a new device to be widely accepted. The reaction time of the economy tends to be long. Consider the privately owned fleet of cars. A sudden rise in gasoline price has little effect on travel, but it increases the demand for fuel efficiency. However, car owners don't rush to buy new vehicles while their old ones are still usable. Thus, the overall fuel consumption will only drop many years later, after a significant fraction of the fleet has been updated. Large investments in obsolete technologies substantially delay the introduction of more desirable and efficient systems.

2.3 Population Grows and energy consumption

The most serious problem that confronts mankind is the rapid grow thin population. The planet has a little more than 6 billion inhabitants, and the growth rate these last few decades has been around 1.4% per year. Almost all projections predict a population of about 7 billion by the year2010. This will be the case even if, right now, everyone were to agree on a limit of two children per family. Under present-day actuarial conditions, the population would eventually stabilize at around 11 billion by the year2050. Thus, population growth alone could account for 1.4% a year increase in energy demand, in the next few decades.

If, in 2050, all the estimated 11 billion inhabitants of Earth were to use energy at the present day USA level (11 kW/capita), the world energy utilization rate would reach 122 TW – a 16-fold increase over the present7.6 TW. Such a rate is probably one order of magnitude higher than can be supplied unless fusion energy becomes practical and inexpensive.

A more modest scenario views the worldwide energy utilization rate stabilizing at the present level of Eastern Europe: 5 kW per capita. This would lead to an overall rate of 65 TW in 2050, which is still too high. Finally, if the world average kept its present 2 kW per capita, the rate would grow to 26 TW by the middle of next century. Clearly, it is difficult to provide adequate energy for 11 billion people. This is one more reason for attempting to limit the planetary population growth.

The rate of per capita energy utilization rose rapidly in the last century. This, combined with the fast increase in population, leads one to the inescapable conclusion that we are facing a serious challenge if we hope to maintain these trends in the foreseeable future. To investigate what can be done to resolve this difficulty we must first inquire what energy resources are available and how we are using the resources at present.

At present the energy used is at least 85% of fossil origin. The fossil fuel reserves seem ample to satisfy our needs for a good fraction of the next millennium.

The problem is Most of the easily accessible sources of oil and gas has already been tapped. What is left is getting progressively more expensive to extract. Thus, one part of the problem is economical. Another is political; |most of the fuel used by developed nations is imported using the large American reserves is unpopular and politicians hesitate to approve such exploration. This creates an undesirable vulnerability. There are also technological difficulties associated with the identification of new reserves and the extraction of fuels from more remote locations. The major obstacle, however, is ecological. Fossil fuels are still the most inexpensive and most convenient of all energy resources, but their use pollutes the environment, and we are quickly approaching a situation in which we can no longer dismiss the problem or postpone the solution.

Effects of environmental, economic, social, political and technical factors have led to the rapid deployment of various sources of renewable energy-based power generation. The incorporation of these generation technologies has led to the development of a broad array of new methods and tools to integrate this new form of generation into the power system network.

In the U.S.A., no nuclear power plants have been ordered since 1978Figure 2.4. Given the potential for cost overruns, safety related design changes during the construction, and local opposition to new plants, most utility executives suggest that none will be ordered in the foreseeable future. Assuming that no new nuclear plants are built, and that the existing plants are not relicensed at the expiration of their 40-year terms, the nuclear power output is expected to decline sharply after 2010.

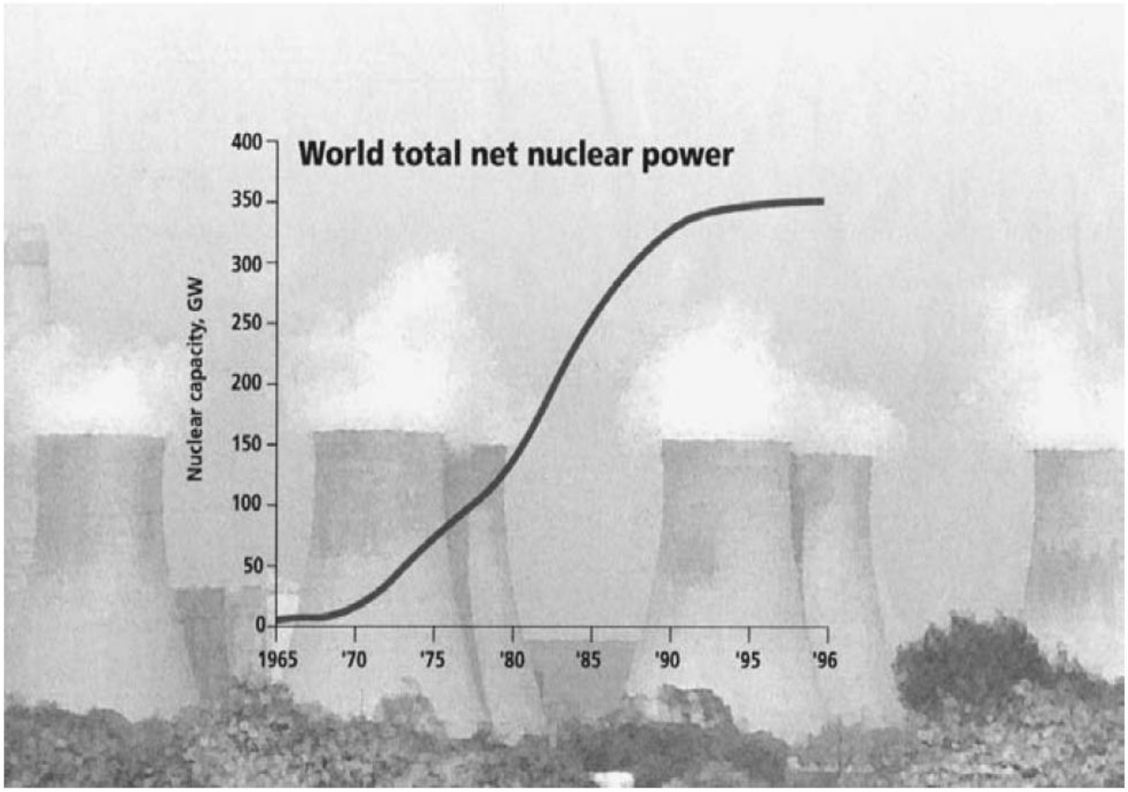

Fig 2.4: The stagnant nuclear power capacity worldwide

2.4 Renewable Energy

An alternative to the nuclear and fossil fuel power is renewable energy technologies (hydro, wind, solar, biomass, geothermal, and ocean). Renewable energy is energy which can be obtained from natural resources that can be constantly replenished. Renewable energy technologies include technologies that use — or enable the use of — one or more renewable energy sources. Types of renewable energy technologies include:

- Bio-energy.
- Geothermal Energy.
- Hydropower energy.

- Ocean Energy.
- Solar Energy.
- Wind Energy.

2.4.1 Bio-energy

Bio-energy is a form of renewable energy derived from biomass to generate electricity and heat or to produce liquid fuels for transport. Biomass is any organic matter of recently living plant or animal origin. It is available in many forms such as agricultural products, forestry products, and municipal and other waste. Traditionally mainly woody biomass has been used for bio-energy; however more recent technologies have expanded the potential resources to those such as agricultural residues, oilseeds and algae. These advanced bio-energy technologies allow for the sustainable development of the bio-energy industry, without competing with the traditional agricultural industry for land and resources.

2.4.2 Geothermal energy

Geothermal energy is the energy stored as heat in the earth. There is a steady flow of heat from the center of the Earth (where temperatures are above 5000°C) through the surface of the Earth (-30 to +40°C) into space (-273°C) - heat flows from hot to cold. The heat is generated by the natural decay over millions of years of radiogenic elements including uranium, thorium and potassium. Energy is brought to the surface by extracting hot water that is circulating amongst the sub surface rocks, or by pumping cold water into the hot rocks and returning the heated water to the surface, to drive steam turbines to produce electricity.

2.4.3 Hydropower

Hydropower is a renewable source of energy which uses the force or energy of moving water to generate power. This power, or 'hydroelectricity', is generated when falling water is channeled through water turbines. The pressure of the flowing water on turbine blades rotates a shaft and drives an electrical generator, converting the motion into electrical energy. Hydropower is the most advanced and mature renewable energy technology, and provides some level of electricity generation in more than 160 countries worldwide. Hydropower plants range from very small to very large individual plants and vast integrated schemes involving multiple large hydropower plants.

Ocean energy is a term used to describe all forms of renewable energy derived from the sea. There are two broad types of ocean energy: mechanical energy from the tides and waves, and thermal energy from the sun's heat. Ocean energy is classified as:

- *Wave energy:* generated by converting the energy of ocean waves (swells) into other forms of energy (currently only electricity). There are many different technologies that are being developed and trialed to convert the energy in waves into electricity.
- *Tidal energy:* generated from tidal movements. Tides contain both potential energy, related to the vertical fluctuations in sea level, and kinetic energy, related to the horizontal motion of the water. It can be harnessed using technologies using energy from the rise and fall of the tides or by technologies using energy from tidal or marine currents.

- *Ocean thermal energy:* generated by converting the temperature difference between surface water and water at depth into useful energy.

2.4.4 Solar energy

Solar Energy is energy which is created from sunlight, or heat from the sun. Solar power is captured when energy from the sun is converted into electricity or used to heat air, water, or other fluids. There are currently two main types of solar energy technologies:

- ***Solar thermal:*** these systems convert sunlight into thermal energy (heat). Most solar thermal systems use solar energy for space heating or to heat water (such as in a solar hot water system). However this heat energy can be used to drive a refrigeration cycle to provide for solar based cooling. The heat can also be used to make steam, which can then be used to generate electricity using steam turbines. It is considered more efficient to build solar thermal electricity generators at large scale, typically in the tens to hundreds of megawatts.
- ***Solar photovoltaic (PV):*** the conversion of sunlight directly into electricity using photovoltaic cells. PV systems can be installed on rooftops, integrated into building designs and vehicles, or scaled up to megawatt scale power plants.

Research and development and deployment in on-grid and off-grid applications is progressing rapidly in Australia, and a range of other solar energy technology innovations are currently being explored, for example photosynthetic based solar energy technologies and solar enhanced fuels.

2.4.5 Wind energy

Wind energy is generated by converting wind currents into other forms of energy using wind turbines. Winds are generated by complex mechanisms involving the rotation of the Earth, the heat capacity of the sun, the cooling effect of the oceans and polar ice caps, temperature gradients between land and sea, and the physical effects of mountains and other obstacles. Wind turbines convert the force of the wind into a torque (rotational force), which is then used to propel an electric generator to create electricity. Wind energy power stations (known as wind farms) commonly aggregate the output of multiple wind turbines through a central connection point to the electricity grid. Across the world there are both on-shore (on land) and off-shore (out to sea) wind energy projects.

Large scale hydroelectric projects have become increasingly difficult to carry through in recent years because of competing use of land and water. Relicensing requirements of existing hydro plants may even lead to removal of some dams to protect or restore wildlife habitats. Among the other renewable power sources, wind and solar have recently experienced a rapid growth around the world. Having wide geographical spread, they can be generated near the load centers, thus simultaneously eliminating the need of high voltage transmission lines running through rural and urban landscapes.

The present status and benefits of the renewable power sources are compared with the conventional ones in Tables 2.1 and 2.2, respectively.

Table 2.1: Status of Conventional and Renewable Power Sources

Conventional	Renewables
Coal, nuclear, oil, and natural gas	Wind, solar, biomass geothermal, and ocean
Fully matured technologies	Rapidly developing technologies
Numerous tax and investment subsidies embedded in national economies	Some tax credits and grants available from some federal and/or state governments
Accepted in society under the 'grandfather clause' as necessary evil	Being accepted on its own merit, even with limited valuation of their environmental and other social benefits

Table 2.2: Benefits of Using Renewable Electricity

Traditional Benefits	Nontraditional Benefits Per Million kWh consumed
Monetary value of kWh consumed	Reduction in emission
U.S. average 12 cents/kWh	750–1000 tons of CO_2
U.K. average 7.5 pence/kWh	7.5–10 tons of SO_2
	3–5 tons of NOx
	50,000 kWh reduction in energy loss in power lines and equipment
	Life extension of utility power distribution equipment
	Lower capital cost as lower capacity equipment can be used (such as transformer capacity reduction of 50 kW per MW installed)

Globally, many countries offer incentives and guaranteed price for the renewable power. Under such incentives, the growth rate of the wind power in Germany and India has been phenomenal.

Doubling the share of renewables in the global energy mix to 36 percent by 2030 could save the world economy up to $4.2 trillion a year, research by the International Renewable Energy Agency (IRENA) showed on Wednesday. Renewable sources, such as wind and solar, accounted for around 18 percent of global energy consumption in 2014. Under existing national policies, the share of renewables is forecast to reach 21 percent by 2030.

Doubling the current share would help achieve a global target to limit the rise in the global average temperature to below 2 degrees Celsius above pre-industrial levels, which was agreed at a summit in Paris last year.

"Achieving a doubling is not only feasible, it is cheaper than not doing so," IRENA's director general Adnan Amin said in a statement.

"It would create more jobs, save millions of lives from reduced air pollution and set us on a pathway to limit global temperature rise to two degrees as agreed in Paris," he added.

Separately on Wednesday, the European Environment Agency said the share of renewable energy in the European Union inched up to 15.2 percent in 2014 from 15 percent in 2013, according to preliminary data for 2014, the latest year available.

This project report will concentrate only in wind power.

2.5 development of wind power

Wind power is the use of wind’s force to generate some form of measurable power or work. The exact origin of the first use of wind power is unknown; however, one of the earliest known uses dates as far back as 3500 B.C. to drive sailboats using aerodynamic lift. Over centuries, sailors developed their understating of lift and made improvements to the sailboat design. These advancements were implemented in the first windmill found in Persia around the year 900. This windmill was a vertical axis Panemone style that used sheet-like wings, similar to sails, to capture the wind, as seen in Figure 2.5. This device was then connected to pulleys or a similar connection method to grind grain or pump water for harvesting. Similar designs were found in China and the Island of Crete in Greece around 1200 A.D.

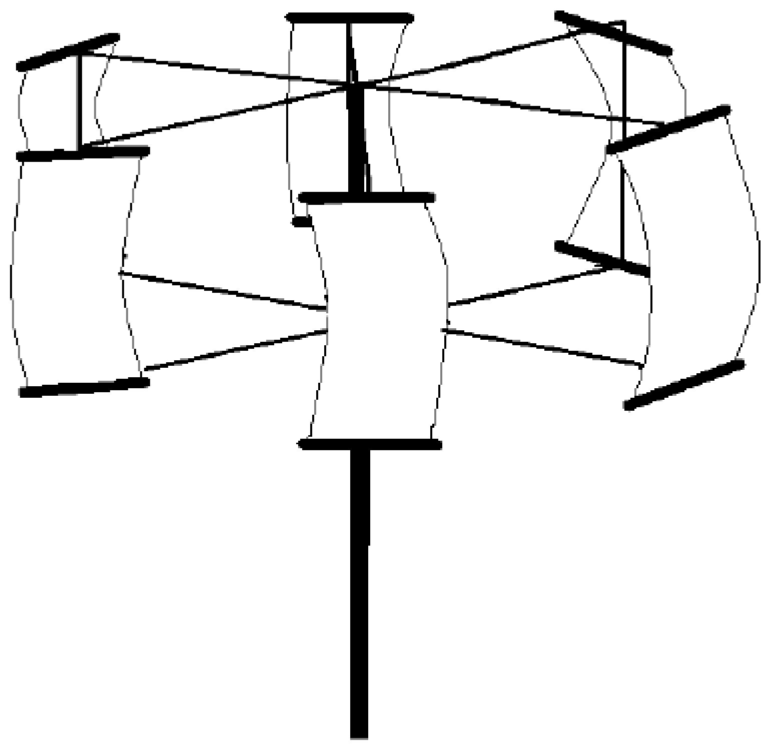

Fig 2.5: Panemone wind mill design

More widespread use of horizontal axis windmills is thought to be a development from horizontal water mills, first seen between 1100 and 1300 in England and Holland. The horizontal axis windmill Figure 2.6 used drag forces for similar purposes of grinding and sawing timber.

Fig 2.6: A Dutch tower mill (1400 A.D.)

One of the major disadvantages of this design was that the blades needed to be manually pushed to face the wind for optimal power generation. Over the next 500 years, the Dutch, as well as other European countries, implemented new technologies designed to improve the efficiency of wind turbines, such as the implantation of aerodynamic camber along the leading edge, twisting of the blade, and appropriate placement of the center of gravity.

Around the same time period, the United States built their first multi-blade turbine for irrigation purposes. From this “American Style” windmill, a trend of homemade windmills used to pump water to farms was replicated across the country. This resulted in numerous homeowner innovations tested throughout the nation. Some windmills were used to collect water for steam engines and were built with rotors as large as 18 meters across. Just before the 20th century, Denmark developed large windmills to generate electricity which was adapted by the United States in 1940 for use to power the local utility network during World War II. Unfortunately, the use of wind power decreases with the price of fossil fuels and for a stretch of 30 years was less desirable. When the price of oil rocketed in the late 20th century, wind energy became a viable choice for sustainable energy and has continued to be a growing field of research.

2.6 Advantages of Wind Power

Today, wind power has the potential to reduce the amount of carbon dioxide and related greenhouse gases that contribute to global warming. As an energy source, wind is free and does not need to be imported from other countries. This is an extremely important advantage of wind power since many countries are dependent upon foreign providers for a large percent of their fossil fuels. As an example, the United States is depended on foreign trade for 49% of their number one energy source, petroleum. In 2009, 83% of the United States' energy was supplied by petroleum, coal, and natural gas, which are three of the major contributors to greenhouse gas emissions. For countries that cannot spend millions of dollars towards fuelling each year, the natural and free use of wind can generate large amounts of energy. Wind has been praised for its modular capacity since wind machinery can be added in increments to fit many different sizes and needs. Its short construction lead time lowers both costs and risks during construction.

2.7 Disadvantages of Wind Power

Even though wind power has many positive aspects, there are numerous disadvantages to overcome as well. Most notably, wind speeds and directions are consistently changing, making it difficult to use wind as a consistent power source. Without connecting to the grid or otherwise storing the available energy, wind power is not consistently available. Another large concern is how expensive construction and installation of wind power machinery can be on or offshore. In 2006, the average investment for a wind turbine was between $1300 and $1700 for every kW the turbine would produce. For perspective, a 5kW turbine would cost between $6500 and $8500 to build and install whereas a 1 MW turbine would cost as high as $1.7 million USD. Large turbines are also plagued with consistent mechanical failures that occur from vibration or misaligned gearbox connections. Furthermore, the most populous regions are usually the regions that require the most power and are the least-suited to house large wind machinery as cities interrupt wind flow and lack appropriate space. Consumers tend to complain about the lack of aesthetic appeal and the noise that is generated from running as well as the potential danger to wildlife.

2.8 Current application of wind power

In the past 20 years, there have been major innovations in wind energy development. From 2008 to 2009 alone, wind powered electricity generation increased 20% worldwide. Still, wind energy only accounted for 1% of the world's electricity use. Many countries have recently seen significant strides in wind technology implementation as wind turbines, both on and offshore, have been installed, wind maps displaying wind patterns from around the world created, and innovative advancements in wind technology researched.

There has also been an increase of wind power use in developing nations as a source of electric power, or as mechanical energy to pump fresh water from wells. Due to the strides taken in high-strength fiber material technology, variable-speed electric generators, and the experience gained through continued development of wind technology, the cost and difficulty of construction of wind power has significantly decreased to provide more feasible and affordable wind powered machinery. Currently the popularity of wind power is still increasing world-wide. Denmark is one of many countries who are continually planning ahead in the development of wind power. Today, 25% of their electrical power is generated from wind with a goal of 50% for the year 2020. Many countries have similar goals while research and development are continuously taking place in an effort to minimize the earlier stated disadvantages.

2.9 Background about Sudan

Although Sudan lies within the tropics, the climate ranges from arid in the north to tropical wet-and-dry in the far southwest. Temperatures do not vary greatly with the season at any location; the most significant climatic variables are rainfall and the length of the dry season. Variations in the length of the dry season depend on which of two air flows predominates, dry northeasterly winds from the Arabian Peninsula or moist southwesterly winds from the Congo River basin.

From January to March, the country is under the influence of the dry north-easterlies. There is practically no rainfall countrywide except for a small area in northwestern Sudan in where the winds have passed over the Mediterranean bringing occasional light rains.

There is a variety of water resources in Sudan including water surfaces, rain and underground water. The amount of renewable water sources are approximated as 149 billion cubic meter. An approximate amount of water available for use is about 30 billion meter cubic, about 4 billion is renewable underground water.

About 50% of the total area of Sudan is filled with underground water (before the separation of Southern Sudan). Only 1% of the 260 billon meter cube is used (2010), 6 billon is renewable.

The main underground water reservoirs are the NOBIAN sand stone and UM-ROWABA reservoir in addition to some in the river regions like BLUE NILE, ATBRA and ALGAZEERA. Figure 2.7 shows the underground storages and their depth.

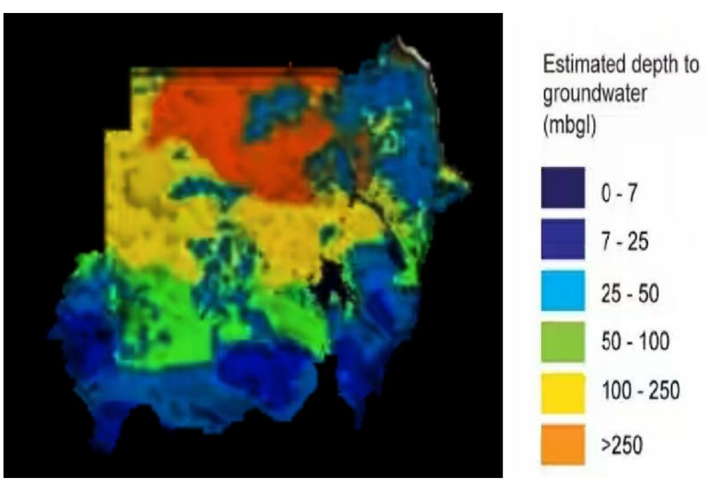

Figure 2.7. Underground water distribution in Sudan

Sudan is endowed with large areas of cultivable land, which are situated between the Blue Nile and the White Nile, and in the region between the Blue Nile and the Atbara-river. Other regions with cultivable land are the valleys of the plains, where irrigation is extensively used, and in the narrow Nile valley. This land has different uses,

About 105 million hectare (259.5 million acre) of the total area of Sudan is suitable for agriculture 8 million hectare (20 million acre) is used, 2 million hectare (5 million acre) is irrigated agriculture. Only 4% of the irrigated area is irrigated with underground water.

After 1980, as the supply of conventional energy has not been able to follow the tremendous increase of the production demand in rural areas of Sudan, a renewed interest for the application of wind energy has shown in many places. Therefore, the Sudanese government began to pay more attention to wind energy utilization in rural areas. Because the wind energy resource in many rural areas is sufficient for attractive Figure 2.8 shows wind speed distribution in Sudan.

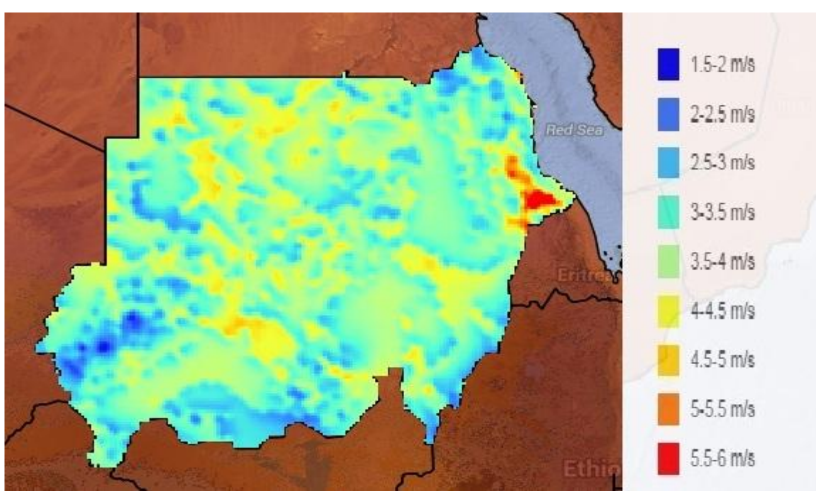

Figure 2.8: wind speed distribution in Sudan.

Application of wind pumps, and as fuel is insufficient, the wind pumps were spread on a rather large scale in the near future.

2.10 Theory

2.10.1 Power in the wind

When wind blows it can move things, depending how strong the wind is. It can rotate a turbine, for instance. So, there is energy in the wind. Any moving object has energy. This type of energy is called **kinetic energy.** For moving air, that is, the wind. The amount of energy of a moving object depends on two factors, its *mass* and its *speed*. Using the proper units for measuring mass and speed, the relationship to determine the energy of a moving object is as follows:

$$Energy = {}^{1}/_{2}\ (mass)(speed)^2 \tag{2.1}$$

This equation implies that, for example, if mass is doubled the energy doubles. But, if the speed is doubled, then the energy is four times more.

Energy in a moving fluid (a gas or a liquid) can be found in the same way as described for a solid body. There are two differences, however, that must be taken into account. The first difference is that for a fluid in motion, we define the moving mass by its volume. This is so because there is no solid object with a definite mass to be considered. The second difference is that for a moving fluid, the whole volume moves.

In the case of a fluid flowing inside a pipe, the moving mass is represented by the size of the pipe and by flow rate. The flow rate is the amount of the volume of the liquid that moves in a minute or a second.

Depending on the size of the pipe, the speed of the flowing fluid can be found. The size of the pipe is defined by its cross-sectional area.

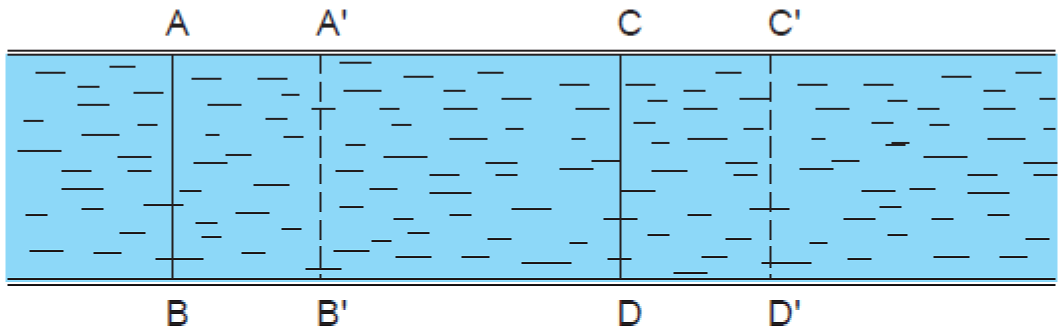

Figure 2.9: movement of fluid inside boundary

One can imagine that a portion of water represented by *ABCD* in figure 2.9 moves along the pipe. After a short period it has moved from the previous position to a new position denoted by *A'B'C'D'*. (In reality, this is not what happens inside a pipe, but it shows the motion of water.) The same is true for any other liquid or gas. If it takes 1 sec for the fluid to travel from *ABCD* to *A'B'C'D'*, then the speed of the fluid is the length of the line from *A* to *A'* (which is the same for *BB'*, *CC'*, and *DD'*).

In order to see how much energy is in the water moving in a pipe it is very important to realize that the whole volume of water in the pipe moves. However, it is not helpful at all to consider this energy, since it depends on the full length of the pipe. Instead the power of the moving fluid is determined.

When a fluid is moving with no boundary, which particularly is the case for wind, then an imaginary boundary is practically generated by the objects that lie along its passage. This is better understood from Figure 2.9.

At some place within the stream denoted here by a plane BB' an object is obstructing the stream. It can be a turbine. For simplicity, assume it is round. Along the wind direction, we can assume an imaginary cylinder, the diameter of which is the size of the object. This is shown in figure 2.6, by the two parallel lines along the wind direction. You can assume that this is the boundary that defines a pipe. But in the case of no boundary flow it is not this imaginary cylinder that defines the boundary. Instead the nearly conical shape shown in the figure is the boundary of the flowing fluid. The reason for this is that, because of the obstruction in the flow, the particles of the fluid start moving outward when approaching the obstacle. Thus, instead of moving ahead in a straight line, they follow the curve shown in the figure. They start moving outward at a point denoted by plane AA'. They resume their parallel flow at some point after the obstacle. This point is represented by plane CC' in figure 2.10.

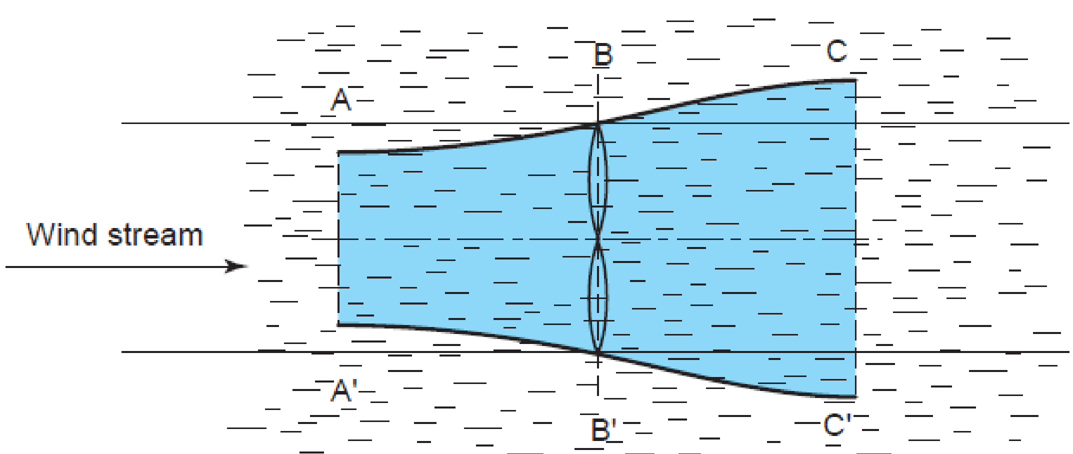

Figure 2.10: Movement of fluid in no boundary

For wind or any other moving fluid it is more practical to find the power rather than the energy. In this sense, in equation 2.1 we can substitute for the mass of the air that flows in 1 sec, and that gives the power in the wind. Note that

$$Mass = (Density)(Volume) \quad (2.2)$$

Also, note that for a fluid moving inside a pipe one can always say that

$$Volume\ moved\ in\ 1\ s = (Cross - sectional\ Area)(speed) \quad (2.3)$$

Substituting from equations (2.2) and (2.3) in equation (2.1) gives the power in a moving fluid, or the amount of energy in 1 sec for the area given by a pipe cross section or the size of an object in the stream of an open flow with no boundary.

$$Power = \frac{1}{2}(Density)(Cross - sectional\ Area)(speed)^3 \quad (2.4)$$

Equation (2.4) shows that the power in a tunnel of wind is proportional to the air density, the cross-sectional area of the tunnel of wind and the cubic power of the wind speed.

The following conclusions can be derived from equation (2.4):

- For the same turbine and at the same time, if the wind speed doubles, the power in the wind increases by a factor of 8.
- For the same turbine and the same wind speed, if the weather is cold (higher density), more power exists in the wind available for the turbine.
- In the same weather conditions and for the same wind speed, a turbine that is two times larger in cross-sectional area than a smaller one has twice as much wind power available to it.

Equation (2.4) is used to calculate the power that exists in wind, a part of which can be extracted by a wind turbine. The cross-sectional area in this equation refers to the size of a turbine.

2.10.2 Power extracted from the wind by wind mill

Wind mill can only absorb a portion of the power in the wind. This depends on the type of turbine, the efficiency, and other conditions in the operation of a turbine such as the height of the rotor, wind speed variation (maximum and minimum), obstacles at the site selected, etc... .

In order to evaluate the fraction of power in the wind that a particular wind turbine can harness from wind a coefficient is used in equation (2.4). Thus,

$$Power = (A\ coefficient)(Power\ in\ the\ wind) \qquad (2.5)$$

Or

$$Wind\ turbine\ power = \tfrac{1}{2}(Power\ coefficient)\ (Density)\ (Cross\text{–}sectional\ area)\ (Speed)^3 \qquad (2.6)$$

The power coefficient C_p is the ratio of power Extracted by the Windmill to the total contained in the wind resource. The power coefficient value is less than 1 and it depends on how good a turbine is designed and how well it can grasp the wind energy. Thus, its value can be small or large. Nevertheless, there is a maximum value that no turbine in its best performance can exceed. It can be theoretically determined and is called the Betz limit. The value for Betz limit is 16/27 = 0.59.

The power coefficients for certain turbines can reach values near the Betz limit. A value of 0.50 for a good design is acceptable. For others, this number can be smaller, say 0.25 or even 0.20. Any claims for coefficient greater than the Betz limit is groundless and can be rejected.

2.10.3 Site selection

The wind speed is the most influential factor to how much power a wind turbine can generate. In fact, for any wind energy project the wind speed is the first decision-making factor. The nature of wind is that it is variable. This implies its direction, speed, and temperature can change. This change can be from minute to minute or sometimes from second to second.

There are four categories of wind speed variation these are:

- Wind speed variation with time.
- Wind speed variation with height.
- Wind speed variation with terrain.
- Wind speed variation with geographic zone.

2.10.3.1 Wind speed variation with time

The variation of wind speed with time, by itself, falls into three categories: momentary changes, daily changes, and seasonal changes.

Wind is generated by a difference in temperature of air between two locations. So, it is subject to the heat from sunshine and the temperature of the surroundings in an area of the Earth. We can sometimes clearly see this variation of wind and notice that wind does not blow with a constant speed. This momentary variation can be clearly seen when the wind speed is recorded.

Figure 2.11 shows an example of recorded wind speed for some short period of time.

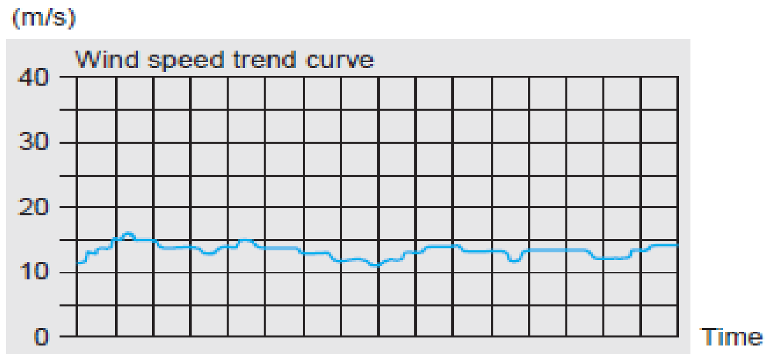

Figure 2.11: Typical variation of wind in 2 min.

The daily changes of wind speed, as the name implies, is the variation of wind speed in 24 hours. For instance, in one region the highest wind speed can occur at a certain time of the day, and at other hours there is less wind or even no wind. In other words, we may be able to identify a specific pattern for the wind in a region for various times of the day. Note that this could also be true for the direction of wind.

The seasonal change in wind refers to variation of wind during a year. Again, for this case one may find a specific pattern for the wind speed for various months of the year. The best example is that in many regions we have more wind in the spring or winter compared to the summer. This means that one cannot expect the same production of power from a turbine at different seasons in a year. Fig 2.10 show an example of wind variation in during year, 1983 to 1984 Khartoum airport, 10 m above the ground.

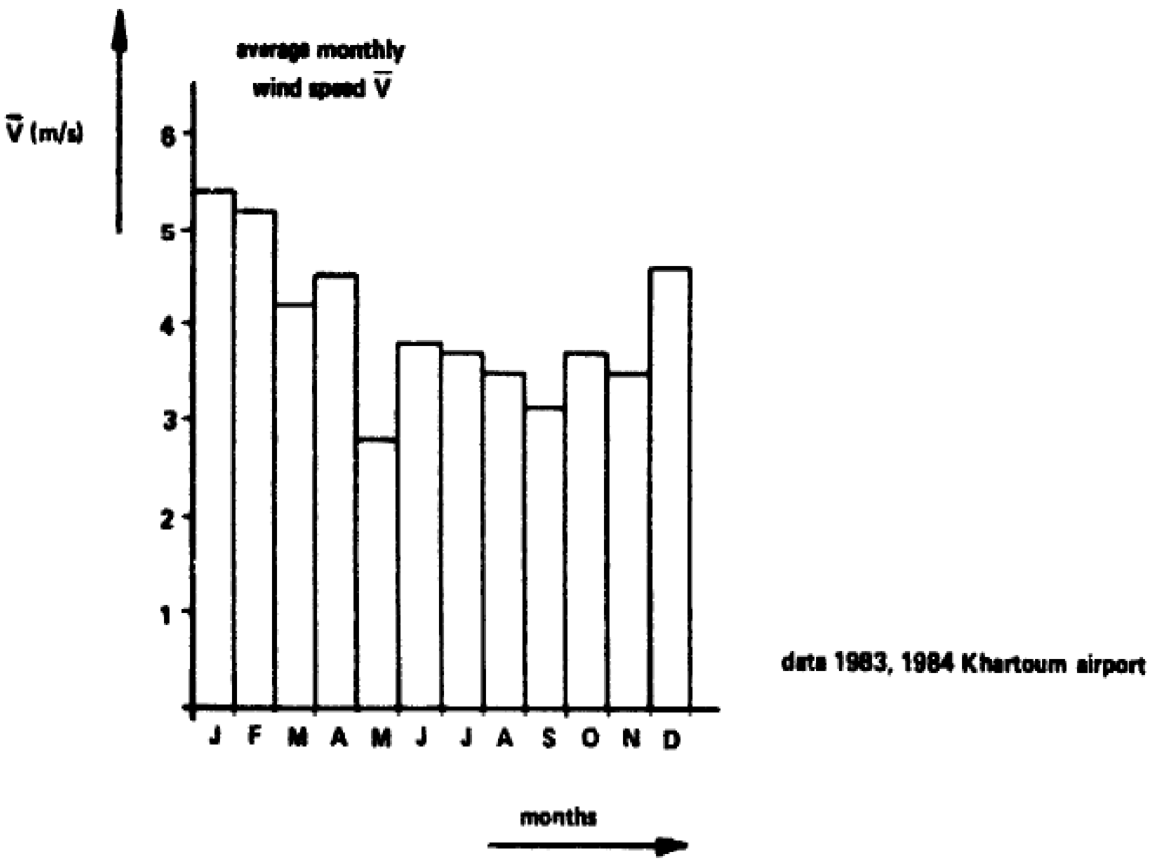

Figure 2.12: wind variation during the year

2.10.3.2 Wind speed variation with height

The speed of wind is not the same at different heights. As we move away from the Earth's surface, the speed of wind gets higher. This variation by height is not the same for all places. This all depends on the nature of the ground in that location.

The relationship between the wind speed and height is not linear. The wind speed at the Earth's surface is lower than that at a relatively distant point above ground. The wind speed increases as the height increases. However, after a certain height, the wind stream has a uniform speed that no longer changes with height.

2.10.3.3 Wind speed variation with terrain

When wind blows, its direction and speed are influenced by all the obstructions that lie on its path. At a height sufficiently away from the ground surface, however, wind direction and speed are not disturbed and there is a steadier wind stream. All the obstacles to the flow of wind can slow it down. Thus, inside cities where there are many buildings, there is more obstruction to slow down the wind. On the contrary, in farmlands with short vegetation or along the surface of a lake there is not much obstruction to slow down the wind.

The effect of a building on the flow of wind is shown in Figure 2.13. Note that the whole wind speed drops because of buildings or other obstructions, but locally, the wind speed is higher on the roof, since more air must move from a narrower area. This is shown by the profile lines being closer to each other above the roof.

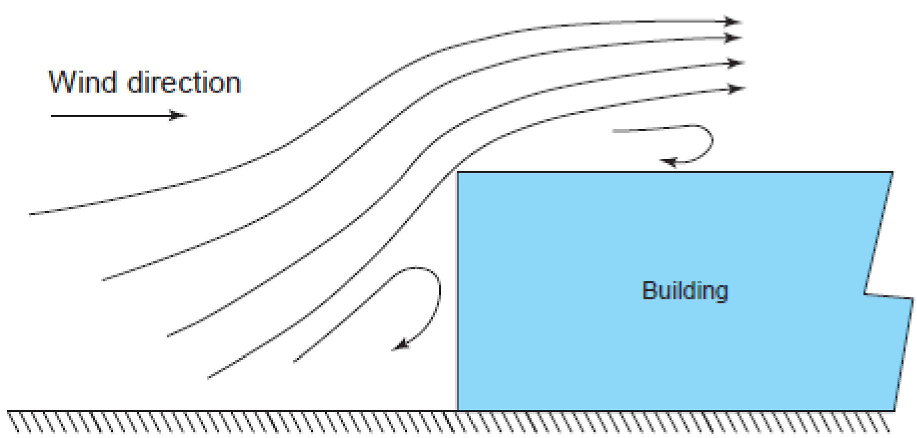

Figure 2.13: the effects of building on wind flow

The same on the larger scale of a hill is shown in Figure 2.14. After wind hits the hill from the left and passes the hilltop it speeds up on the right-hand side. In such a situation, the right-hand side of the hill is the best place to install wind turbines.

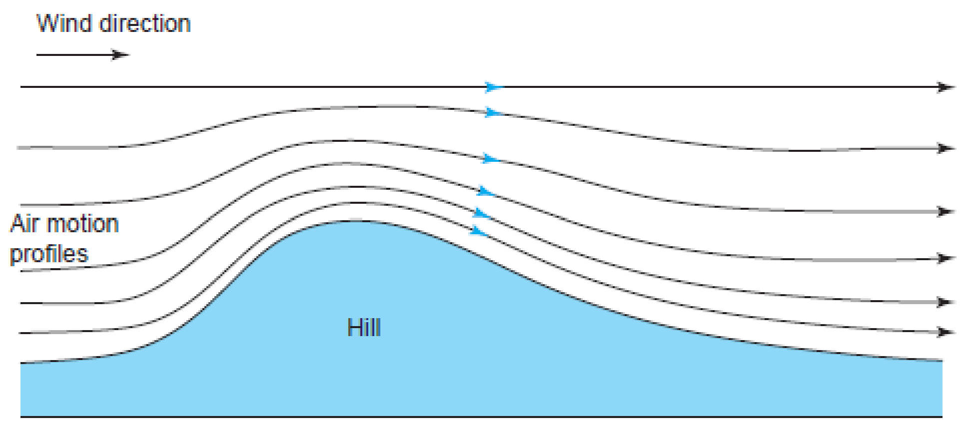

Figure 2.14: Profile of the wind passing over a hill

2.10.3.3 Wind speed variation with geographic zone

The climate is not the same everywhere. The formation of wind is affected by the change in the temperature (and thus, pressure) of air. The cooling down or warming up of a region depends on a number of factors, all related to the geographic location. For example, if a region is near the sea or surrounded by mountains, whether or not it is affected by large storms, and so on, determine the wind specifications.

2.10.4 Force from the wind

When wind blows, it exerts some forces on all the objects that are touched by the wind. The size and direction of these forces are evident in some cases, and the effect can be easily observed.

When an object is in the path of the wind it is subject to two forces from wind. Assume a rectangular plate with and angle to the wind direction as shown in figure 2.15. When wind blows it pushes the plate. This is due to a force component parallel to the wind direction. On the other hand, as wind passes through, depending on the angle of the plate with the direction of wind, it causes the pressure at the two sides of the plate to be different. The result of this pressure difference is a force that pushes the plate in the direction of the side where the pressure is lower. One more effect of the wind is to cause a rotation of the plate. This rotation is due to a torque.

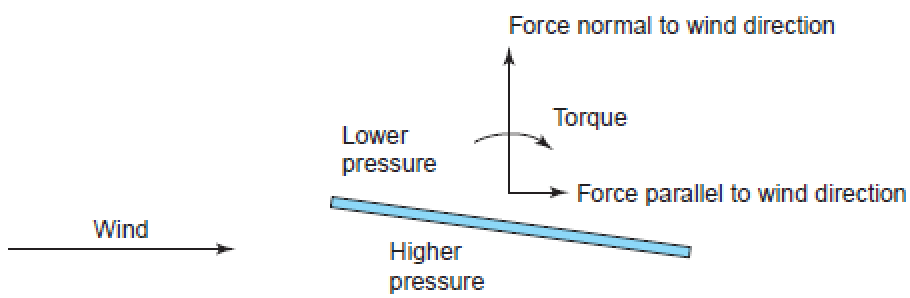

Fig 2.15: Force and torque on a plate

The angle of the plate to the wind direction called The *Angle of Attack*; the force component parallel to the direction of the wind is called the *Aerodynamic Drag* or just simply the *Drag*; the force component perpendicular to the direction of the wind is called the *Aerodynamic Lift* or just simply the *Lift*. The lift force is not necessarily upward. It depends on the angle of attack (figure 2.15).

When the angle of attack is small the lift force is larger than the drag force. As the angle becomes larger the lift decreases and the drag increases. When the angle of attack is 90, the lift is zero (for this plate) and the magnitude of drag is the maximum as shown in figure 2.16. The drag force is the resistance of air on something that moves in the air or the force from air when wind flows over an object. On the other hand, lift is a force that moves an object to a side (it can be upward).

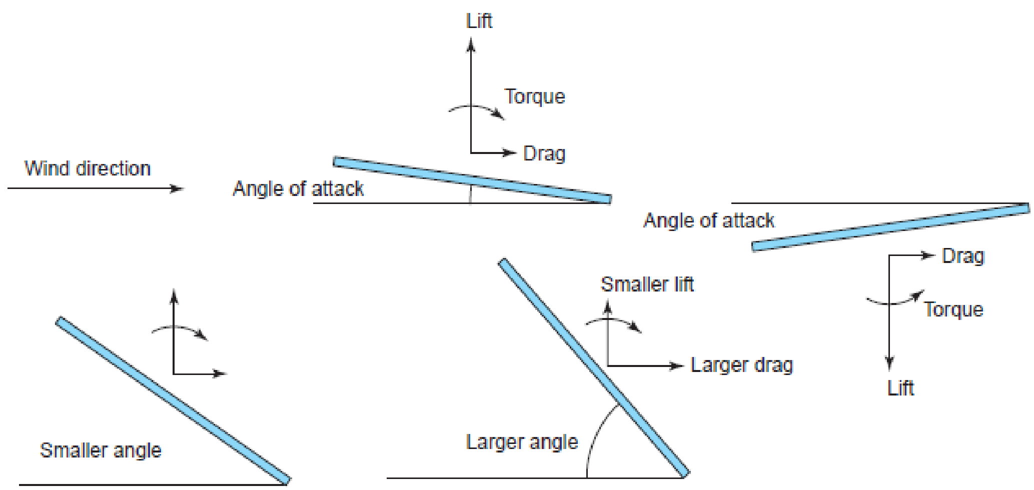

Fig 2.16: Lift, Drag and Angle of Attack

2.10.5 Aerodynamic force extracted by the plate

The lift force and the drag force are the two components of the aerodynamic force on the plate under consideration. These two components are perpendicular to each other; that is, they make an angle of 90° with each other.

The force extracted on any surface can be calculated using:

$$Force = (Area)(Pressure) \tag{2.7}$$

The pressure from wind on a surface initially depends on the wind speed and the air density at the temperature under consideration. The exact relationship is

$$Pressure\ of\ the\ air = \frac{1}{2}(Density)(Speed\ of\ the\ air)^2 \qquad (2.8)$$

Substituting the (2.7) in (2.6) we have the net force on the plate

$$Pressure\ of\ the\ air = \frac{1}{2}(Area)(Density)(Speed\ of\ the\ air)^2 \qquad (2.8)$$

The force is in addition to the atmospheric pressure that is exerted on both sides of the plate. It can be assumed to be concentrated at the center of mass (here, the geometric center) of the plate.

The magnitudes of the lift and drag forces depend on the angle of attack, but at each angle their values can be defined in terms of the aerodynamic force; that is,

$$Lift\ Force = Lift\ coefficient * Aerodynamic\ force \qquad (2.9)$$

$$Drag\ Force = Drag\ coefficient * Aerodynamic\ force \qquad (2.10)$$

As the aerodynamic force depend on the shape of an object. Based on equation (2.8), the definition for lift coefficient and drag coefficient are as follows:

$$Lift\ coefficient = \frac{Lift\ force}{Areodynamic\ force}$$

$$Drag\ coefficient = \frac{Drag\ force}{Areodynamic\ force}$$

Although the *lift* and *drag* coefficients change with the angle of attack, they are highly dependent on the shape of an object. Moreover, they are the same for objects of the same shape, since these two quantities are ratios. The following table shows data for the different shapes.

Table 2.3: Data for some common plate's cross-sections

Section	Sketch	Drag/Lift Ratio	Optimum angle of attack	Lift Coefficient (C_L)
Flat plate		0.1	5^0	0.8
Curved Plate (10% curvature)		0.02	40^0	1.25
Curved plate with tube on concave side		0.003	4^0	1.1
Curved plate with tube on convex side	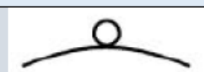	0.2	14^0	1.25
Aerofoil		0.01	4^0	0.8

2.10.6 Twisting the blade

Since the drag is in the downwind direction, it may seem that it wouldn't matter for a wind turbine as the drag would be parallel to the turbine axis, so wouldn't slow the rotor down. It would just create "thrust", the force that acts parallel to the turbine axis hence has no tendency to speed up or slow down the rotor. When the rotor is stationary (e.g. just before start-up), this is indeed the case. However the blade's own movement through the air means that, as far as the blade is concerned, the wind is blowing from a different angle. This is called apparent wind. The apparent wind is stronger than the true wind but its angle is less favorable: it rotates the angles of the lift and drag to reduce the effect of lift force pulling the blade round and increase the effect of drag slowing it down. It also means that the lift force contributes to the thrust on the rotor. The result of this is that, to maintain a good angle of attack, the blade must be turned further from the true wind angle.

The closer to the tip of the blade the faster the blade is moving through the air, and so the greater the apparent wind angle is. Thus the blade needs to turn further as the tips than the root, in other words it must be twisted along its length typically 10 – 20 degree from root to tip as shown in the figure below.

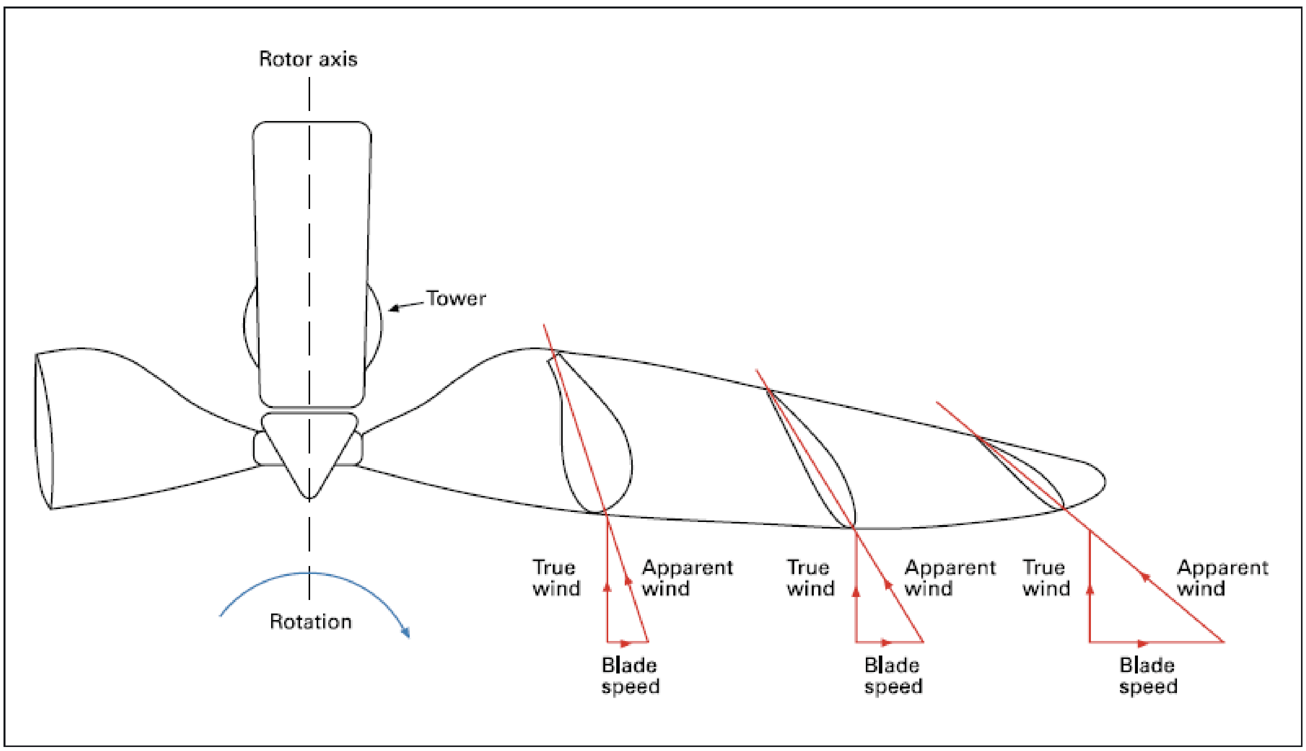

Figure 2.17: An airfoil twisted to benefit the apparent wind

2.11 Categories of wind turbines

A variety of wind machine can be used to produce power; the main classification which based on the application of the wind machine which are the *Wind turbine* for production of electricity and *Windmill* for pumping water or grinding –as used back in time in Germany. Other classification of wind machine is based the *Vertical Axis Wind Turbine* (VAWT) and the *Horizontal Axis Wind Turbine* (HAWT)**,** the classification based on the axis of orientation of the rotor.

2.11.1 Vertical Axis Wind Turbine (VAWT)

This has blades which are arranged on the vertical axis and are rotated by wind and therefore it doesn't require a yaw mechanism since it can harness wind from any direction. It does not rely on the direction of the wind to generate power as in the case of the horizontal axis. They usually operate closer to the ground which has an advantage of allowing for placement or replacement of heavy equipment. However this is a disadvantage as winds are lower near ground level hence less power output.

In the past quite some researches effort has been put into vertical axis machines for pumping, especially Savonius rotors. However, this has not led to practical applications for two main reasons: high cost per unit of water pumped (heavy machine6 combined with low efficiency), and poor reliability (it is difficult or impossible to incorporate a safety system in such a design). Vertical axis Darrieus wind rotors are hardly suitable for a water pumping By Stem, as they need an external power source for starting, figure 2.16a show a Darrieus vertical axis turbine.

2.11.2 Horizontal Axis Wind Turbine (HAWT)

It has blades that are similar in design to aircraft propellers where air flow over the airfoil shaped blades produces a lifting force that turns the rotor. They should be placed on towers to ensure maximum use of the winds at higher levels.

For large scale types, they have an active yaw mechanism with wind direction sensors and motors that will rotate the nacelle. In both upwind and downwind the rotors should be perpendicular to the direction of wind and if the rotor is held in a fixed position, only 21% of the wind energy will be captured. For upwind type, the rotor rotation is accomplished by using a vain to measure the direction of the wind and then the information is communicated to the yaw drive. The yaw drive then drives the rotor so that the turbine is facing the direction of wind for maximum harness. They don't suffer from wind shade phenomenon as the wind is tapped early enough before obstruction by the tower.

For downwind types, they don't use a yaw drive because the wind itself orients the turbine. The blades are situated on the downwind side and therefore capture the wind and rotate following its direction. These designs are prone to "wind shade" a process in which the wind flow is obstructed by an object e.g. the tower thus reducing amount of wind and therefore a reduction in the power output. Figure 2.16b show a horizontal upwind and downwind wind turbine.

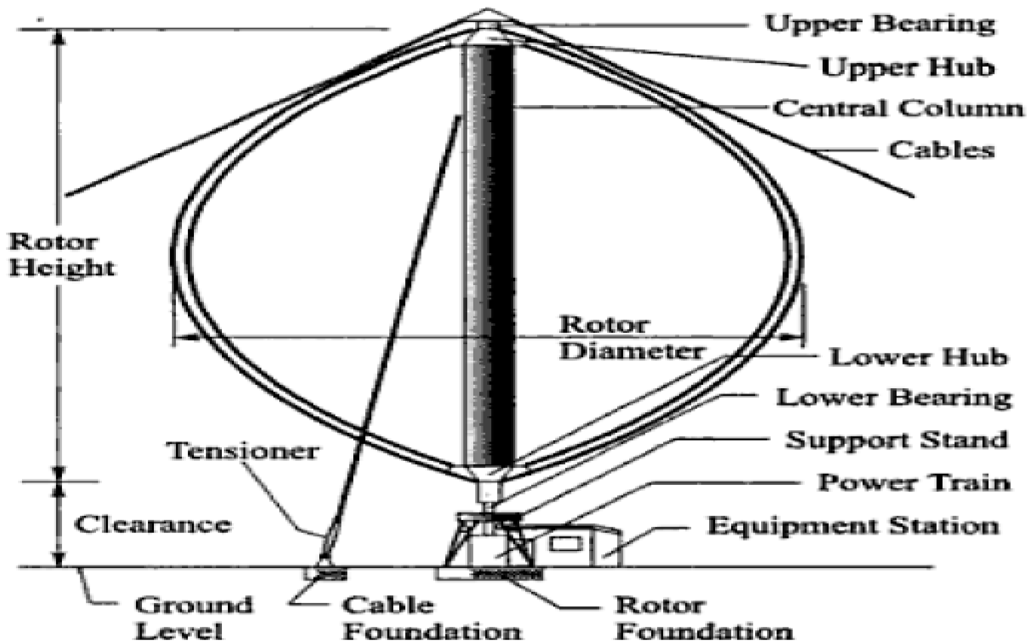

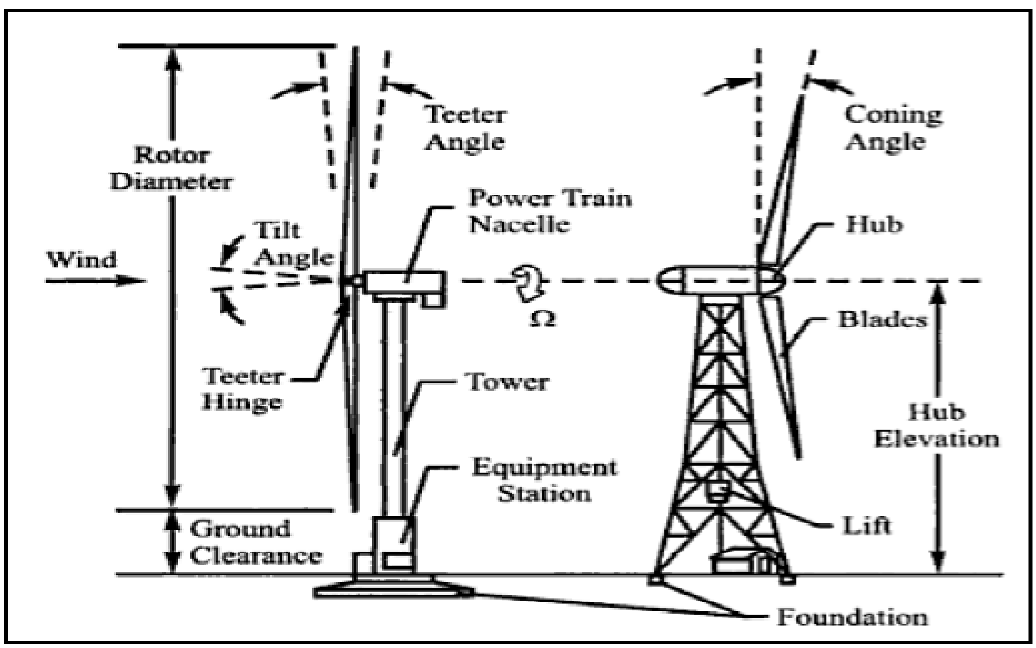

Fig 2.18: Examples of wind turbine categories. a) Schematic drawing of Darrieus wind turbine. b) Schematic drawing for Horizontal Up wind and downwind wind turbine.

2.12 Types of wind turbines

There are many different types of wind turbines, each with their own advantages and disadvantages. Many of these different wind turbine designs were researched in order to better understand them and choose one that fit with the proposal of pumping water for a village in a third-world country.

2.12.1 Savonius Turbine

One of the more prevalent types of VAWTs is the Savonius Rotor. The Savonius rotor is less powerful than most HAWTs, and it has a high power to weight ratio. However, the Savonius rotor is particularly useful for situations that do not require a large amount of electric power. Also, because of the simple design of the Savonius, it is relatively simple to build. Figure 2.19 shows a simple Savonius rotor.

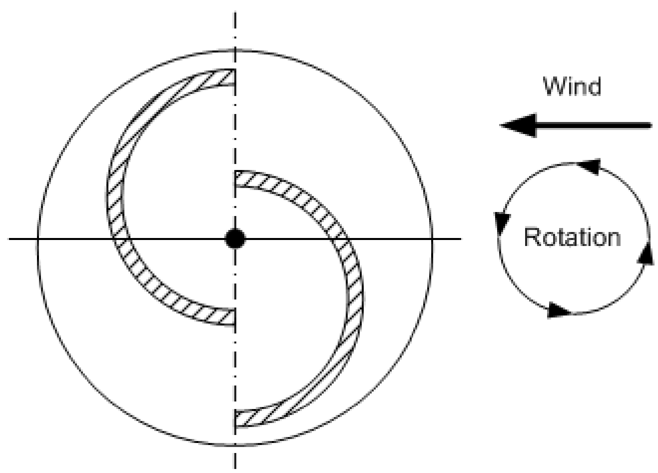

Figure 2.19: A simple Savonius concept

2.12.2 Darrieus Turbine

Because it is a VAWT, the Darrieus turbine has certain advantages over a standard HAWT. Most HAWTs require some sort of yaw control mechanism to ensure that that turbine is oriented appropriately with respect to the wind. Because the Darrieus turbine does not rely on wind direction, it avoids this problem entirely. The Darrieus turbine is also typically designed to keep the heavy machinery at ground level, reducing the total weight of the vertical section. However, this type of turbine is not self-starting.

The Darrieus turbine, in its most general sense, works by generating lift using the rotating motion of the blades. Essentially, most of the “apparent wind” is coming from the air pressing on the blade due to the rotation, and not from the wind itself. The ambient wind on the blade creates a rearward change in momentum, and it is this that propels the blade in the direction of rotation. This phenomenon does not occur unless the blades are already rotating, however. This is why a separate means of starting is requires for the Darrieus turbine.

A simpler type of Darrieus, known as the H-Darrieus turbine, does not utilize curved blades to move, making it easier to design and manufacture. Instead, it uses a number of straight airfoils (usually two or three) to generate the requisite lift. The Darrieus is known for having very low torque (Table 1), though its size can be manipulated to provide sufficient torque for different applications.

The Darrieus type relies on two or more curved blades that rely on wind to revolve around a central column.

2.12.3 Hybrid Savonius - Darrieus

A turbine design consisting of both a Savonius and a Darrieus wind turbine joins both turbines together in order to gain advantages from each. The advantages of each of the turbines help offset the disadvantages of the other turbine. Combining these two wind turbines results in a turbine that is able to start itself, operate in low wind speed, and produce a high enough efficiency to be able to transfer wind energy over to electrical power.

Figure 2.20: Combined Savonius-Darrieus wind turbine

2.12.4 Helix Turbine

A helix wind turbine uses long blade scoops that are helically shaped to catch the wind from any direction. The helix is similar to the Savonius since it uses drag forces provided by the wind and is self-starting. This is one of the more innovative designs that manipulate the direction of the wind through its blades to increase its rotational velocity. An example of this design is provided in Figure 2.19.

Figure 2.21: Helix Wind Turbine

2.12.5 Panemone turbine

A Panemone windmill is a vertical-axis wind turbine. The rotating axis is positioned vertically and the blades move parallel to the wind to catch the wind. The Panemone primarily uses drag force to turn the blades. Wind moves the vanes of a Panemone in a circle to make the drive shaft turn. However, a disadvantage to the Panemone is that it is one of the least efficient types of wind turbines because the wind panels generate no work when returning to the part of the turbine that is upwind.

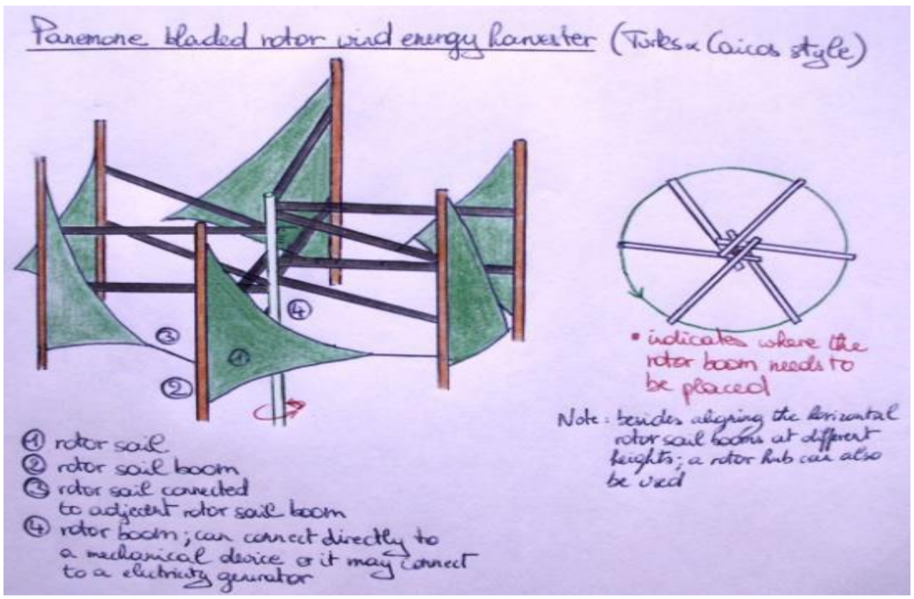

Figure 2.22: A drawing of a Panemone wind turbine

2.12.6 Aerocam turbine

An Aerocam is a HAWT that uses multiple aerodynamic blades which cut a profile in the air that is similar to a water wheel. This also allows it to follow the path of the wind as the blades rotate, which means it requires no mechanical yaw correction. This wind turbine is used for electricity production. One disadvantage of this type of wind turbine is that it is stationary, meaning that it is only one-directional.

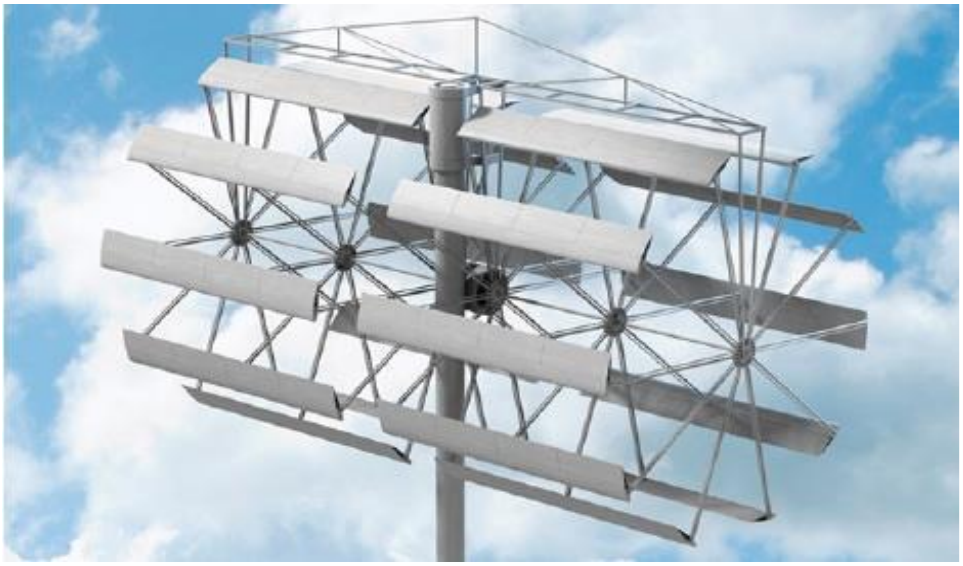

Figure 2.23: An Aerocam wind turbine design

2.12.7 Eco whisper silent turbine

The Eco Whisper Turbine is an Australian-made horizontal axis wind turbine (HAWT) that is quieter and more compact than popular 3-blade turbines. Eco Whisper Turbines may be deployed to offset electricity loads in a variety of applications, including residential, commercial, industrial and manufacturing sites, as well as farms and urban locations such as schools. The Eco Whisper Turbine eliminates the noise and vibration of traditional three bladed wind turbines.

Figure 2.24: Eco whisper silent wind turbine

2.12.8 Traditional Windmill

A traditional windmill operates at low speed and produces high torque. It is generally used to produce mechanical power for pumping water for domestic uses, irrigation or even for fish farms. This design has also been around for many decades allowing for many design advancements and a large data base.

Figure 2.25: American multi-blades windmill

2.12.9 Wind Turbine Comparisons

For the many wind turbines introduced previously, Table 2.4 compares some of the desired characteristics important to this project. Speed, torque, and the power coefficient are important factors to take into consideration as they help determine the performance of the wind turbine. The wind device torque is needed to predict the turbine's compatibility with its intended application. Different characteristics are more relevant for different applications.

Table 2.4: comparison of desired characteristics of some types of wind turbine types

Ref No.	Design	Orientation	Use	Propulsion	* Peak Efficiency	Diagram
1	Savonius rotor	VAWT	Historic Persian windmill to modern day ventilation	Drag	16%	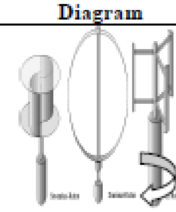
2	Cup	VAWT	Modern day cup anemometer	Drag	8%	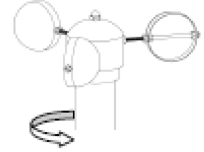
3	American farm windmill	HAWT	18th century to present day, farm use for Pumping water, grinding wheat, generating electricity	Lift	31%	
4	Dutch Windmill	HAWT	16th Century, used for grinding wheat.	Lift	27%	
5	Darrieus Rotor (egg beater)	VAWT	20th century, electricity generation	Lift	40%	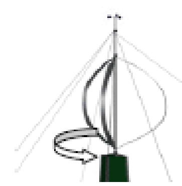
6	Modern Wind Turbine	HAWT	20th century, electricity generation	Lift	Blade Qty / efficiency: 1 – 43% 2 – 47% 3 – 50%	

Chapter Three

Research Methodology

CHAPTER THREE

RESEARCH METHODOLOGY

The work of this project were carried out in sequential stages. The project started with pointing out the problem to be solved. An information about the project problem was gathered in different ways. Literature studies and internet search were conducted during the whole project period to find the information needed. The aim and objective, scope of the project and the Project plan and time table were made to visualize the dead line of the project.

According to the information gathered, a clear understanding of the concept of the solutions, identification and selection of the types of the systems where developed over past time and an understanding of the theory and principles of the selected system obtained.

The Design parameters which are in this case the swept area *(A)*, total water required per day *(Q)*, average wind speed *(V)* and the total head of water to be lifted *(H)* were identified according.

The design were divided into two main subsystems:

- Design of rotor assembly
- Design of pump assembly.

3.1 Design of Rotor assembly:

In this project he rotor assembly consists of the rotor, Transmission mechanism and Directing tail.

The design of the rotor was initiated with the evaluation of the power requirement to lift water for the required elevation considering the various losses during the whole system (frictions on pipe, efficiencies of pump, pump rod, transmission mechanism and losses in the rotor) to calculate the power that should be obtained from the rotor assembly. The power needed were calculated using equation (3.1), (3.2) (3.3)

$$P_h = \rho\ g\ Q\ H \tag{3.1}$$

$$H = H_s + H_f + H_d \tag{3.2}$$

$$efficiency = \frac{output}{input} \tag{3.3}$$

The power obtained from the rotor were calculated to calculate rotor swept area and hence the blades area and dimensions that are needed to obtain the evaluated power using equations (3.4), (3.5), (3.6) and (3.7).

$$P_{Wind} = \frac{1}{2} * \rho * v^3 * A \tag{3.4}$$

$$A = \pi R^2 \tag{3.5}$$

$$\sigma = \frac{n * Ab}{As} \tag{3.6}$$

$$\sigma = \frac{n * Ctip}{\pi * D} \tag{3.7}$$

Since the wind speed is varying with time the velocities of wind at which the rotor will start spinning and stop was calculated using equations (3.8), (3.9) and (3.10) as follows:

$$Vd = \sqrt{\frac{\eta_{vol} * V_s * \rho_w * g * H * \lambda_d * i}{\rho * \pi^2 * R^3 * (C_p \eta)_{max}}} \tag{3.8}$$

$$Vstart = 1.8\,Vd \tag{3.9}$$

$$Vstop = 1.2\,Vd \tag{3.10}$$

In order to specify the shaft diameter the bending and twisting moments has been calculated using equations

$$T_e = \sqrt{M^2 + T^2} \tag{3.11}$$

$$T_e = \frac{\pi}{16} * \tau * d^3 \tag{3.12}$$

$$M_e = \frac{\pi}{32} * \sigma * d^3 \tag{3.13}$$

$$\tau = 0.186 * \sigma_u \tag{3.14}$$

$$\sigma = 0.36 * \sigma_u \tag{3.15}$$

3.2 Design of pump assembly:

The size of the pump and the torque required to pump water was calculated according to water required per day and the optimum tip speed ration of the design using equations:

$$\lambda_{opt} = \frac{4\pi}{n} \tag{3.16}$$

$$\lambda = \frac{\omega\, R}{V} \tag{3.17}$$

$$Q\ pipeflow = \frac{Q}{f} \tag{3.18}$$

$$R_{pump} = \sqrt{\frac{Q\ pipeflow}{\pi * h_{pump}}} \tag{3.19}$$

$$T = \frac{P_{Mech}}{\omega} \tag{3.20}$$

The forces acting on the pump rod static and dynamic loads were calculated to select the material that have the ability to overcome those loads, the equations were used are:

$$\omega_{max} \approx 3\,\lambda_d \frac{V_{rated}}{R} \tag{3.21}$$

$$F_{st,\ w} = \rho_w\, g\, H\, A_p \tag{3.22}$$

$$F_{Pr} = K\, F_{St,\ w}[1 + \frac{1}{2}\, s\ \omega^2/g\left(\frac{A_p}{A_{rm}}\right)] \tag{3.23}$$

3.3 Modeling and analysis:

The configuration of the rotor assembly and pump assembly has been sketched and then modeled using SolidWorks Version 14 which a trial version that worked for only 30 days. The components include the:

1. Rotor;
    - Blade.
    - Supporting arm and fixtures.
    - Hub.
2. Transmission assembly:
    - Crank shaft.
    - Base, base stands and cabs.
    - Lifting bully.
    - Bully- crank link and cabs.
    - Guiding pin.
3. Directing tail:
    - Tail straight bar.
    - Tail rod.

- Tail structure.
- Vain.

4. Pump assembly:
    - Pump rod.
    - Plunger.
    - Pump cylinder.
    - Valves.
    - Cylinder cabs.
    - Pump rod connections.

An analysis was carried out using Solid Works based on static manner in which the forces acting on each member of the system was identified and the materials were selected based on the criteria of weight and yield strength. The simulation process were made to monitor the behavior of the component due to applied forces. The analysis processes iterated several times accompanied with modification, until all the stresses, strain and displacement resulted from the applied loads were suitable to the material selected and the working conditions. The dimensions of each component on the system was specified. A detailed drawing was made (see appendix).

Summary of the work presented in the methodology flowchart as figure (3.1)

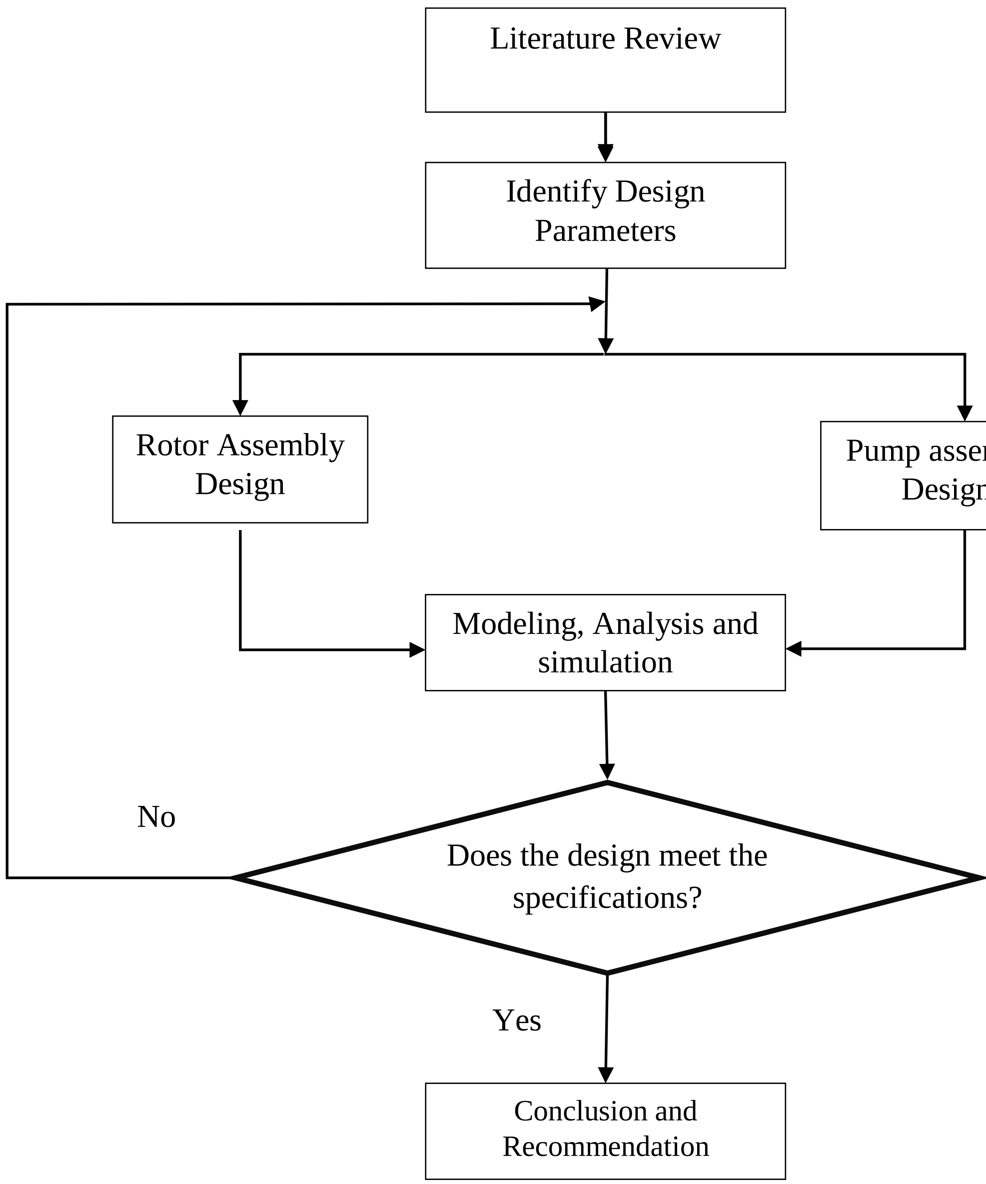

Figure 3.1: Work flow chart

Chapter Four

Design, Analysis and Results

CHAPTER FOUR

DESIGN, ANALYSIS AND RESULTS

4.1 Rotor radius calculations

In order to calculate the rotor radius we first need to calculate the desired power output from the rotor.

Starting with the hydraulic power required (P_h) by the pump in order to lift the water to the tank level, which can be calculated using:

$$P_h = \rho\ g\ Q\ H$$

ρ = the density of the water (1000Kg/m3).

g = the acceleration Due to gravity (9.81 m/s²).

Q = the flow rate of water

H = the total Head of to be lifted

The total amount of water required to fill the take was taken to be $15\ m^3$ per day. Accordingly the flow rate was found to be ($0.1736\ m^3/s$).

The elevation of the water to be lifted (H_s) was taken to be 15 m. considering the loss due to friction in the pipe(H_f) and stroke length (H_d) was taken to be (*0.1 m*), the total head can be calculated using the equation:

$$H = H_s + H_f + H_d$$

The loss due to friction can be found using the following chart at (Q = $0.1736*10^{-3}m^3/s$) and clear pipe diameter of *26 mm*, which was found to be (*0.24 m*)

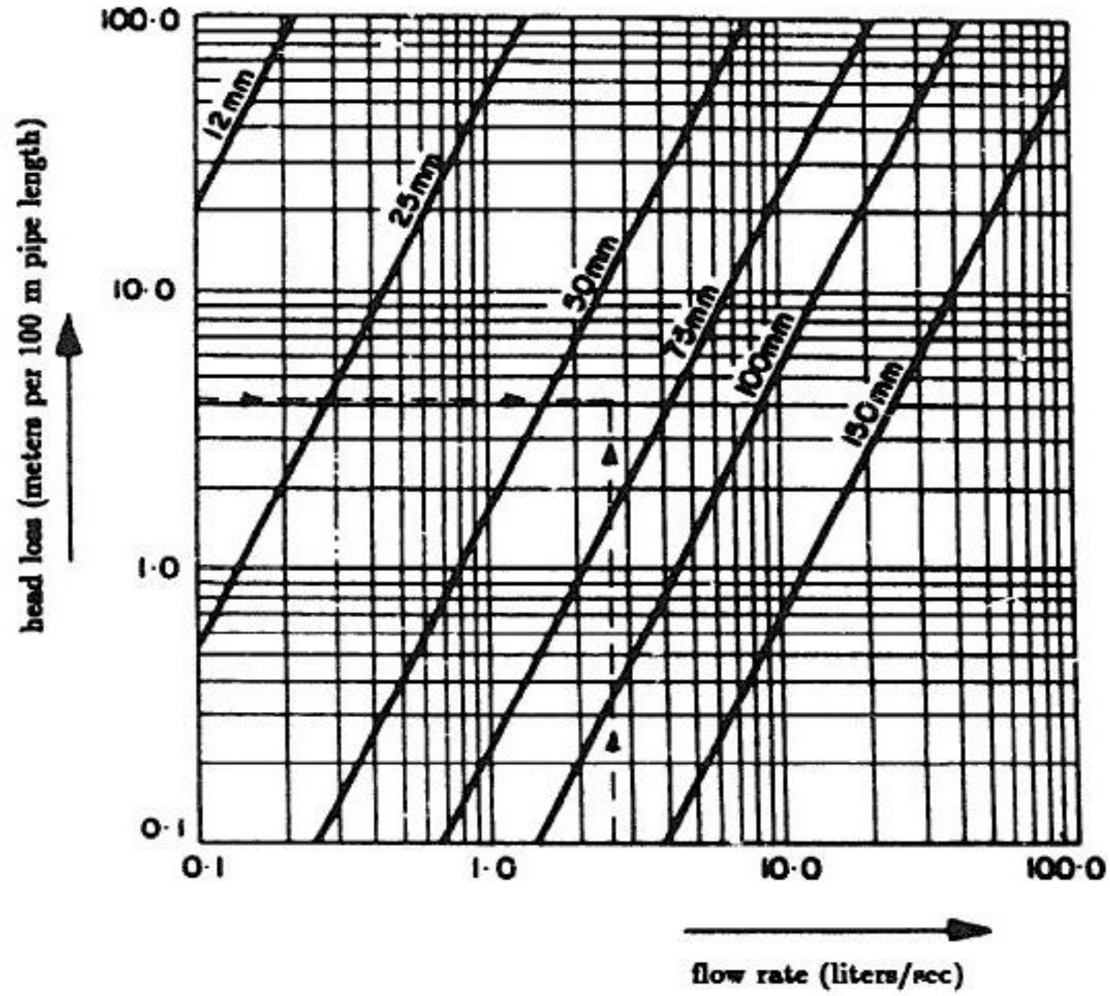

Figure 4.1: Total head loss in smooth pipes

The total head can be:

$$H = 15 + 0.24 + 0.1 = 15.34\ m$$

Then the power the power required to lift the water to the tank level is:

$$P_h = 1000 * 9.81 * 0.1736 * \ 10^{-3} * 15.34$$

$$P_h = 26.12\, Watt$$

In order to calculate the power required from the rotor various loss should be considered, table 3.1 shows the various losses *(WE Handbook)*

Table 4.1: Power Loss in Windmill

Factor	Efficiency
Rotor to shaft	92-97 %
Shaft to crank	93 – 96 %
Crank	99 %
Pump	60 – 75 %

$$efficiency = \frac{output}{input}$$

Hence before losses occur, the input power to the system is given by:

$$input = \frac{output}{efficiency}$$

1. Before pump loss

   Taking the average efficiency of 67.5%

   $$P = \frac{26.12}{0.675} = 38.7\, Watt$$

2. Before vertical shaft losses

   Taking the average efficiency of 94.5%

   $$P = \frac{38.7}{0.945} = 40.95\, Watt$$

3. Before crack shaft

   Taking the average efficiency of 99%

$$P = \frac{40.95}{0.99} = 41.36\, Watt$$

4. Before Horizontal shaft losses

Taking the average efficiency of 0.945%

$$P_{Mech} = \frac{41.36}{0.945} = 43.77\, Watt$$

However, according to the Betz limit, the efficiency in wind power extraction is a function Power Coefficient C_p, where C_p is the ratio of power Extracted by the Windmill to the total contained in the wind resource.

The maximum practical power coefficient for the American wind mill is 30%, the power in the wind can be calculate as:

$$P_{Wind} = \frac{43.77}{0.3} = 145.9\, Watt$$

P_{Wind} = 43.77/ 0.3 = 145.9 *Watt*

Since the power extracted is mainly depend on the wind speed (*3.5 m/s)* and the swept area of the rotor, using equation (2.4) the swept area that of the rotor (A) can be calculated as:

$$P_{Wind} = \frac{1}{2} * \rho * v^3 * A \tag{3.2}$$

The density of the air at 25^{o}C average and atmospheric pressure of 1 bar was found to be (*1.18 kg/m^3).*

$$A = \frac{145.9}{\frac{1}{2} * 1.18 * 3.5^3}$$

$$A = 20.19\, m^2$$

The radius of the rotor can be found using the following equation:

$$A = \pi R^2$$

Then the radius of the rotor was found to be:

$$R = \sqrt{\frac{20.19}{\pi}}$$

$$R = 1.352\ m$$

4.2 Blade Design Calculations

Rotor Solidity (σ) is a fairly graphic term for the proportion of a windmill rotor's swept area that is filled with solid blades. It is generally defined as the ratio of the sum of the width, or "chords" of all the blades to the circumference of the rotor.

The blade is designed such that it is narrower at the root (C_{root}) and wider at the tip (C_{tip}). The projected area of the blade is a trapezium.

The practical maximum solidity of an American wind mill fill in the range of 0.3 to 0.6, using 0.6 as solidity based on area ratio the area of the blade (A_b) can be found as:

$$\sigma = 0.6 = \frac{n * Ab}{As}$$

$$0.6 = \frac{12 * Ab}{\pi * 1.352^2}$$

$$Ab = 0.29\ m^2$$

Taking the solidity of the rotor as 0.6 on circumference basis the width of the plate at top (C_{tip}) can be found as:

$$\sigma = 0.6 = \frac{n * Ctip}{\pi * D}$$

$$0.6 = \frac{12 * Ctip}{\pi * 2.704}$$

$$Ctip = 0.425\ m$$

In order to find the width of the plate at root and since the area in trapezium, the area of the trapezium can be calculated using the following equation:

$$Ab = \frac{Ctip + Croot}{2} * R$$

Hence the width of the blade at the root calculated as:

$$0.29 = \frac{0.425 + Croot}{2} * 1$$

$$Croot = 0.153\ m$$

4.3 The rotor performance

The design speed of the rotor is defined as the wind speed for which the ratio of Hydraulic power output to the available wind power is maximum.

The ratio of the hydraulic power to the available wind power is known as the overall power coefficient.

The efficiency of the pump at constant head, depends strongly on the speed of operation, and reaches a sharp maximum at one speed only which is the design speed.

There is special problem of windmills driving a piston pumps. To start running a wind mill its need a high wind speed to over com the peak of the pump torque, this speed called the start speed *(V_{start})*. As the wind mill the rotor only fills the average torque demands, at decreasing wind the windmill keeps running below *(V_{start})* until its stop at certain wind speed called stop speed *(V_{stop})*.

The start speed is higher than the design speed and the stop speed is less than the design speed *(fig (4.2))*.

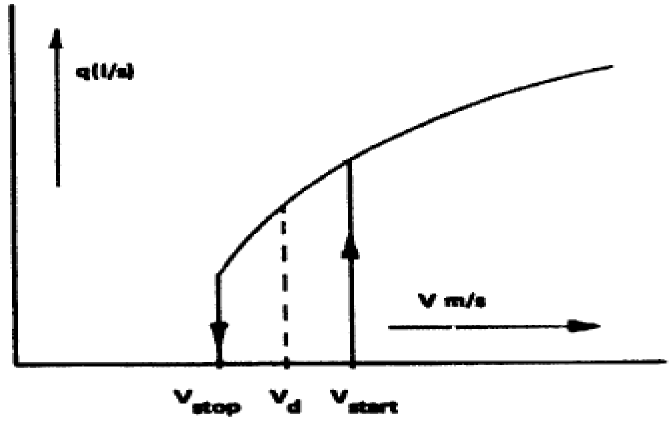

Figure 4.2: Vstart / Vstop Behavior

The design speed can be calculated as:

$$Vd = \sqrt{\frac{\eta_{vol} * V_s * \rho_w * g * H * \lambda_d * i}{\rho * \pi^2 * R^3 * (C_p\eta)_{max}}}$$

Where:

η_{vol} = *the volumetric efficiency, 0.8 to 1.0*

V_s = *stroke volume* (m^3).

ρ_w = *the water density* (kg/m^3)

g = *acceleration due to gravity* (m/s^2)

H = *pumping height (m).*

λ_d = *design tip speed ratio.*

i = *Transmission ratio = 1*

ρ = *air density* (kg/m^3).

R = *radius of the rotor (m).*

$C_p\eta$ = *overall power coefficient.*

The design tip speed can be chosen from table 4.2

Table 4.2: Choice of Design wind speed V_d, Energy production coefficient C_E, Output Availability:

	$V_d/\bar{V}$	C_E	Output availability
Windmills driving piston pumps			
- Classical deep well	0.6	0.40	60%
- Classical shallow well or deep well with balanced pump rod	0.7	0.55	60%
- Starting nozzle and balanced	1.0	0.90	50%
- Ideal (future)	1.3	1.20	50%
Wind machines driving rotating pumps	1.2	0.80	50%

The design tip speed ratio was found to be 0.6.

The overall power coefficient can be found from table 4.3.

Table 4.3: Peak Overall Power Coefficient $(C_p\ \eta)_{max}$:

Pumping head:	H < 3 m	H = 3 m	H = 10 m	H > 20 m
Windmills driving piston pumps				
- Classical	0 to 0.15	0.15	0.20	0.30
- Starting nozzle	0 to 0.13	0.13	0.18	0.27
Wind machines driving rotating pumps				
- Mechanical transmission		0.15 to 0.25		
- Electric transmission		0.05 to 0.10		

$$Vd = \sqrt{\frac{0.8 * 4.956 * 10^{-4} * 9.81 * 1000 * 15 * 0.6}{1.18 * \pi^2 * 1.36\hat{}3 * 0.3}}$$

$$Vd = 1.8\ m/s$$

The start speed and the stop speed can be found using the diagram (4.2):

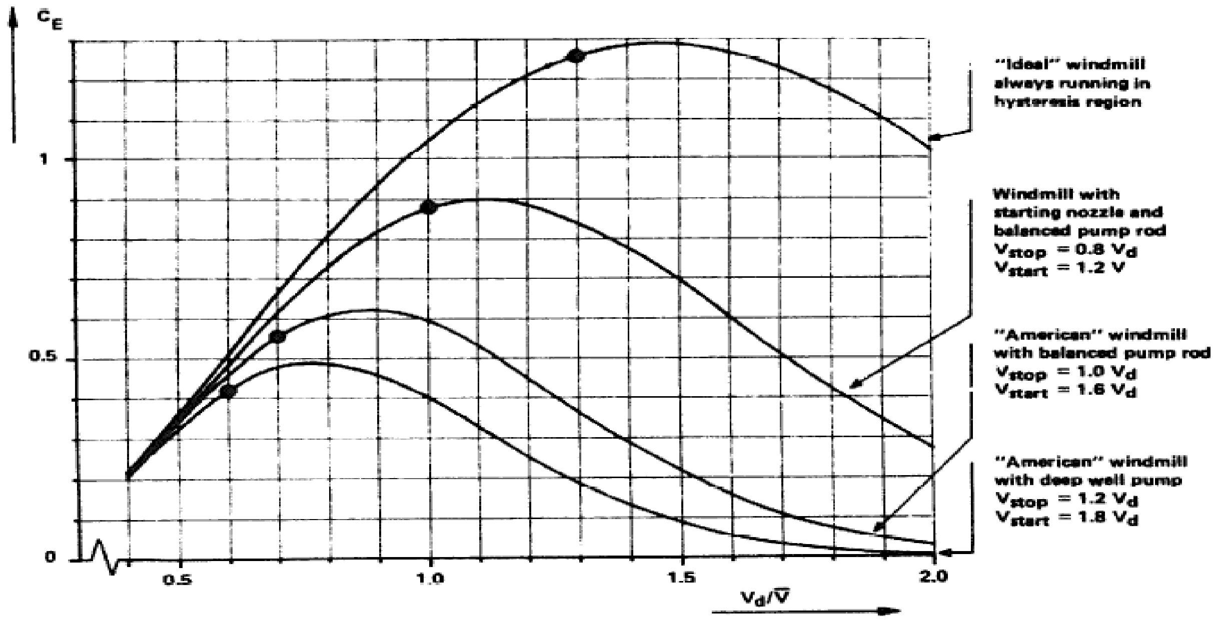

Figure 4.3: change of tip speed design with energy coefficient

$$Vstart = 1.8\, Vd$$

$$Vstart = 1.8 * 1.8 = 3.24\ m/s$$

$$Vstop = 1.2\, Vd$$

$$Vstop = 1.2 * 1.8 = 2.16\, m/s$$

4.4 Pump design

The optimal tip speed ratio (λ_{opt}) can be found using the equation:

$$\lambda_{opt} \approx \frac{\omega_{opt} * R}{V} \approx \frac{2\pi}{n}\left(\frac{R}{s}\right)$$

Where:

ω_{opt} = the optimal rotation speed (rad/s)

R = the radius of the rotor (m).

S = the displacement of the blade tip (m)

n = Number of blades.

The optimal tip speed ratio for an n bladed machine it has been empirically observed that *(s)* is equal to about half the rotor radius or:

$$\frac{s}{R} \approx \frac{1}{2}$$

Then the optical tip speed ration depend on the number of blades *(n)* as shown below:

$$\lambda_{opt} = \frac{4\pi}{n}$$

The optimal tip speed ratio can be calculated as follows:

$$\lambda_{opt} = \frac{4\pi}{12} = 1.05$$

Since the tip speed ratio is the ratio of the rotor speed to the wind speed then the tip speed ratio can be calculated using the equation.

$$\lambda = \frac{\omega\ R}{V}$$

$$1.05 = \frac{\omega\ 1.36}{3.5}$$

$$\omega = 2.7\ rad/s$$

The frequency of rotation of can be found using the equation:

$$f = \frac{\omega}{2\pi} = \frac{2.7}{2\pi} = 0.43\ rev/s$$

The pipe flow will be or volume per stroke:

$$Q\ pipeflow = \frac{Q}{f}$$

$$Q\ pipeflow = \frac{0.1736 * \ 10^{-3}}{0.43} = 0.404 * 10^{-3}\ m^3/rev$$

The pipe flow represent the volume per stroke then the radius of the pump can be found a

$$r\ pump = \sqrt{\frac{Q\ pipeflow}{\pi *\ hpump}}$$

$$r_{\ pump} = \sqrt{\frac{0.404 * 10^{-3}}{\pi *\ 0.10}} = 0.036\ m\ or\ 3.6\ cm$$

The maximum torque *(T)* can be calculated using the following equation:

$$T = \frac{P_{Mech}}{\omega}$$

$$T = \frac{43.77}{2.7} = 16.21\ Nm$$

4.5 Crank shaft

The loads applied to the crank shaft are as in figure (3.4) where all the distances are in mm:

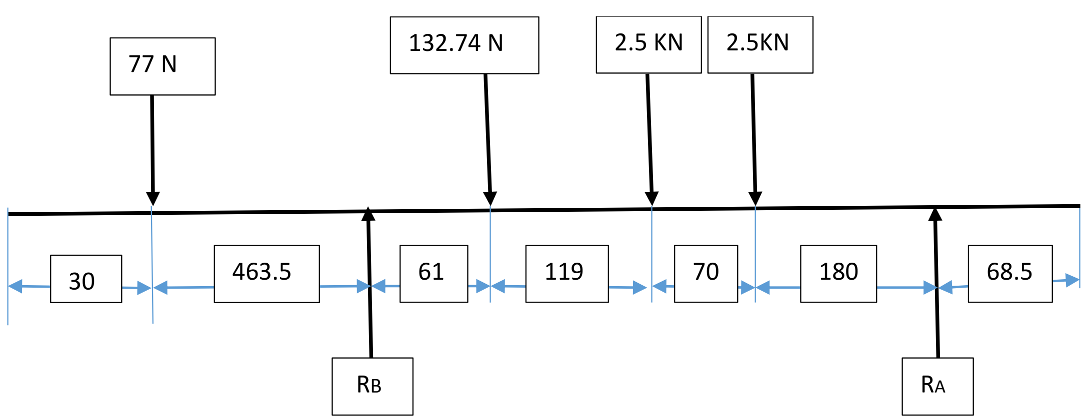

Figure 4.4: the loads on the crank shaft

Taking the moments around A:

$$\sum M_A = 0$$

$$R_B = 2765.2\ N$$

$$R_A + R_B = 5209.74\ N$$

$$R_A = 2444.5\ N$$

The diameter of the shaft can be calculated as follows:

$$T_e = \frac{\pi}{16} * \tau * d^3$$

Where:

T_e = the equivalent twisting moment Nm.

τ = the allowable shear stress N/m^2.

d = the diameter of the shaft mm

$$\tau = 0.186 * \sigma_u$$

$$\tau = 0.186 * 356.9 * 10^6 = 64.24\ MPa$$

$$T = \frac{power}{\omega} = \frac{510.73}{2.7} = 189.16\ Nm$$

$M = 440\ N.m$ (max $bendin\ g\ moment$)

$$T_e = \sqrt{M^2 + T^2} = 479\ Nm$$

$$d = 33.61\ mm \qquad say\ 35\ mm$$

Or it can be calculated using the equivalent bending moment (M_e) as follows:

$$M_e = \frac{\pi}{32} * \sigma * d^3$$

$$M_e = \frac{1}{2}(M + T_e) = 459.45\ Nm$$

$$\sigma = 0.36 * \sigma_u$$

$$\sigma = 0.36 * 356.9 = 128.48\ MPa$$

$$d = 33.15\ mm \qquad say\ 35\ mm$$

4.6 Pump rod

A reliable wind pump will have a pump rod capable to cope with the occurring forces under design conditions. For a given head and pump size, these forces vary in congruence with the rotational speed of the pump and the rotor. The total fatigue load on the pump rod depends on the distribution frequency of the pump rod loads.

At rated wind speed, the wind rotor turns at a tip speed ratio close to the maximum tip speed ratio max. The effective maximum pump speed follows the equation:

$$\omega_{max} \approx 3\ \lambda_d \frac{V_{rated}}{R}$$

$$\omega_{max} \approx 3 * 1.5 * \frac{15}{1.352}$$

$$\omega_{max} = 23.3\ Rad/s$$

Due to the cyclical variations, the pump rod force is a fatigue load. The only load considered is the static and dynamic load in order to determine the maximum load applied to the pump rod.

The static force F_{st}, w due to the water column is equal to the weight can be found as follows:

$$F_{st,\ w} = \rho_w\ g\ H\ A_p$$

$$F_{st,\ w} = 1000 * 9.81 * 15.34 * 0.004407$$

$$F_{st,\ w} = 612.5\ N$$

The dynamic forces represented in the acceleration and deceleration phases of the pump, by summing all the forces the forces the maximum load on the pump rod F_{Pr} can be calculated as follows:

$$F_{Pr} = K\ F_{St,\ w}[1 + \frac{1}{2}\ s\ \omega^2/g\left(\frac{A_p}{A_{rm}}\right)]$$

Where:

K = over shot factor usually taken as 2

A_p/A_{rm} = the ratio of the piston area to the rising main area usually taken as 0.84.

- F_{Pr} (on design ω)

$$F_{Pr} = 2 * 612.5[1 + \frac{1}{2}\ 0.1\ \ 2.7^2/9.81\,(0.84)]$$

$$F_{Pr} = 1263\ N$$

- F_{Pr} (on rated ω)

$$F_{Pr} = 2 * 612.5[1 + \frac{1}{2}\ 0.1\ \ 23.3^2/9.81\,(0.84)]$$

$$F_{Pr} = 4072.2\ N$$

4.7 Welding:

Welding is a fabrication or sculpture process that joints materials usually metals or thermoplastics by causing fusion.

The thickness of materials to be jointed and the type of material to be jointed should be considered in order to perform a reliable weld joint.

In this design weld joint is used on the base and the crank arms which they are made of alloy steel with a thickness of 30mm.

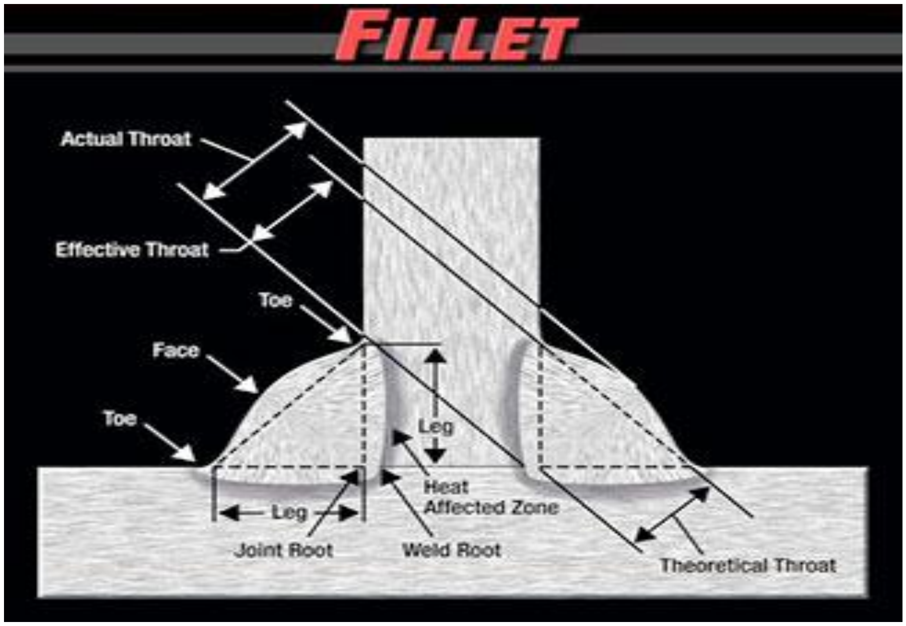

Figure 4.5: weld fillet

By knowing the thickness of the sections we can determine the minimum weld size from the table (4.4)

Table 4.4: Minimum Weld Size

Base Metal Thickness (T)[1]		Minimum Size of Fillet Weld[2]	
in.	mm	in.	mm
T ≤ 1/4	T ≤ 6	1/8 (Note 3)	3 (Note 3)
1/4 < T ≤ 1/2	6 < T ≤ 12	3/16	5
1/2 < T ≤ 3/4	12 < T ≤ 20	1/4	6
3/4 < T	20 < T	5/16	8

From the table and according to the thinness the weld size (leg) of 8mm.

The weld throat then can be calculated as follows:

$$weld\ throat = (0.707 * a) + 0.11$$

Where:

a = the weld size (leg).

So the throat equals:

$$weld\ throat = (0.707 * 8) + 0.11$$

$$weld\ throat = 5.766$$

After the determination of the weld joint dimensions it's time to determine the electrode type and for alloy steel the suitable electrode is: E7018 G.

This electrode is especially designed for alloy steel.

The (70) in the electrode code indicate that how strong this electrode when welded measured in thousands of pounds per square inch.

To determine the allowable stress on our weld joint we can use the next relation:

$$\delta_{allowable} = 0.3 * nominal\ tensile\ strength\ of\ the\ filler\ material$$

$$\delta_{allowable} = 0.3 * 7000 = 21000\ psi$$

So welding type selected to admit the following properties:

Parts to be jointed: base and shaft arms.

- Type of joint: T filet joint.
- Type of material: Alloy steel.
- Sections thickness: 30mm
- Weld size (leg): 8mm
- Weld throat: 6mm
- Electrode type: E7018G
- Allowable stress on joint: 2100 psi.

4.8 Fitting

We used the force fitting in our design to join the shaft and the hub and also to join the shaft arms.

When it comes to using force fitting for joining two parts it is important to determine the degree of Interference between the parts for our design we toke the ISO H7/p6 as our fit relation because it gives a really strong rigidity between the parts while in the same time it doesn't need great pressing force that may be an issue in the assembly stage (see appendix A2).

4.9 Bolts and nuts

The bolts were used to join the support arm to the hub. The following equation determines which size of the bolt to be used:

$$A_s = {P_t}/{\sigma_t}$$

(3.24)

Where:

A_s = bolt effective cross-section area mm^2

σ_t = bolt maximum allowable stress N/mm^2

The tensile load on the bolts is 600 N resulting from the force generated on the blade to rotate the rotor.

$$\sigma_t = {\sigma_b}/{safty\ factor}$$

(3.25)

From the table for yield strength class 12.9, σ_b = 112 n/mm^2 and the safety factor for repeated load for steel = 5, so:

$$\sigma_t = {112}/{5} = 22.4\ N/mm^2$$

The cross-section area of the bolt will be:

$$A_s = {600}/{22.4} = 26.7\ mm^2$$

Which is in the range of M8 bolt class (see appendix A4)

4.10 Bearing

These are machine components designed to provide support for rotating machine elements by taking pure radial loads, pure thrust loads or a combination of the two.

In this design there four types of bear selected according to the applied load,(appendix A5 and A6 identify the selection criteria of the bearing selected).

4.10.1 Types of the bearing:

There are various types of bearing which they fail in two main categories as follows:

4.10.1.1Ball bearing.

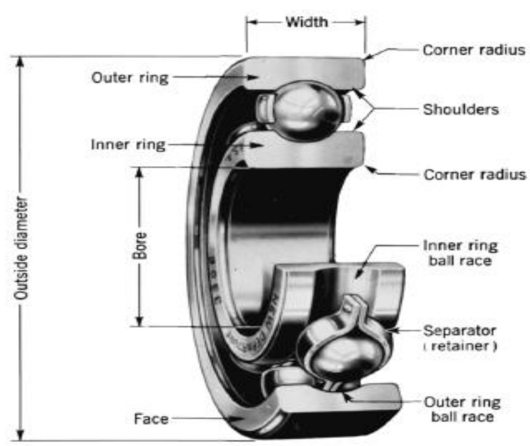

Figure 4.6: Ball bearing

These are made of an inner race and outer race with incorporated hardened steel balls which geometrically have contact with the two races at a point.

4.10.1.2 Roller bearing

These have two tracks of races but the balls in ball bearings are replaced by various types of hardened steel cylindrical rollers which may be straight, barrel-shaped or truncated cones. The line of contact deforms into areas larger than ball bearings hence are capable of carrying higher radial loads.

Figure 4.7: Roller bearing

The bearings were used in the following components

- The middle of the crank shaft (horizontal) has two roller bearing one for each arm linking the bully. The roller bearings were used due to their ability to support both radial and axial loads and an increased contact surface area (NU1008).
- Two tapered roller bearing were used to support the crank shaft to the rotor base stands. The tapered roller bear were chosen due to their ability to support radial, axial and thrust loads (32908XU).
- Two unit ball bear were used to support the tail rod at the right base stand due to their ability to support light radial loads (ASPB204).
- One thrust roller bearing were used to the turn table base according to their ability to support radial and thrust load and prevent slippery (29412).

Appendix (A7), (A8) and (A9) shows the specification of each bearing:

4.10.2 Bearing life time:

Even in bearings operating under normal conditions, the surfaces of the raceway and rolling elements are constantly being subjected to repeated compressive stresses which causes flaking of these surfaces to occur.

The relationship between the basic rating life, the basic dynamic load rating and the bearing load is given in formulas.

For Ball bearing:

$$L_{10} = \left(\frac{C}{P}\right)^{3}$$

For roller bearing:

$$L_{10} = \left(\frac{C}{P}\right)^{\frac{10}{3}}$$

Where:

L_{10} =the basic rating life 10^6 revolution.

C = Basic Dynamic load rating (N).
(C_r: Radial bearing; C_a: Thrust bearing)

P = equivalent dynamic load (N).
(P_r: Radial bearing; P_a: Thrust bearing)

For the tapper roller bearing:

The basic dynamic load for tapper roller bearing were found to be:

C = 32.5 *KN*

The equivalent dynamic load can be calculated as follows:

$$P_r = xF_r + yF_a$$

$$if\ {}^{F_r}/_{F_a} \le e \gg x = 1\ , y = 0\ and\ e = 0.29\ (see\ appendix\ A11) \tag{3.28}$$

$$\left(\frac{600}{2444.5}\right) = 0.245\ \le e$$

For the bearing at the right side:

$$P_r = 1 * 2444.5 = 2652.62$$

The basic dynamic load were found to be C = 32.5 *KN*

Then the rated life is:

$$L_{10} = \left(\frac{32500}{2444.5}\right)^{\frac{10}{3}} = 5567.3 * 10^6\ revolution$$

For the bearing at the left side:

$$\left(\frac{600}{2765.2}\right) = 0.217\ \le e$$

$$P_r = 1 * 2765.2 = 2557.08$$

Then the rated life is:

$$L_{10} = \left(\frac{32500}{2765.2}\right)^{\frac{10}{3}} = 3691.38 * 10^6\ revolution$$

For the cylinder roller bearing:

The basic dynamic load for cylindrical roller bearing were found to be:

C = 27.3 *KN*

The equivalent dynamic load can be calculated as follows:

$$P_r = xF_r + yF_a$$

$$P_r = 1 * 2500 = 2500\ N$$

Then the rated life time:

$$L_{10} = \left(\frac{27300}{2500}\right)^{\frac{10}{3}} = 2888.96 * 10^6\ revolution$$

For the spherical thrust bearing:

P = 5809 N

$$L_{10} = \left(\frac{283000}{5809}\right)^{\frac{10}{3}} = 422295.9 * 10^{6}\ revolution$$

4.11 ANALYSIS AND RESULTS

4.11.1 Solid works analysis steps

After the definition of the power required, the components and its configuration of the wind pump system has been made using solid works. The analysis of the forces and stresses on the component with their resultant strain and displacement has been carried out in steps as follows:

- For the individual components:
  1. The static structure study has been made in which the type of the study, the units, type of result and component results and number of plots with the definition of each plot (eg. Stress type: nodel stresses) has been identified.

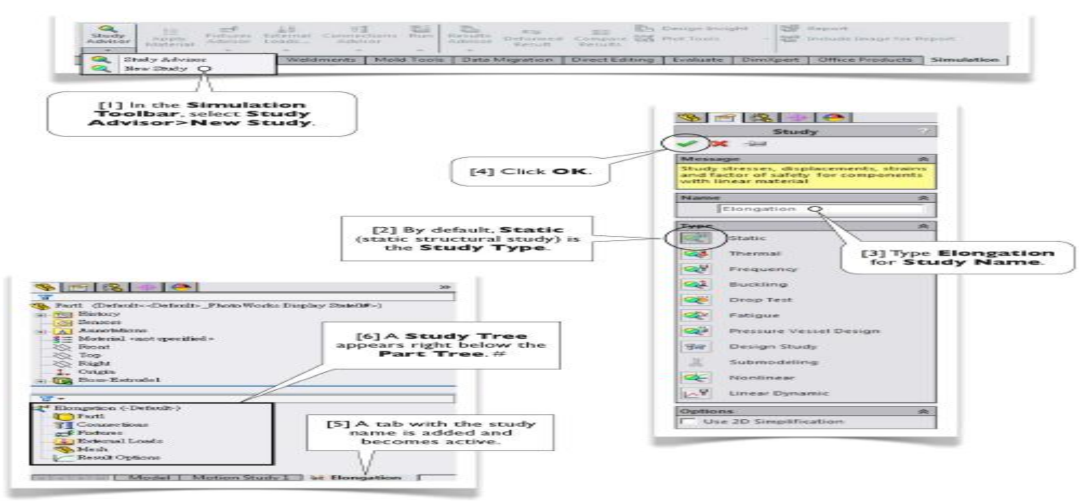

Figure 4.8: Initiating the static structure study

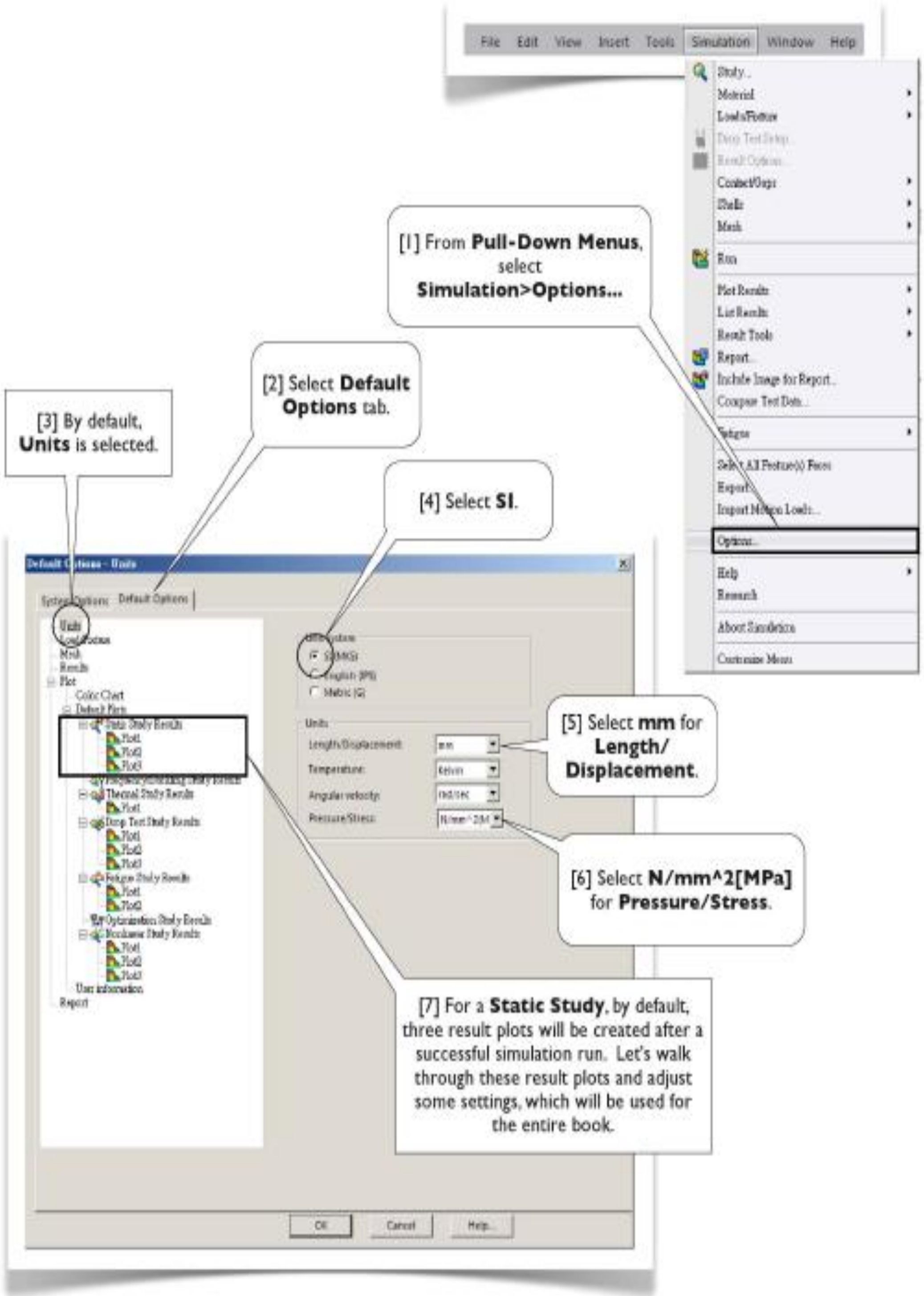

Figure 4.9: identifying units and number of plots

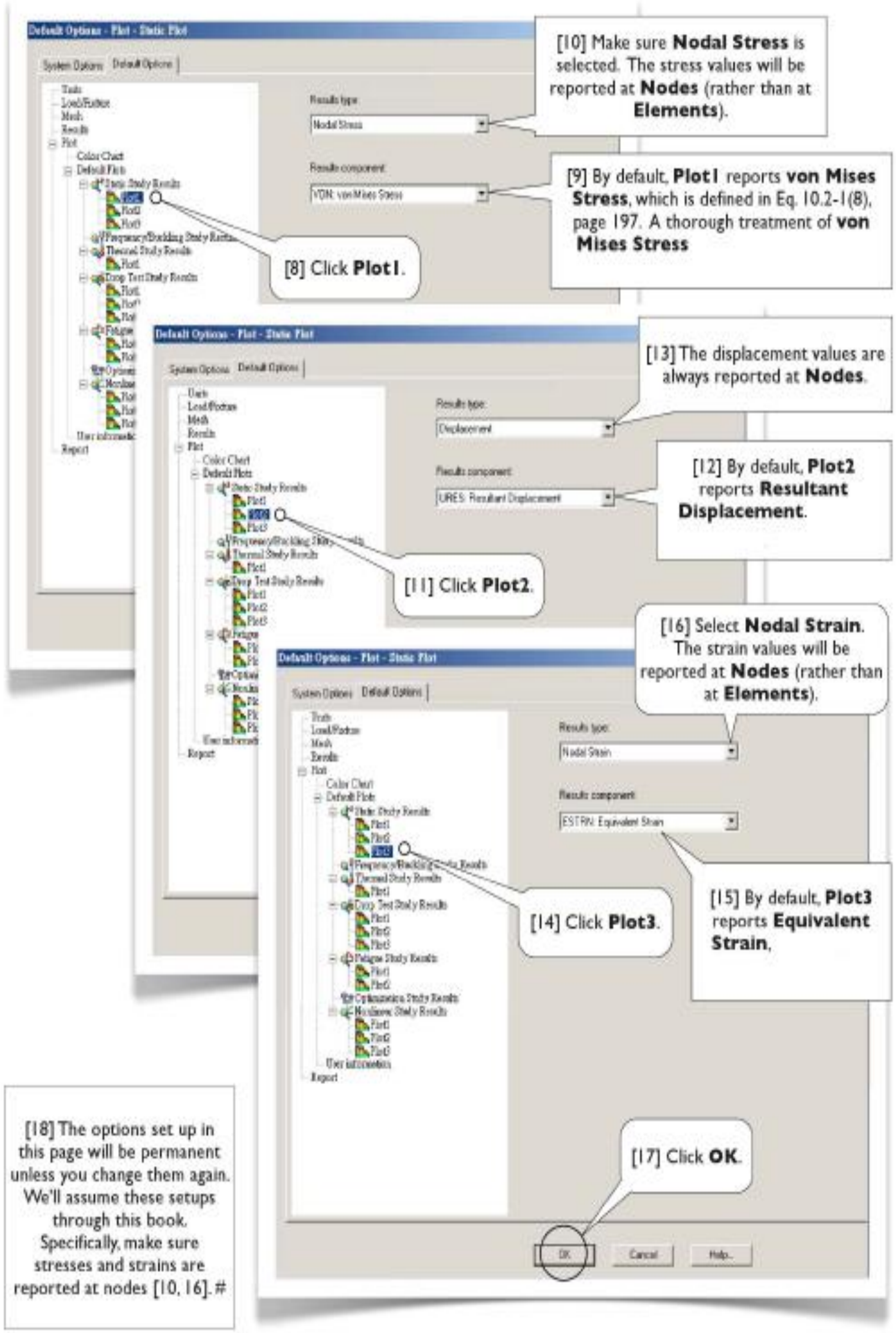

Figure (4.10): Finalizing static structure study

2. Apply the material, supports and loads.
3. Solve the model (create mesh and run simulation).
4. Show results (stress, strain and displacement).

- For the parts or assembly the concerned with fluid flow (rotor assembly and tail assembly):

1. Flow simulation has been created
2. Run wizard option in which the units, system analysis type (external), fluid (air) and the parameters which include:
   a. Pressure of 1*atm.*
   b. Temperature of 35^{o}C.
   c. Air direction (z direction)
   d. Air velocity of 18 *m/s*.

   And results resolution has been identified.

3. Wind load has been identified in which:
   a. The computational domain (the region where the condition will be applicable).
   b. Goals (velocity, dynamic pressure forces and shear stress).
   c. The run of the simulation has been made.
   d. The results are shown.
4. Static structural study has been created and the material and support were applied. For the applicable loads the flow effect from step (3) is imported to complete analysis as in the process made for the individual parts.

4.11.2 Rotor

4.11.2.1 Wind on the rotor:

The wind velocity decreases due to loss part of its kinetic energy that has been captured by the rotor as shown in figure (4.11)

Name	Type	Min	Max
Rotor	**velocity**	0.00 m/s	24.661 m/s

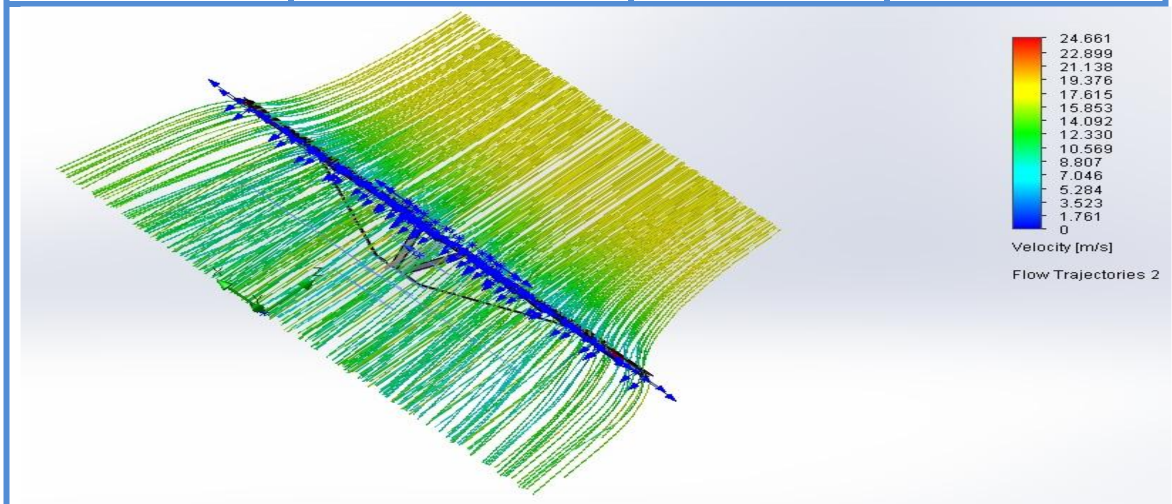

Figure 4.11: Wind velosity

4.11.2.2 Rotor Material Properties

Table 4.5: Rotor Material Properties

Name:	**7075-T6, Plate (SS)**
Model type:	**Linear Elastic Isotropic**
Default failure criterion:	**Max von Mises Stress**
Yield strength:	**5.05e+008 N/m^2**
Tensile strength:	**5.7e+008 N/m^2**
Elastic modulus:	**7.2e+010 N/m^2**
Poisson's ratio:	**0.33**
Mass density:	**2810 kg/m^3**
Shear modulus:	**2.69e+010 N/m^2**
Thermal expansion coefficient:	**2.4e-005 /Kelvin**

4.11.2.3 Loads and Fixtures

Table 4.6: loads at the rotor

Fixture name	Fixture Image	Fixture Details	
Fixed	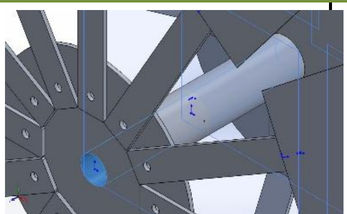	**Entities:** **Type:**	**1 face(s)** **Fixed Geometry**

Resultant Forces

Components	**X**	**Y**	**Z**	**Resultant**
Reaction force(N)	**0.386719**	**-0.742469**	**596.778**	**596.779**

4.11.2.4 The Rotor Stresses

The stress at certain position in a solid material as the force per unit surface area on an infinitesimally small body placed at that position.

$$\sigma = \frac{F}{A}$$

The maximum stress apply at the fixing points at the supporting rim and the supporting back arm as shown in the figure (4.12).

Name	Type	Min	Max
Stress	VON: von Mises-Stress (effective stress)	14.8802 N/m^2 Node: 22894	1.13511e+007 N/m^2 Node: 21735

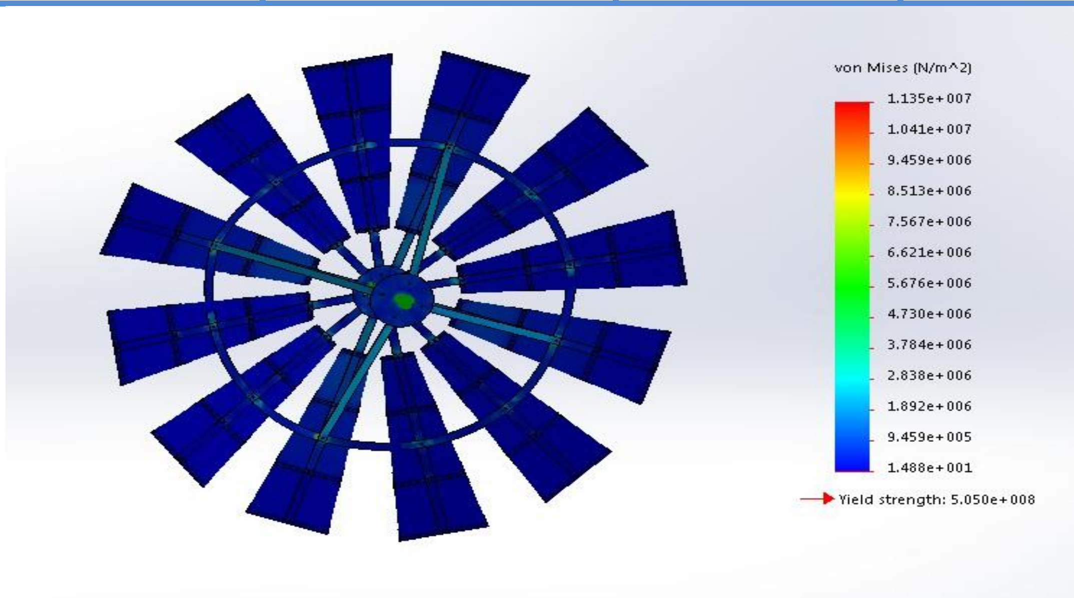

Figure 4.12: The Stresses on the rotor

4.11.2.5 Strain on the Rotor

The strain can be defined based in the concept of the deformation which is defined as the variation of any two points inside the solid body. Hence the strain is the quantities to describe the displacement of point relative to another point inside the solid body.

$$\sigma = E * \varepsilon$$

Figure (4.13) below describe the strain which occur due to the applied forces acting on the rotor, as shown in the figure shows that the maximum stress occurs at the points at the supporting rim corresponds to points where there is no supports – back arm.

Name	Type	Min	Max
Strain	ESTRN: Equivalent Strain	2.10383e-010 Element: 65836	0.000426824 Element: 63600

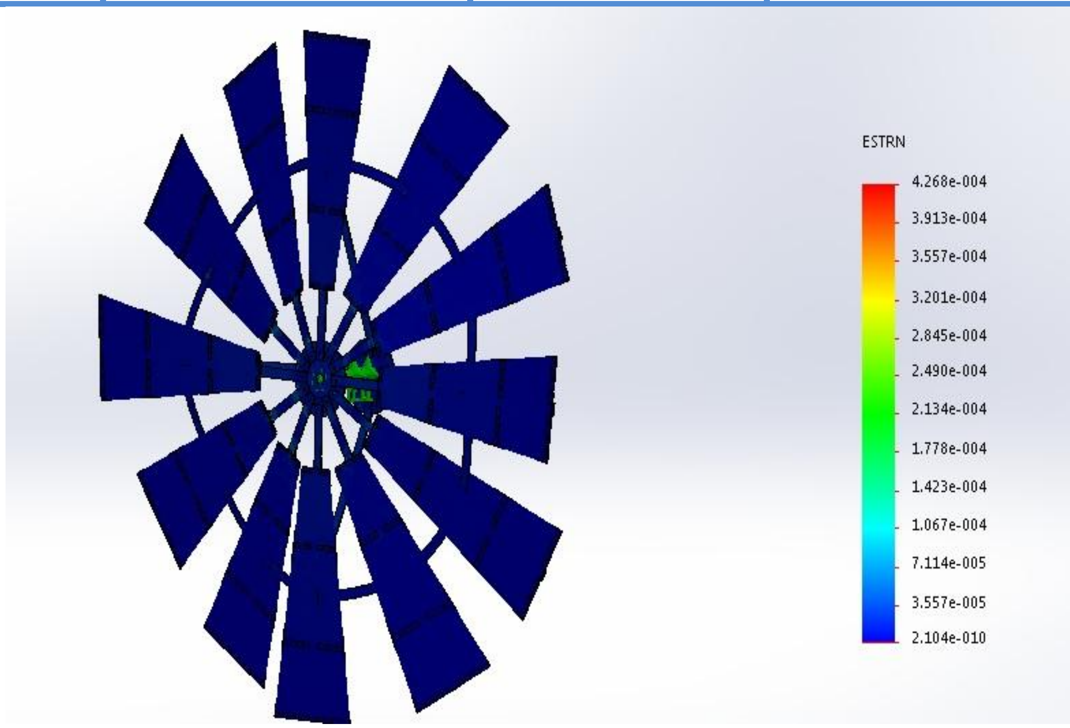

Figure 4.13: The strain on the rotor

4.11.2.6 Displacement analysis results:

The displacement can be defined in term the rigid body motion which is defined as the displacement of a body which do not change the distance between the points inside the body. Hence the displacement is the quantities to describe the displacement of point relative to another point which does not change the distance between points inside the solid body.

Figure (4.14) shows the displacement results due to the forces acting on the blades, the far the point of force application the greater the displacement. The blades with the least displacement values (blue region) represents the ones with support of the back arm.

Name	Type	Min	Max
Displacement	URES: Resultant Displacement	0 mm Node: 22460	1.18808 mm Node: 12911

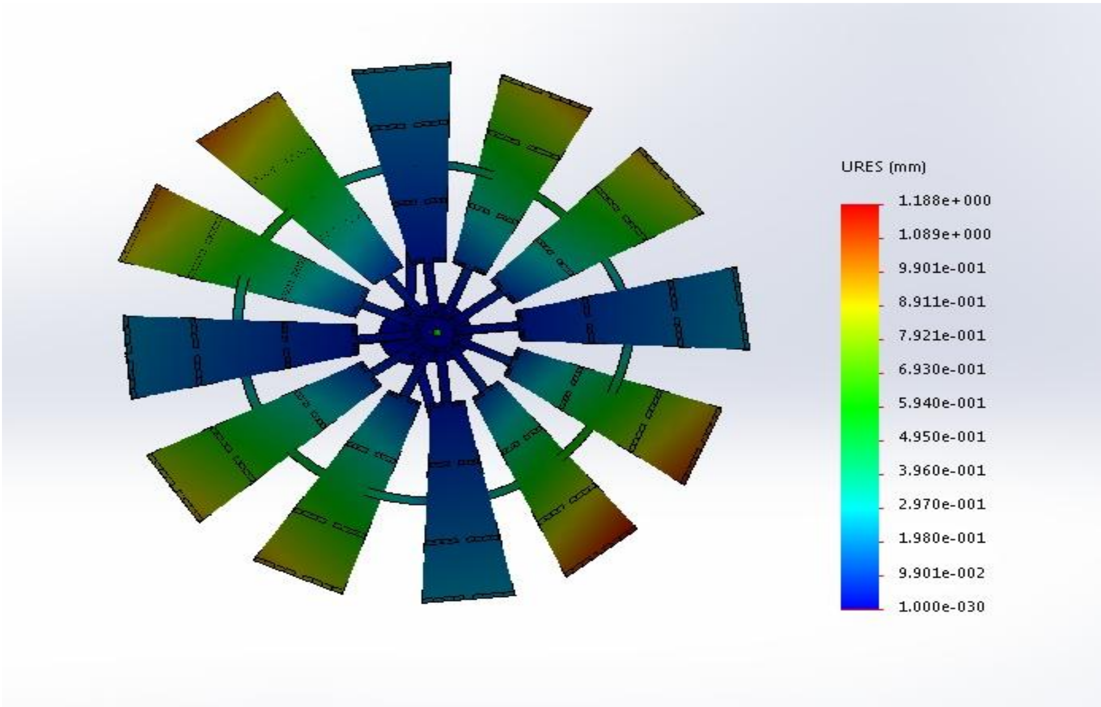

Figure 4.14: The rotor Displacement

4.11.3 Crank Shaft

Material properties 4.11.3.1

Table 4.7: Crank Shaft Material Properties

Name:	**Galvanized Steel**
Model type:	**Linear Elastic Isotropic**
Default failure criterion:	**Max von Mises Stress**
Yield strength:	**2.03943e+008 N/m^2**
Tensile strength:	**3.56901e+008 N/m^2**
Elastic modulus:	**2e+011 N/m^2**
Poisson's ratio:	**0.29**
Mass density:	**7870 kg/m^3**

4.11.3.2 Crank shaft loads

Table (4.8): The Applied Loads and Location of Application in the Crank Shaft.

Load name	Load Image	Load Details
Force-7	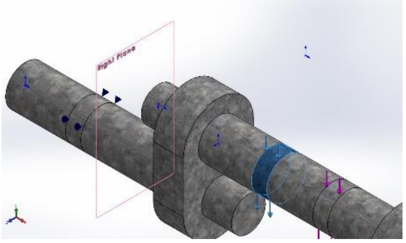	**Entities:** 1 face(s), 1 plane(s) **Reference:** Right Plane **Type:** Apply force **Values:** ---, -2500, --- N
Force-8	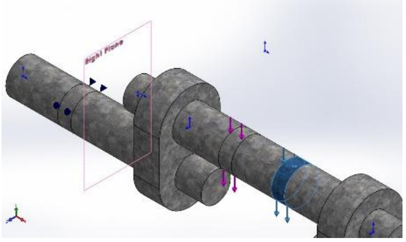	**Entities:** 1 face(s), 1 plane(s) **Reference:** Right Plane **Type:** Apply force **Values:** ---, -2500, --- N
Force-9	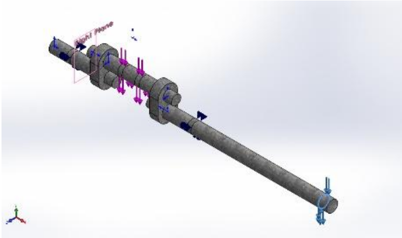	**Entities:** 1 edge(s), 1 plane(s) **Reference:** Right Plane **Type:** Apply force **Values:** ---, -77, --- N

4.11.3.3 The crank Shaft stresses

Figure (4.15) shows the location where stress due the applied forces, the green regions on the shaft middle rod represents the stress due the forces applied because of the shaft- bully arm which in turn transfer the load of weight of the water, pump, and pump rod to the shaft.

The red regions at the connection faces between the shaft arm and the shaft rods represents the stress at the shaft arm cause its act as a support to the shaft middle rod, and as shown in the figure it holds the maximum amount of the stress, which is occur when the middle rod at position of 270 and 90 degree.

Name	Type	Min	Max
Stress	VON: von Mises-Stress (effective stress)	24969.7 N/m^2 Node: 3857	4.76222e+007 N/m^2 Node: 4808

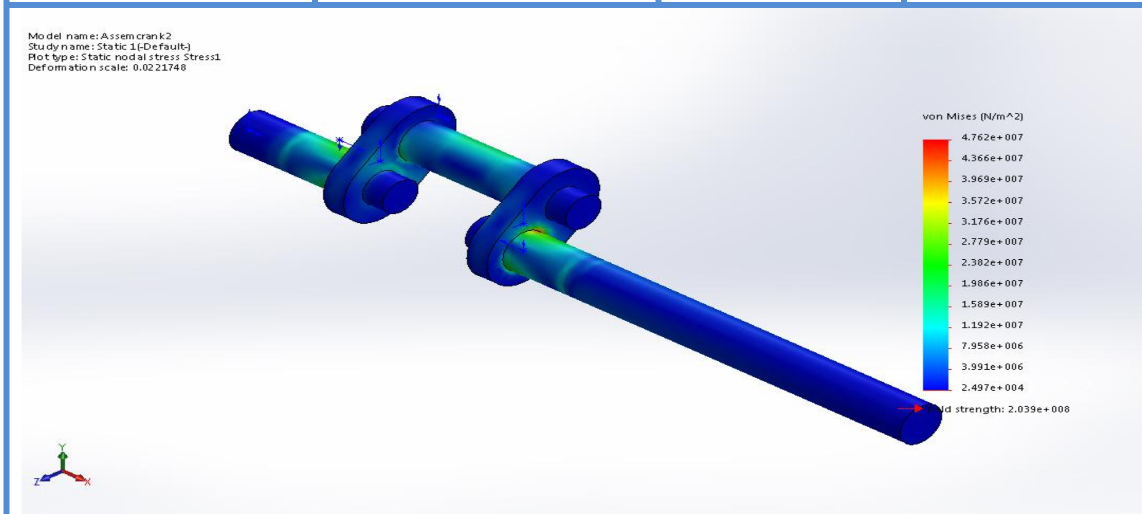

Figure 4.15: The Stresses on the crank shaft

4.11.3.4 The strain on the Crank Shaft

The amount of strain is related to a corresponding amount of load applied, hence the red region represents the highest strain in the rod. Figure (4.16) shows the stresses at the crank shaft.

Name	Type	Min	Max
Strain	ESTRN: Equivalent Strain	1.07917e-007 Element: 1149	0.000209618 Element: 2670

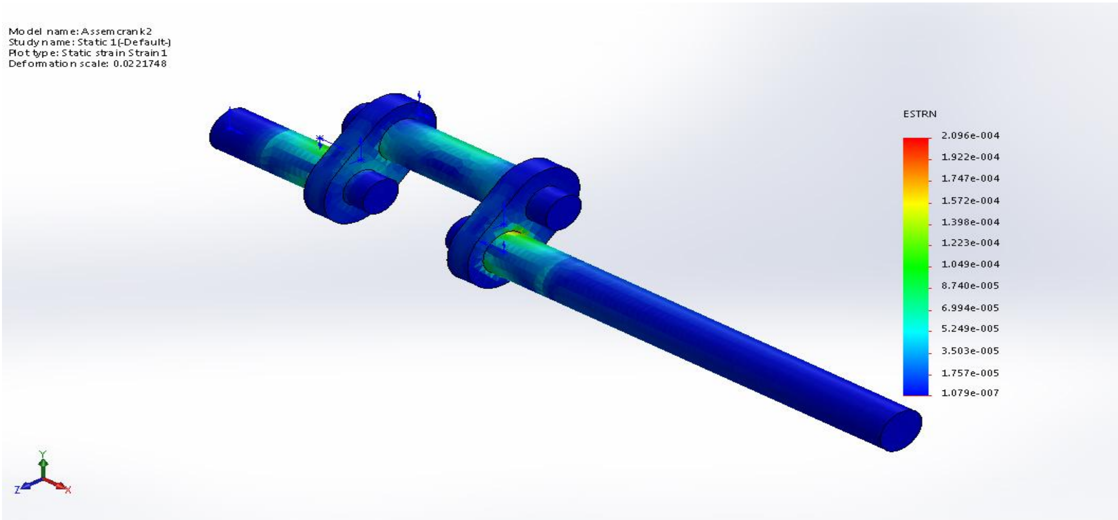

Figure 4.16: The Strain on the crank shaft

4.11.3.5 The Crank Shaft Displacement

Figure (4.17) shows the resultant displacement.

Name	Type	Min	Max
Displacement	URES: Resultant Displacement	0.281621 mm Node: 3234	4473.55 mm Node: 29220

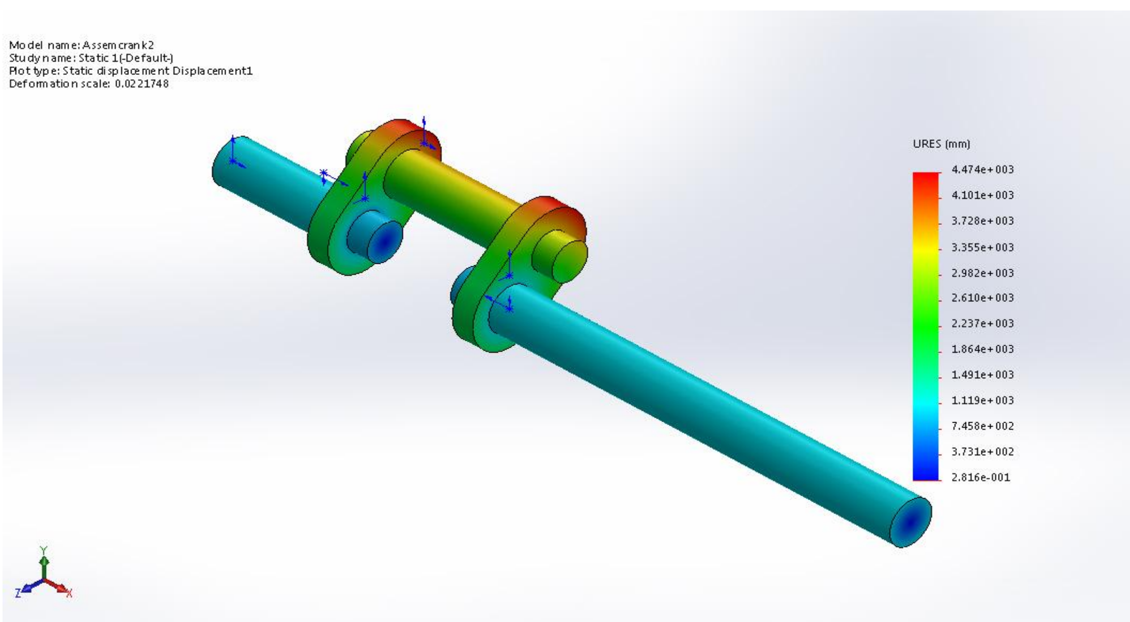

Figure 4.17: The Crank Shaft Displacement

4.11.4 The Tail:

4.11.4.1 The Wind on the tail:

Name	Type	Min	Max
Tail	Flow velocity	0.000 m/s	23.180 m/s

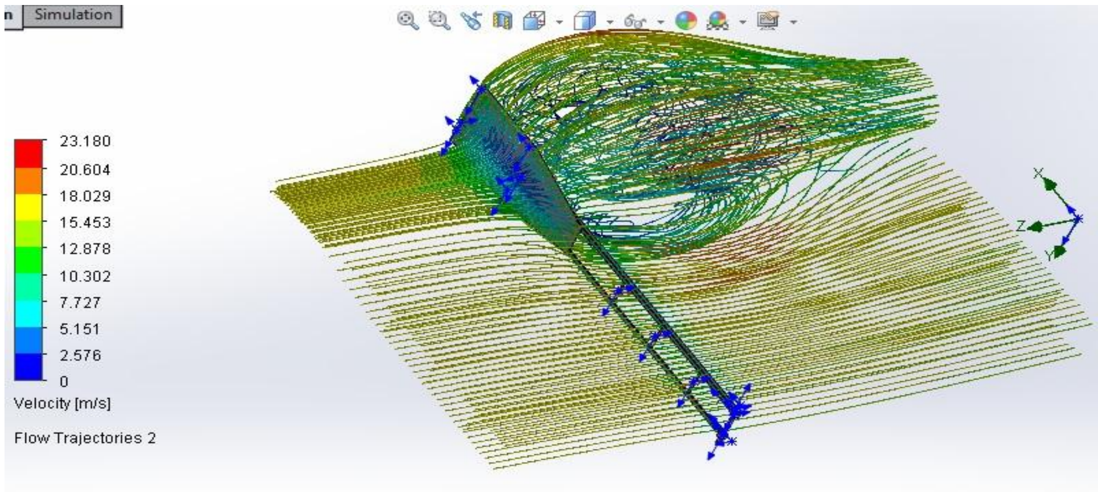

Figure 4.18: Wind speed at the Tail

4.11.4.2 The Tail Assembly Material Properties

Table 4.9: The Tail Assembly Material Properties:

Name:	**Alloy Steel**
Model type:	**Linear Elastic Isotropic**
Default failure criterion:	**Max von Mises Stress**
Yield strength:	**6.20422e+008 N/m^2**
Tensile strength:	**7.23826e+008 N/m^2**
Elastic modulus:	**2.1e+011 N/m^2**
Poisson's ratio:	**0.28**
Mass density:	**7700 kg/m^3**
Shear modulus:	**7.9e+010 N/m^2**
Thermal expansion coefficient:	**1.3e-005 /Kelvin**

4.11.4.3 The Tail assembly Load results

The loads represented in the following figure is load applied by the air when the tail held fixed acting as a break.

Table (4.10): The Loads at the Tail Assembly:

Fixture name	Fixture Image	Fixture Details
Fixed-3	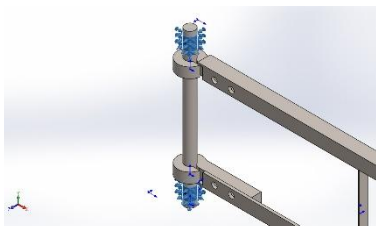	**Entities:** 2 face(s) **Type:** Fixed Geometry

Resultant Forces

Components	X	Y	Z	Resultant
Reaction force(N)	**0.268494**	**129.655**	**119.66**	**176.434**

4.11.4.4 The Stress on the Tail assembly

Since the tail assembly is connected with the base through a sleeve bearing then there are no effective stress due to the force generated by the wind, in case of the tail is fixed – acting as a break at high wind speed – the amount of the stress generated is not sufficient to yield the material of the tail as represented by the blue region, as shown in figure (4.19).

Name	Type	Min	Max
Stress	VON: von Mises Stress (effective stress)	997.19 N/m^2 Node: 31305	3.57262e+008 N/m^2 Node: 16247

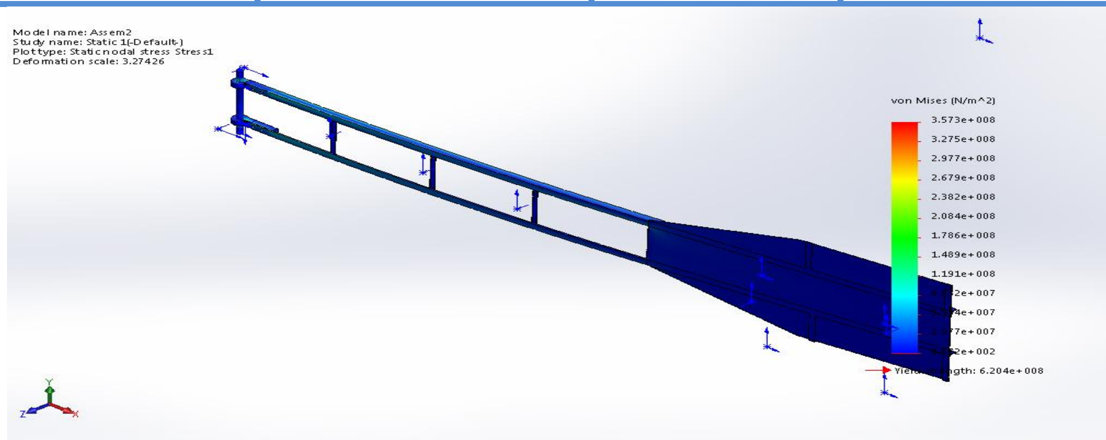

Figure 4.19: The stresses on The Tail assembly

4.11.4.5 Strain analysis results:

When the wind act on the vain of the tail, the force acting on the vain generate a bending moment about the axis of the tail rod which is in turn result in deforming the tail bars as represented by the green areas as shown in figure (4.20).

Name	Type	Min	Max
Strain	ESTRN: Equivalent Strain	2.58804e-009 Element: 14199	0.000707924 Element: 7433

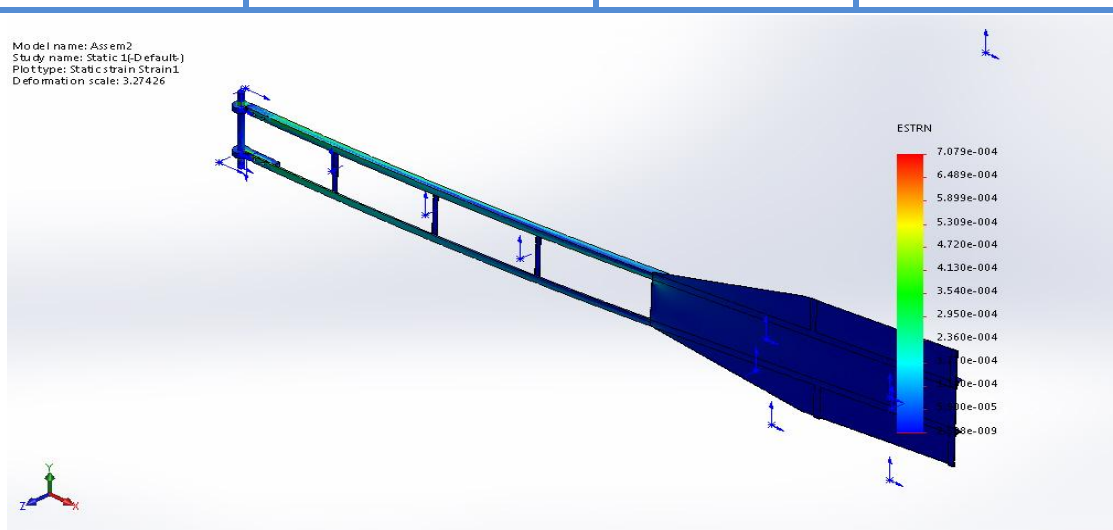

Figure 4.20: The strain on the Tail assembly

4.11.4.6 Displacement analysis results

As the bending moment increases with the distance from the axis of rotation, the amount of displacement increases, the amount displacement represented by the color code from green to red as shown in the figure (4.21).

Name	Type	Min	Max
Displacement	URES: Resultant Displacement	0 mm Node: 29136	74.8251 mm Node: 33074

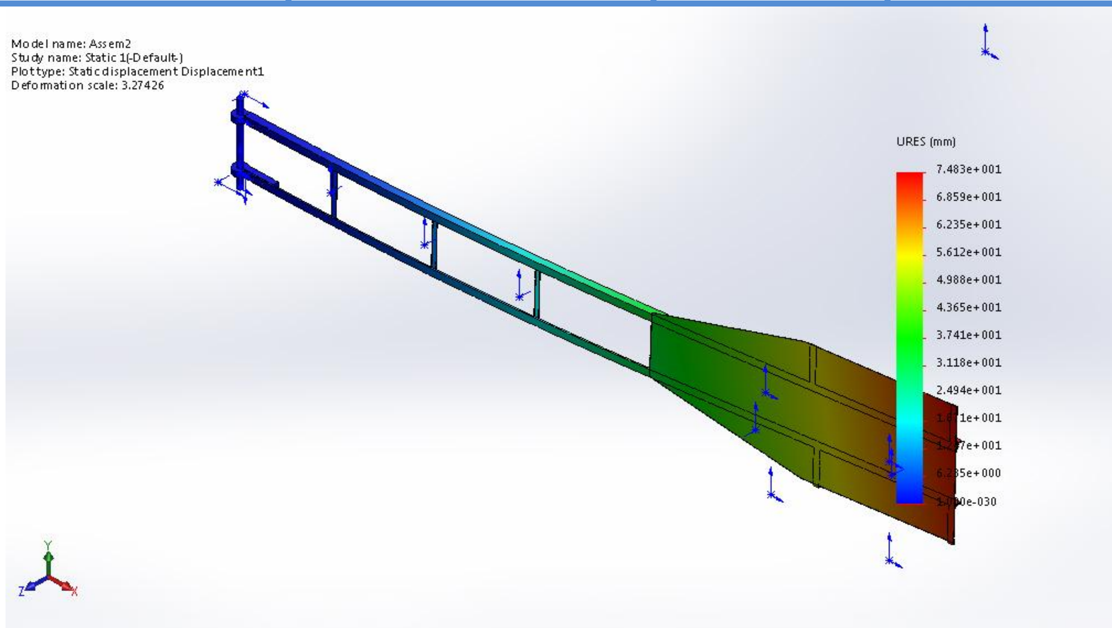

Figure 4.21: The Tail Assembly Displacement

4.11.5 The Base

4.11.5.1 The Base Material properties

Table 4.11: The Base Material Properties

Name:	**Alloy Steel**
Model type:	**Linear Elastic Isotropic**
Default failure criterion:	**Max von Mises Stress**
Yield strength:	**6.20422e+008 N/m^2**
Tensile strength:	**7.23826e+008 N/m^2**
Elastic modulus:	**2.1e+011 N/m^2**
Poisson's ratio:	**0.28**
Mass density:	**7700 kg/m^3**
Shear modulus:	**7.9e+010 N/m^2**
Thermal expansion coefficient:	**1.3e-005 /Kelvin**

4.11.5.2 Load on the Base

The base hold the various component of the transmission mechanism, thus it support multiple loads as it supported by the bearing at the top tower base. The loads are shown in the table (4.8).

Table (4.12): The Loads at the Base

Load name	Load Image	Load Details
Force-1	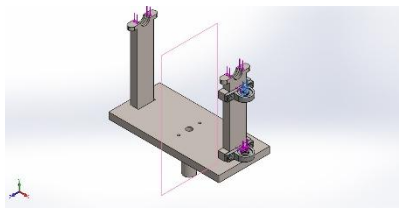	**Entities:** 2 face(s), 1 plane(s) **Reference:** Right Plane **Type:** Apply force **Values:** ---, -64.85, --- N
Force-2	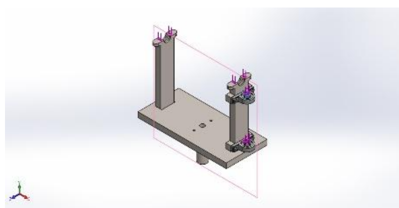	**Entities:** 1 face(s), 1 plane(s) **Reference:** Front Plane **Type:** Apply force **Values:** 64.85, ---, --- N
Force-3	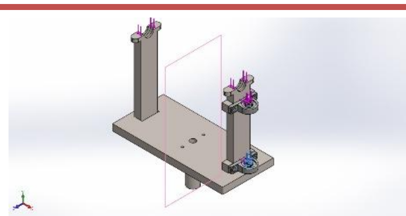	**Entities:** 2 face(s), 1 plane(s) **Reference:** Right Plane **Type:** Apply force **Values:** ---, -64.85, --- N
Force-4	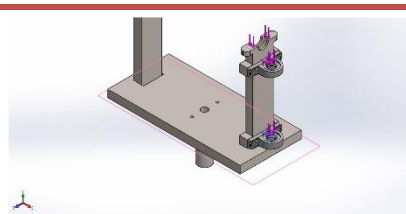	**Entities:** 1 face(s), 1 plane(s) **Reference:** Top Plane **Type:** Apply force **Values:** 64.85, ---, --- N
Force-5	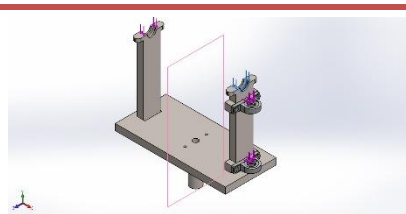	**Entities:** 1 face(s), 1 plane(s) **Reference:** Right Plane **Type:** Apply force **Values:** ---, -2444.5, --- N

Load name	Load Image	Load Details
Force-6	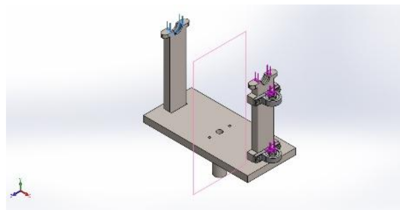	**Entities:** 1 face(s), 1 plane(s) **Reference:** Right Plane **Type:** Apply force **Values:** ---, -2765.2, --- N

4.11.5.3 The Stress on the Base

The maximum value of the stresses applied at the middle of the base as a results of the weights applied at the base left and right stands which act as a bending couple and bearing support at the bottom surface of the base as figure (4.22) shows the color code of the stress.

Name	Type	Min	Max
Stress	VON: von Mises Stress (effective stess)	65.03 N/m^2 Node: 8162	1.93613e+007 N/m^2 Node: 4450

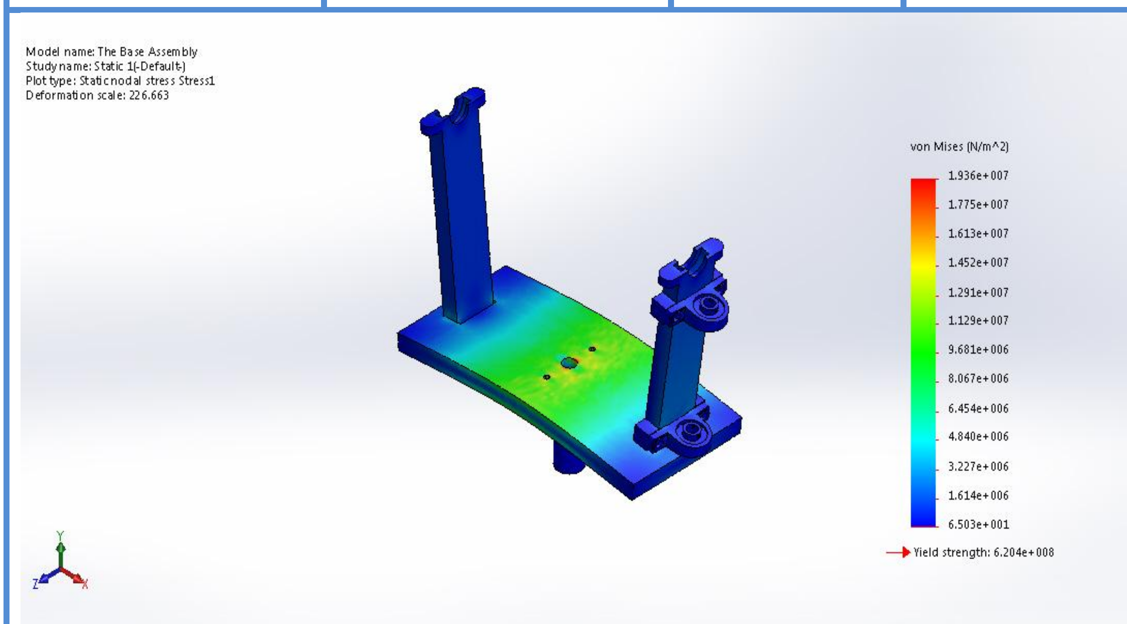

Figure 4.22: Stresses on the Base

4.11.5.4 The Strain on the Base

The maximum amount of strain represented by the color code in figure (4.23) where the maximum amount of stress are applied.

Name	Type	Min	Max
Strain	ESTRN: Equivalent Strain	2.35664e-010 Element: 112645	0.000111768 Element: 20433

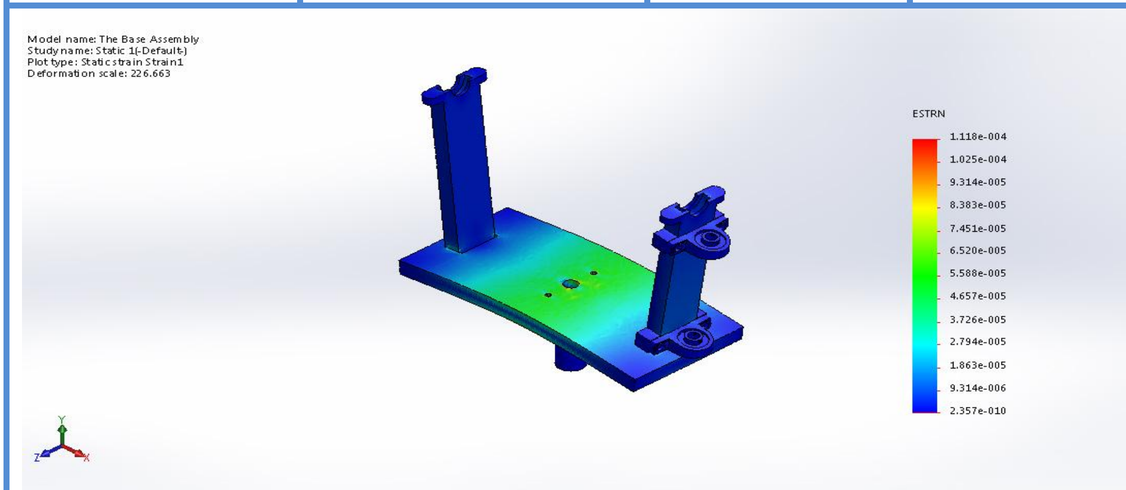

Figure 4.23: The Strain on the Base

4.11.5.5 The Base Displacement

Since the loads are concentrated at the stands which they are at the edges of the base beside the weights of the tail and the rotor the stands tends to move outward as shown in figure (4.24).

Name	Type	Min	Max
Displacement	URES: Resultant Displacement	0 mm Node: 7976	0.264712 mm Node: 36473

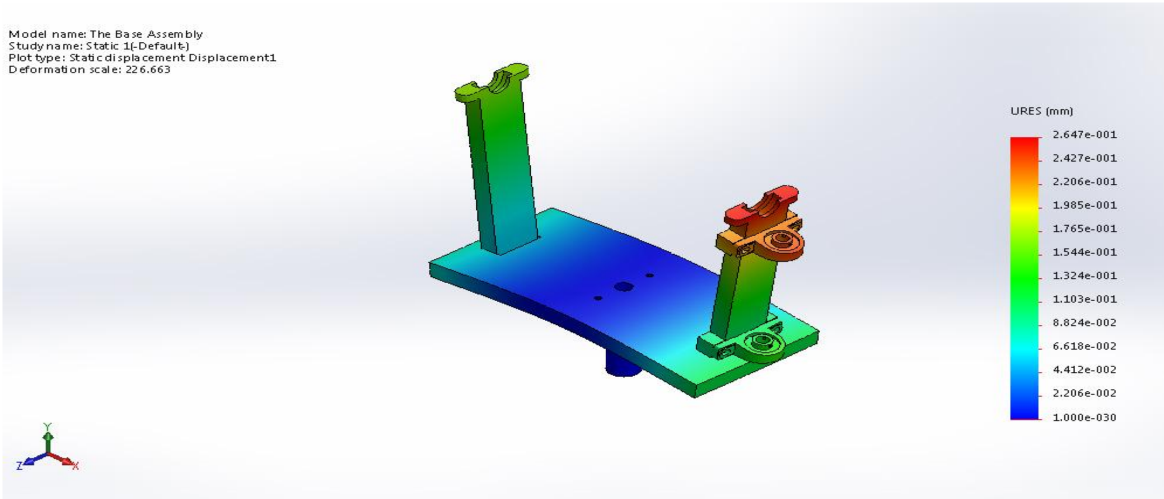

Figure 4.24: The Base Displacement

4.11.6 The bully - crank arm

4.11.6.1 The bully - crank arm Material properties

Table (4.13): The Bully-Crank Arm Material Properties

Name:	**Alloy Steel**
Model type:	**Linear Elastic Isotropic**
Default failure criterion:	**Max von Mises Stress**
Yield strength:	**6.20422e+008 N/m^2**
Tensile strength:	**7.23826e+008 N/m^2**
Elastic modulus:	**2.1e+011 N/m^2**
Poisson's ratio:	**0.28**
Mass density:	**7700 kg/m^3**
Shear modulus:	**7.9e+010 N/m^2**
Thermal expansion coefficient:	**1.3e-005 /Kelvin**

4.11.6.2 Loads on The bully - crank arm

The bully- shaft arm responsible of transferring the rotary motion of the crank shaft to translation motion through the bully, hence the loads applied at the inner rings of both the one connected to shaft bearing and the one connected to the bully. Table (4.10) shows the loads applied to the arm.

Table (4.14): the Loads at the Shaft-bully Link:

Fixture name	Fixture Image	Fixture Details
Fixed	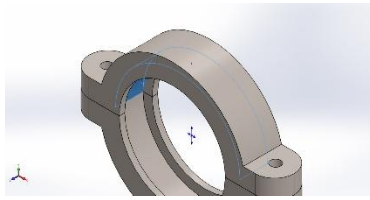	**Entities:** **1 face(s)** **Type:** **Fixed Geometry**

Resultant Forces

Components	**X**	**Y**	**Z**	**Resultant**
Reaction force(N)	**-0.0083847**	**2499.94**	**-0.0799284**	**2499.94**

4.5.3 The Stress on the bully - crank arm

The maximum value of stress is applied when the shafts at upper point of the stroke (90 degree) where all the loads pulling downward, figure (4.25) shows the stress on the link. The point where mostly stressed out are the points where the link is connected to the shaft and the bully.

Name	**Type**	**Min**	**Max**
Stress	VON: von Mises Stress (effective stress)	1144.46 N/m^2 Node: 3374	4.28158e+007 N/m^2 Node: 3767

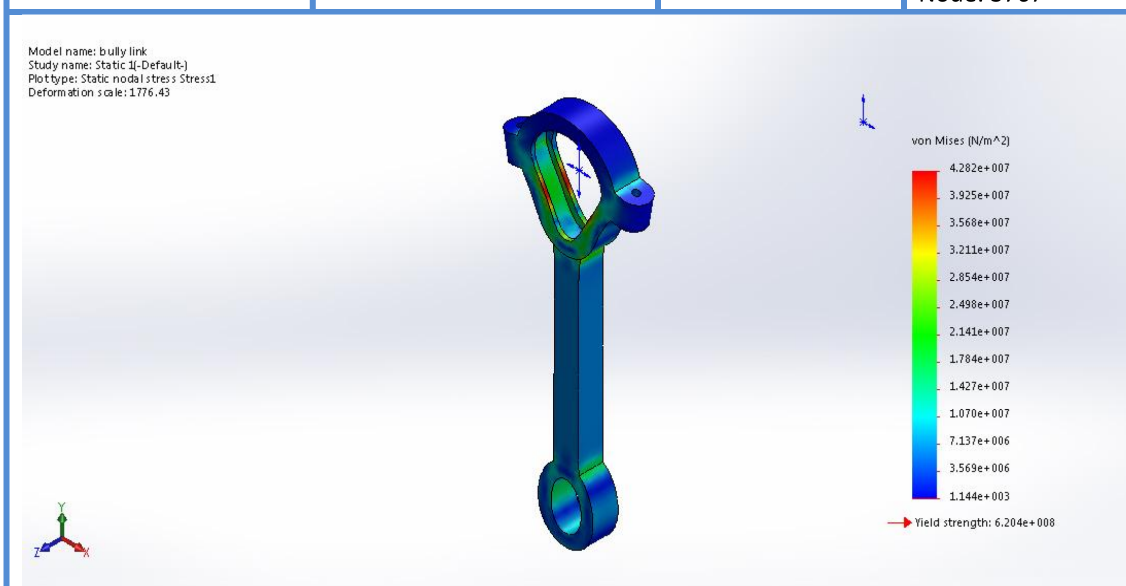

Figure 4.25: The stresses on bully-crank arm

4.11.6.4 Strain analysis results

The deformation due to the applied load is shown in figure (4.26) where the strain dependent to the stresses.

Name	Type	Min	Max
Strain	ESTRN: Equivalent Strain	2.73599e-008 Element: 488	0.000163588 Element: 6542

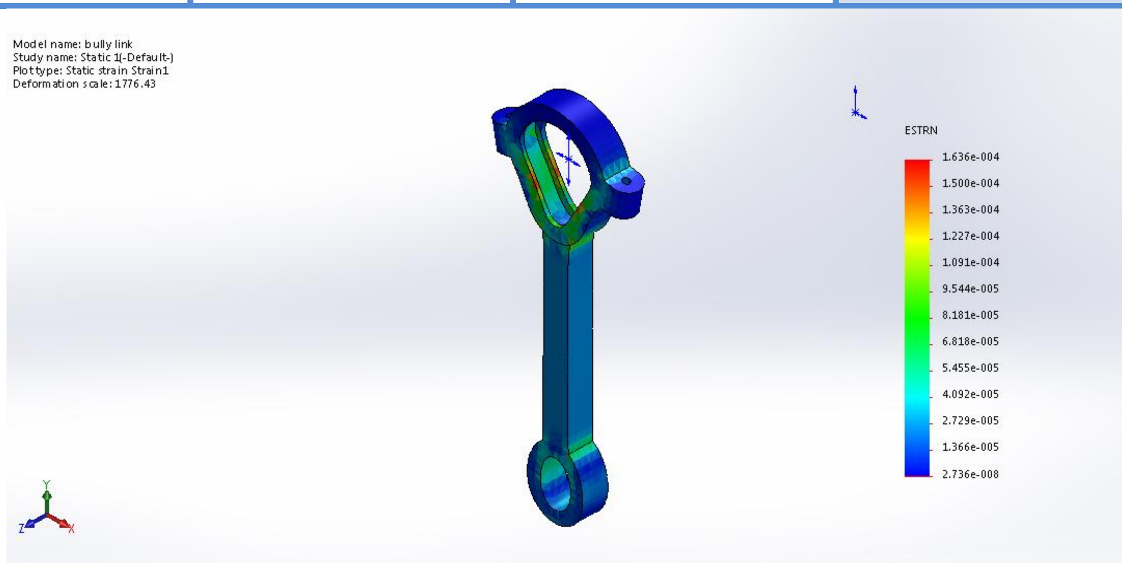

Figure 4.26: The Strain on the bully-crank arm

4.11.6.5 The bully - crank arm Displacement:

Since the main loads acting on the link are caused by the weights of the water, pump plunger, the pump rod and lifting bully the displacement of the link in the direction of the loads at the point where its connected to the lifting bully as shown in the figure (4.27)

Name	Type	Min	Max
Displacement1	URES: Resultant Displacement	0 mm Node: 1	0.0150374 mm Node: 13403

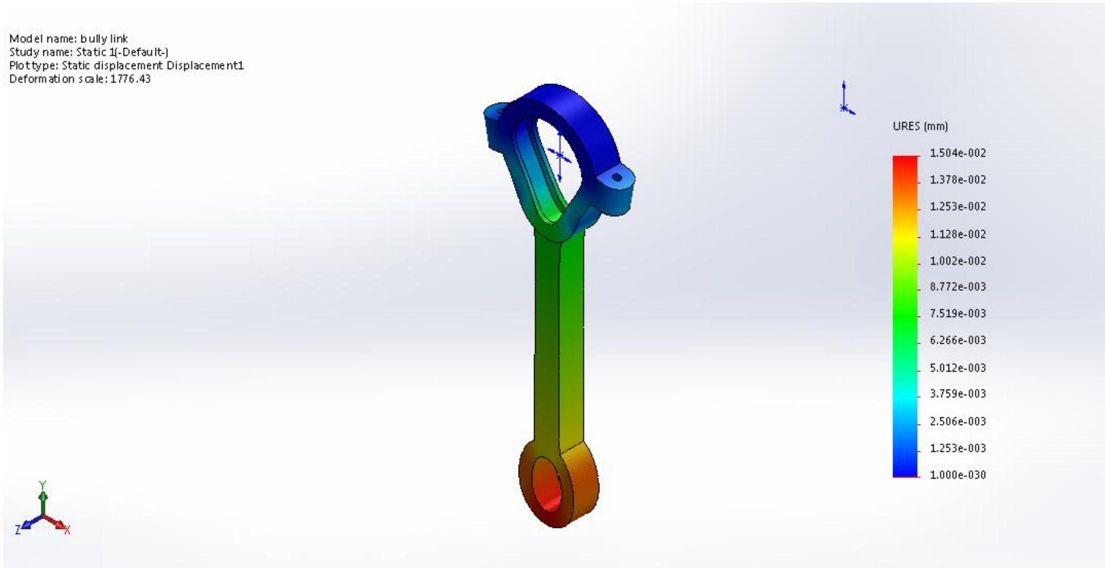

Figure 4.27: the at the bully-crank arm Displacement

4.11.7 The lifting bully

4.11.7.1 The lifting bully Material properties

Table (4.15): The Lifting Bully Material Properties

Name:	**Alloy Steel**
Model type:	**Linear Elastic Isotropic**
Default failure criterion:	**Max von Mises Stress**
Yield strength:	**6.20422e+008 N/m^2**
Tensile strength:	**7.23826e+008 N/m^2**
Elastic modulus:	**2.1e+011 N/m^2**
Poisson's ratio:	**0.28**
Mass density:	**7700 kg/m^3**
Shear modulus:	**7.9e+010 N/m^2**
Thermal expansion coefficient:	**1.3e-005 /Kelvin**

4.11.7.2 The Loads on The lifting bully

The lifting bully support the loads applied by the bully-shaft link and the pump rod as it fixed to it as shown in table (4.16). The loads are maximum when the shaft is about to move from the lower point of the stroke.

Table (4.16): The Loads at the Lifting Bully

Fixture name	Fixture Image	Fixture Details
Fixed-1	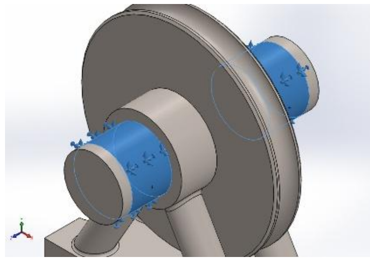	**Entities:** **2 face(s)** **Type:** **Fixed Geometry**

Resultant Forces

Components	**X**	**Y**	**Z**	**Resultant**
Reaction force(N)	**0.449012**	**4944.95**	**-0.323017**	**4944.95**

4.11.7.3 The Stress on The lifting bully

The weights of the water lifted, pump rod and the pump plunger where applied directly to bully, the maximum amount of the stress applied at the point where the shaft-bully link and the pump rod are connected, the amount of the stress by the color code as shown in figure (4.28).

Name	**Type**	**Min**	**Max**
Stress	VON: von Mises Stress (effective stress)	2314.21 N/m^2 Node: 2159	5.94643e+007 N/m^2 Node: 32475

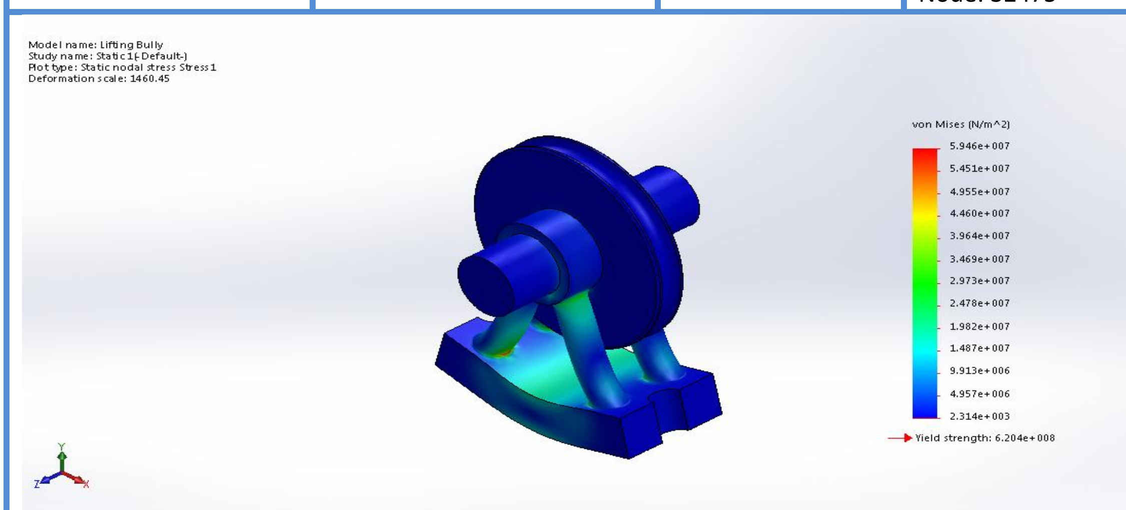

Figure 4.28: The stresses on the lifting bully

4.11.7.4 Strain on The lifting bully

The strain due to the applied loads and relative to the stress on the bully is shown at figure (4.29).

Name	Type	Min	Max
Strain	ESTRN: Equivalent Strain	8.64468e-009 Element: 6293	0.000171049 Element: 7054

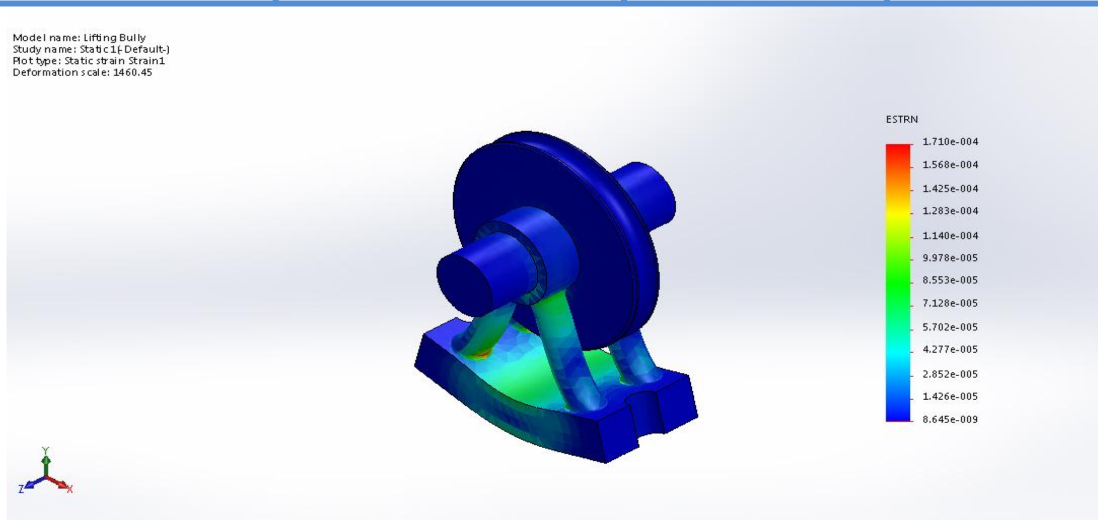

Figure 4.29: the strain on the lifting bully

4.11.7.5 The lifting bully Displacement

The maximum distance the base of bully move at the middle base of it due to that the maximum load concentrated their as shown in figure (4.30).

Name	Type	Min	Max
Displacement	URES: Resultant Displacement	0 mm Node: 219	0.00890174 mm Node: 34770

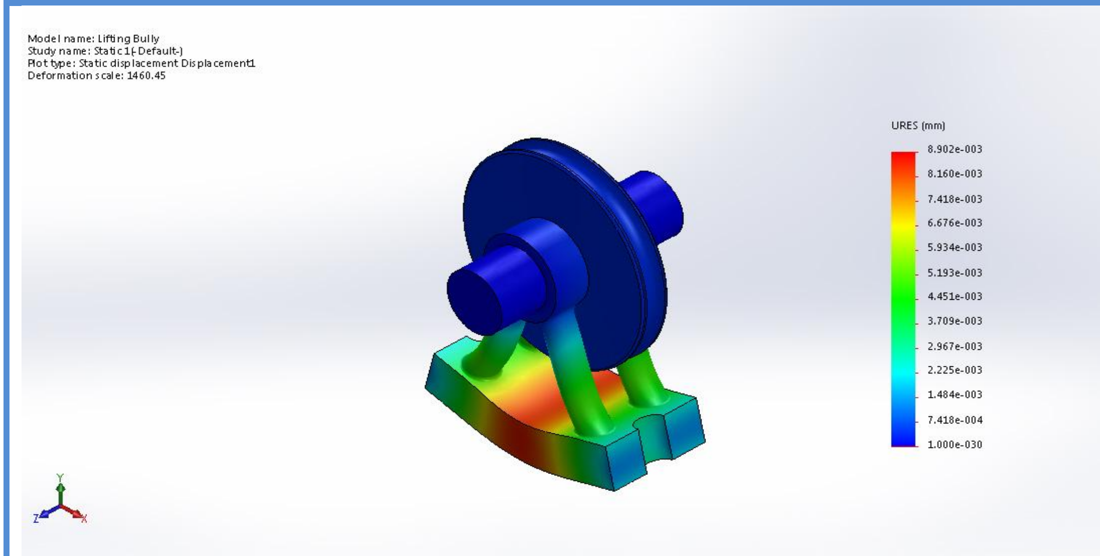

Figure 4.30: The lifting bully displacement

4.11.8 The top tower base

4.11.8.1 The top tower base Material properties

Table 4.13: The Top Tower Base material Properties

Name:	**Alloy Steel**
Model type:	**Linear Elastic Isotropic**
Default failure criterion:	**Max von Mises Stress**
Yield strength:	**6.20422e+008 N/m^2**
Tensile strength:	**7.23826e+008 N/m^2**
Elastic modulus:	**2.1e+011 N/m^2**
Poisson's ratio:	**0.28**
Mass density:	**7700 kg/m^3**
Shear modulus:	**7.9e+010 N/m^2**
Thermal expansion coefficient:	**1.3e-005 /Kelvin**

4.11.8.2 Load on The top tower base

The tower top base support the loads of the rotor assembly through the bearing the loads and its reaction are shown in table (4.14). Where all the loads are concentrated at the area occupied by the bearing.

Table (4.14): The Loads at the Top Tower Base

Fixture name	Fixture Image	Fixture Details
Fixed-1	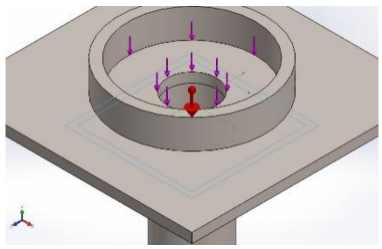	**Entities:** **1 face(s)** **Type:** **Fixed Geometry**

Resultant Forces

Components	X	Y	Z	Resultant
Reaction force(N)	**0.0082531**	**6069.35**	**-0.0244009**	**6069.35**

4.11.8.3 The Stress on the top tower base

The stress is concentrated in the middle of the top-tower base where the bearing is placed specially at the edges of the inner cylinder, since the top tower base is fixed at tower at the lower edges of the square plate. Figure (4.31) shows the stresses on the top- tower base. The yield strength of the material is much higher of the stresses caused by the loads so satisfies the design requirements.

Name	Type	Min	Max
Stress	VON: von Mises Stress (effective stress)	145.59 N/m^2 Node: 2955	4.96781e+006 N/m^2 Node: 600

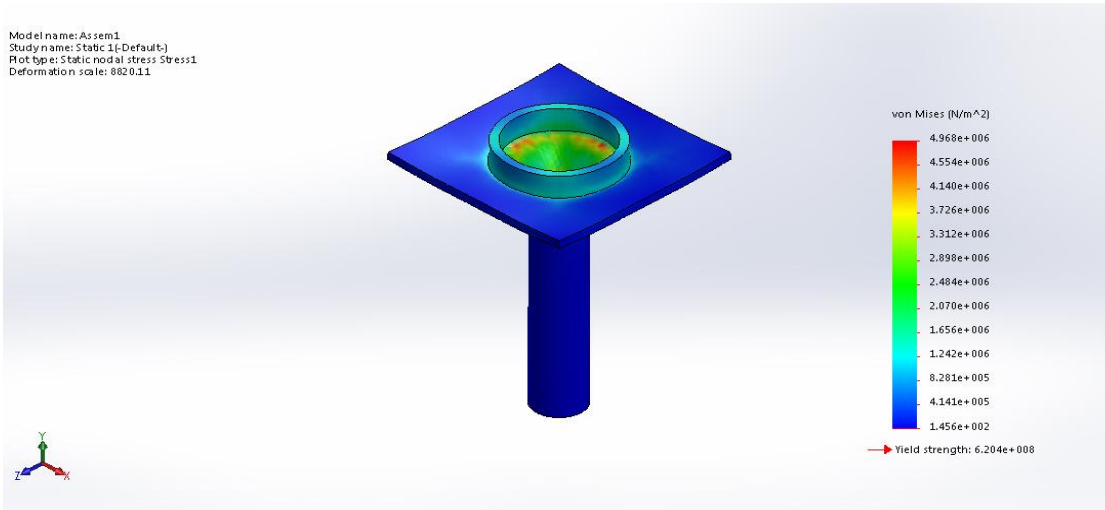

Figure 4.31: The stresses on the Top tower base

4.11.8.4 The Strain on the top tower base

As the loads applies resulting in stress, strain occurs. The strain is shown in figure (4.32).

Name	Type	Min	Max
Strain	ESTRN: Equivalent Strain	6.55287e-010 Element: 13675	3.33708e-005 Element: 33445

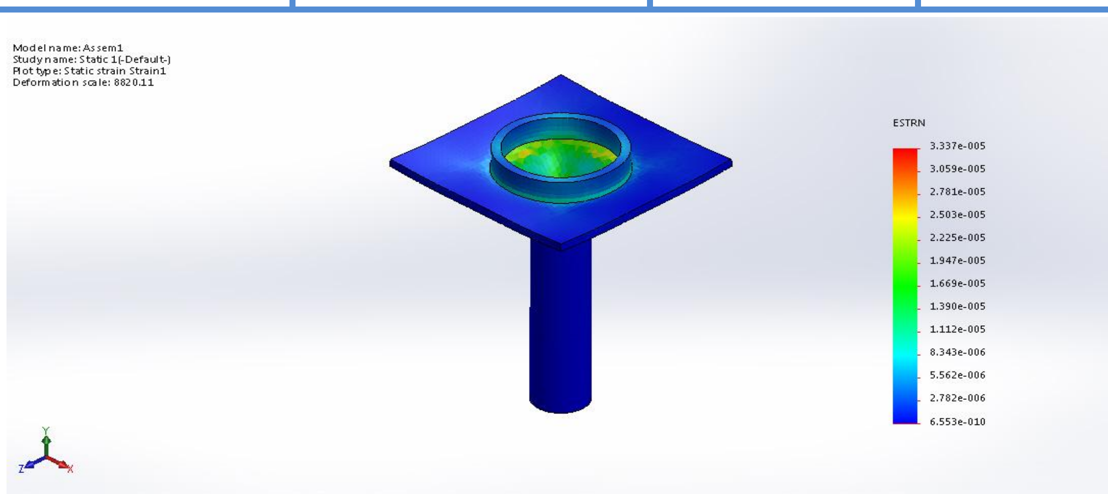

Figure 4.32: the strain on the Top tower base

4.11.8.5 The Top Tower Base Displacement

Since the top tower base is supported by the bottom edges of the base the cylinder of the base will have the maximum displacement as shown at figure (4.33).

Name	Type	Min	Max
Displacement1	URES: Resultant Displacement	0 mm Node: 161	0.00388082 mm Node: 4982

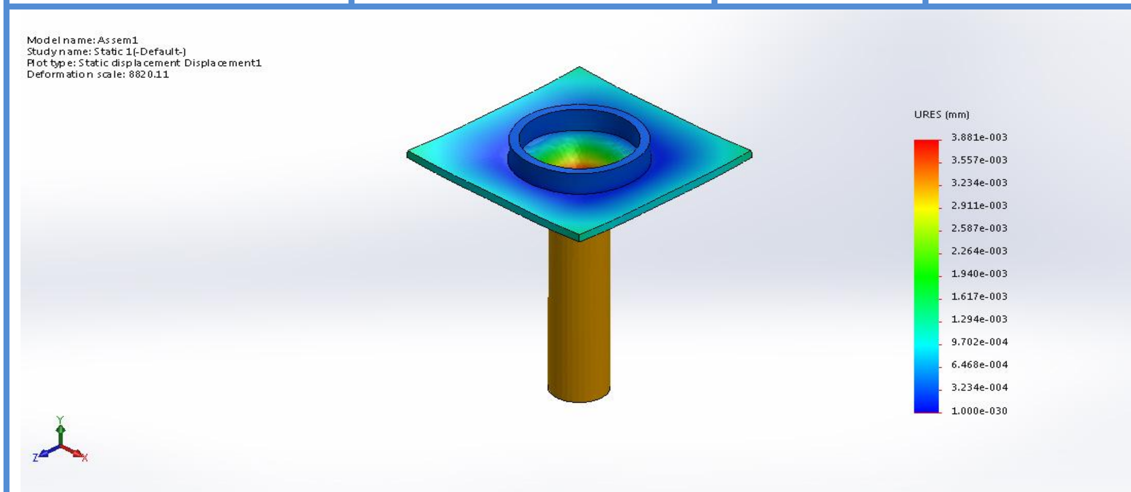

Figure 4.33: the Top tower base displacement

Chapter Five

Conclusion and Recommendation

CHAPTER FIVE

CONCLUSION AND RECOMMENDATION

5.1 Conclusion

1. The project concluded that the power required to elevate water for a total maximum head of 15 *m* at average wind speed of 3.5 *m/s* when the rotor is placed 10 *m* above the ground level is 43.77 *Watt* with torque output of 16.21 *Nm.*
2. The rotor of 12 blades with a solidity of 0.6 (maximum solidity for American windmill) and with total swept area of 20.19m^2.
3. The blades are trapezium shape with length of 1.352*m* and width of 0.425*m* at the tip of the blade and 0.153*m* at the root of the blade, having a total blade area of 0.29m^2.
4. The piston pump of diameter of 7.2*cm* and stroke of 10*cm* with a total volume of $0.404 * 10^{-3} m^3$ to produce a flow rate of $0.1736 * 10^{-3}$ *m3/second*.

5.2 Recommendations

After the completion of the design it’s recommended that:

1. The project should be fabricated and tested.
2. The focus should then be shifted to the effectiveness of the windmill by studying the efficiency and reducing Losses that might be in the present design.

3. Study should be conducted to improve overall efficiency of power extraction from the wind by the windmill which might include changing the tower height, construct the system in a different areas in Sudan where there is a difference in weather condition or improve the performance of the rotor by using another types of blades.
4. Study should be conducted based on other windmill types namely the vertical axes windmills such as SVONIUS, DARRIEUS and the HYBRID SAVONIUS DARRIEUS and compare their efficiencies to the efficiency of the horizontal axes American windmill used in our design.
5. Study should be conducted about lifting water from revers using windmills instead of diesel pumps for irrigation purpose especially in the Northern part of the country where the river Nile is the main source of irrigation water and also the wind speed there is significantly higher.
6. Study should be conducted about using water aeration using windmills for the purpose of water circulation specially in Western part of the country where people are using water pools (locally named as HAFFEER) as a source of water and also on the field of fish farms.

REFERENCES

[1] T. Burton, D. Sharpe, N. Jenkins, and E. Bossanyi, Wind energy handbook: John Wiley & Sons, 2001.

[2] A. V. Da Rosa, Fundamentals of renewable energy processes: Academic Press, 2012.

[3] P. Fraenkel, Water pumping devices: a handbook for users and choosers: Intermediate Technology Publications Ltd (ITP), 1997.

[4] R. Harrison and E. S. Hau, Large wind turbines: design and economics, 2000.

[5] A. Hemami, Wind turbine technology: Cengage Learning, 2012.

[6] W. A. Jansen and P. T. Smulders, Rotor design for horizontal axis windmills: Steering committeee for windenergy in developing countries, 1977.

[7] S. Lancashire, J. Kenna, and P. Fraenkel, Windpumping handbook: Intermediate Technology Publications Ltd.(IT), 1987.

[8] M. R. Patel, Wind and solar power systems: design, analysis, and operation: CRC press, 2005.

[9] J. Van Meel and P. Smulders, "Wind pumping: a handbook," International Bank for Reconstruction and Development, Washington, DC (USA)1989.

[10] A. J. Wortman, "Introduction to wind turbine engineering," NASA STI/Recon Technical Report A, vol. 84, p. 33699, 1983.

[11] A. F. Zobaa and R. C. Bansal, Handbook of renewable energy technology: World Scientific, 2011.

[12] WOT. (2012). Retrieved Dec, 2013,

[12] Machini N. Mercyline,Okero Julius Mokaya,'' DESIGN OF A WINDMILL FOR PUMPING WATER'', 2013.

[13] Gregory Ford, Victoria Hewey, Nicholas Lima, An Analysis of Small-Scale wind pump Design for Use in Developing Countries'', 2013.

[14] Sara Salomonsson, Helena Thoresson, 'Windmill Driven Water Pump or Small-Scale Irrigation And Domistic Use', 2010.

[15] Valerie Bulter, Jeffrey Corado, Kimberly Joback, "Redesign of the WPI Kite- Powered Water Pump and Wind Turbine Systems", 2013.

[16] Peter J Schubel, Richard J Crossley, "Wind Turbine Bladde Design", Energies, 2012.

[17] John McCosker, "Design and Optimization of a small Wind Turbine", 2012.

[18] Mwangi Michael Mbaci, Mungi Gee Gatabaki, "Prototype Design of a savonius Wind Turbine, 2010.

[19] John Larson, "The effects of Chord Length and tapper on Wind Turbine Blade Design", 2008.

[20] Qiyue Song, "Design, Fabrication and testing of a New Wind Turbine Blade", 2012.

[21] M. Rageb, "Optimal Rotor Tip Speed Ratio", 2014.

[22] Australian Government – Australian Renewable Energy Agency2012.

[23] International Renewable Energy agency (IRENA), 17th Mar 2016.

[24] Ages, E. M. Wind Power Overview. Akvopedia. Retrieved 27th February 2013.

[25] Cole, J. (2013). Denmark 25% wind-powered, going for 50% in 8 years. Retrieved, 2013.

[26] PES. (2012). Eight common turbine failures – and how to fix them. Retrieved, 2013.

[27] Telsonet. (n.d.). Wind Power's Beginnings. Retrieved from Telsonet

[28] U.S. Energy Information Administration. (2011). Trends in renewable energy consumption and electricity 2009, March 19, 2012.

[29] NTN Ball and Roller Bearing – CAT No. 2202 IX/E.

[30] R.S. khurmi – J.K. Gupta, Machine Design, Eurasia Publishing House (PVT.) LTD., 2005.

APPENDICES

APPENDIX A: Tolerance and Fits

APPENDIX A1: ISO STANDARD FOR FIT AND TOLERANCE (HOLE BASES)

FITS		*EXAMPLES*	
H11-c11 Slack running fit	Used to give flexibility under load, easy assembly or a close fit at elevated temperatures.	*I.C. engine exhaust valve in guide*	
H9-d10 Loose running fit	Used for gland seals, loose pulleys and very large bearings.	*Idler gear on spindle*	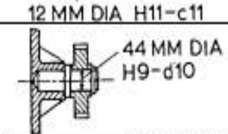
H9-e9 Easy running fit	Used for widely separated bearings or several bearings in line.	*Camshaft in bearing*	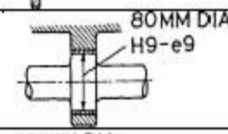
H8-f7 Normal running fit	Suitable for applications requiring a good quality fit that is easy to produce.	*Gearbox shaft in bearing*	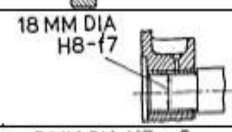
H7-g6 Sliding and location fit	Suitable for precision and location fits.	*Valve mechanism link pin*	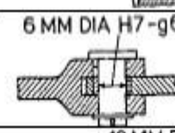
H7-h6 Location fit	Suitable for many non-running assemblies.	*Valve guide in head*	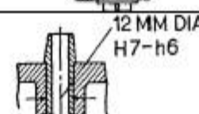
H7-k6 Push fit	Used for location fits when slight interference to eliminate movement is an advantage.	*Clutch member keyed to shaft*	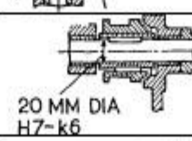
H7-n6 Tight assembly fit	Used when the degree of clearance that can result from a H7-k6 fit is unacceptable.	*Commutator shell on shaft*	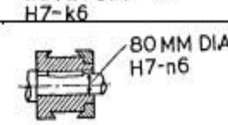
H7-p6 Press fit	Ferrous parts are not over-strained during assembly and dismantling.	*Split journal bearing*	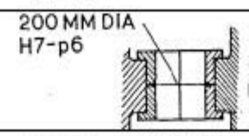
H7-s6 Heavy press fit	Mainly used for permanent assemblies.	*Cylinder liner in block*	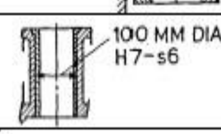

APPENDIX B: Bolts and Nuts

APPENDIX B1: UNWIN SAFETY FACTOR A BASED ON TENSILE STRENGTH:

M	Static load	Repeated load		Impact load
		Pulsating	Alternating	
Steel	3	5	8	12
Cast iron	4	6	10	15
Copper, soft metals	5	5	9	15

APPENDIX B2: BOLT FATIGUE STRENGTH:

Nominal thread size	Effective cross-section area As mm^2	Strength class			
		12.9		10.9	
		Fatigue strength*	Maximum allowable load	Fatigue strength*	Maximum allowable load
		kgf/mm^2	kgf	kgf/mm^2	kgf
M 4	8.78	13.1	114	9.1	79
M 5	14.2	11.3	160	7.8	111
M 6	20.1	10.6	213	7.4	149
M 8	36.6	8.9	326	8.7	318
M10	58	7.4	429	7.3	423
M12	84.3	6.7	565	6.5	548
M14	115	6.1	702	6	690
M16	157	5.8	911	5.7	895
M20	245	5.2	1274	5.1	1250
M24	353	4.7	1659	4.7	1659

APPENDIX C: Bearings

APPENDIX C1: CLASSIFICATION AND CHARACTERISTICS OF ROLLING BEARINGS

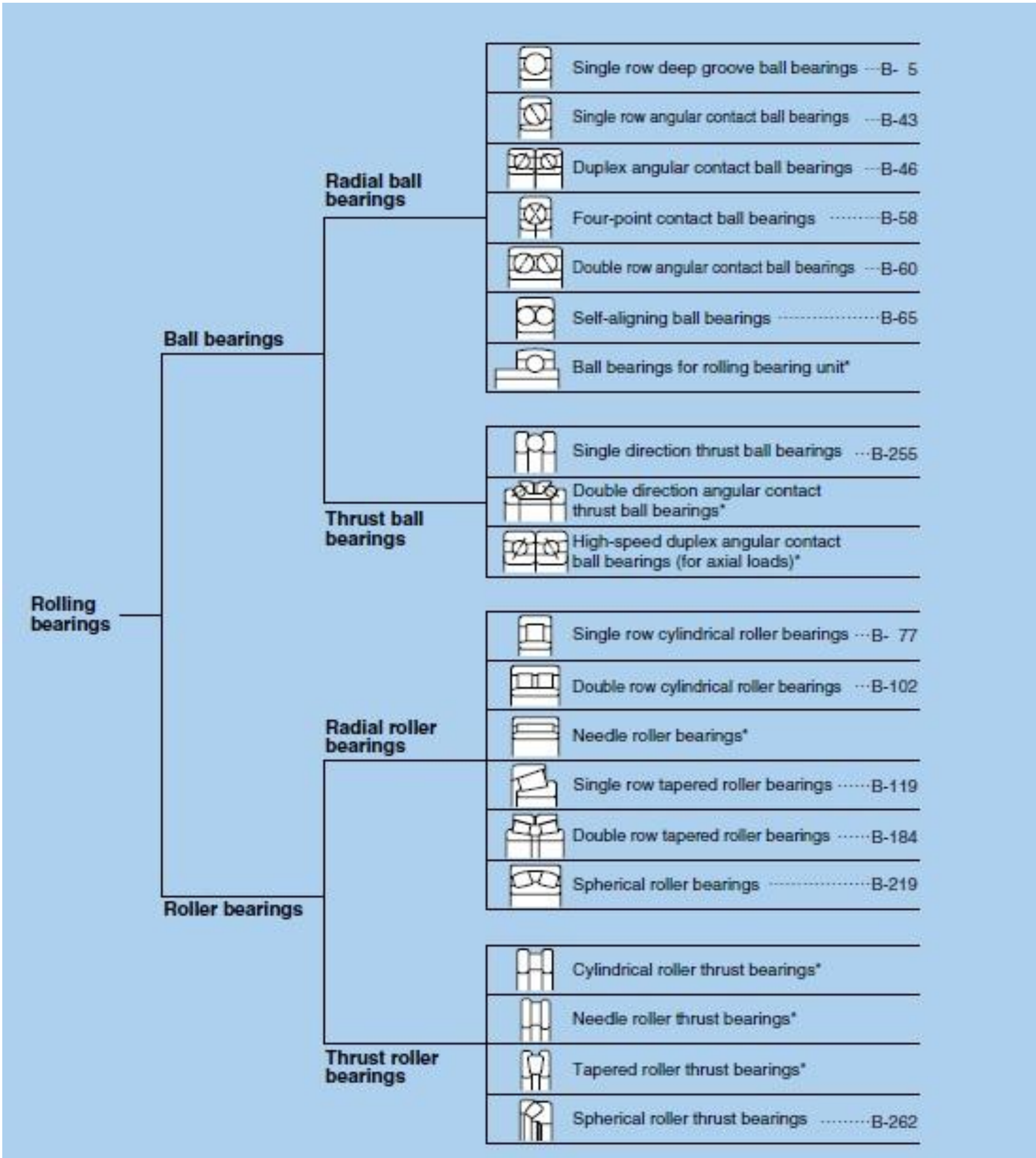

APPENDIX C2: TYPE OF ROLLING BEARINGS AND PERFORMANCE COMPARISON

Characteristics \ Bearing types	Deep groove ball bearings	Angular contact ball bearings	Double row angular contact ball bearings	Duplex angular contact ball bearings	Self-aligning ball bearings	Cylindrical roller bearings	Single-flange cylindrical roller bearings	Double-flange cylindrical roller bearings	Double row cylindrical roller bearings	Needle roller bearings
Load Carrying Capacity (Radial load / Axial load)										
High speed❶	☆☆☆☆	☆☆☆☆	☆☆	☆☆☆	☆☆	☆☆☆☆	☆☆☆	☆☆☆	☆☆☆	☆☆☆
High rotating accuracy❶	☆☆☆	☆☆☆	☆☆	☆☆☆		☆☆☆	☆☆	☆	☆☆☆	
Low noise/vibration❶	☆☆☆☆	☆☆☆		☆		☆	☆	☆	☆	☆
Low friction torque❶	☆☆☆☆	☆☆☆		☆☆	☆	☆				
High rigidity❶			☆☆	☆☆		☆☆	☆☆	☆☆	☆☆☆	☆☆
Vibration/shock resistance❶			☆		★	☆☆	☆☆	☆☆	☆☆	☆☆
Allowable misalignment❶ for inner/outer rings	☆				☆☆☆	☆				
Stationary in axial direction❷	◎	○	◎	◎ For DB and DF arrangement	◎		○	◎		
Moveable in axial direction❸	○		○	○ For DB arrangement	○	◎			◎	◎
Separable inner/outer rings❹						○	○	○	○	○
Inner ring tapered bore❺					○	○			○	
Remarks		For duplex arrangement				NU, N type	NJ, NF type	NUP, NP, NH type	NNU, NN type	NA type
Reference page	B-5	B-43	B-60	B-43	B-65	B-77	B-77	B-77	B-102	—

Tapered roller bearings	Double-row, 4-row tapered roller bearings	Spherical roller bearings	Thrust ball bearings	Cylindrical roller thrust bearings	Spherical roller thrust bearings	Reference page	Bearing types / Characteristics
							Load Carrying Capacity (Radial load / Axial load)
☆☆☆	☆☆	☆☆	☆	☆	☆	A-70	High speed❶
☆☆☆	☆		☆			A-35	High rotating accuracy❶
			☆			—	Low noise/vibration❶
						A-71	Low friction torque❶
☆☆	☆☆☆☆	☆☆☆		☆☆☆	☆☆☆	A-58	High rigidity❶
☆☆	☆☆☆	☆☆☆		☆☆☆	☆☆☆	A-21	Vibration/shock resistance❶
☆		☆☆☆		★	☆☆☆	A-85	Allowable misalignment❶ for inner/outer rings
○	◎	◎	○	○	○	A-15	Stationary in axial direction❷
	○	○	○			A-15	Moveable in axial direction❸
○	○		○	○	○	—	Separable inner/outer rings❹
		○				A-85	Inner ring tapered bore❺
For duplex arrangement				Including needle roller thrust bearing		—	Remarks
B-119	B-119	B-219	B-255	—	B-255		Reference page

❶ ☆ The number of stars indicates the degree to which that bearing type displays that particular characteristic.
★ Not applicable to that bearing type.

❷ ◎ Indicates dual direction. ○ Indicates single direction axial movement only.

❸ ◎ indicates movement in the axial direction is possible for the raceway surface; ○ indicates movement in the axial direction is possible for the fitting surface of the outer ring or inner ring.

❹ ○ Indicates both inner ring and outer ring are detachable.

❺ ○ Indicates inner ring with tapered bore is possible.

APPENDIX C3: TAPPER ROLLER BEARING

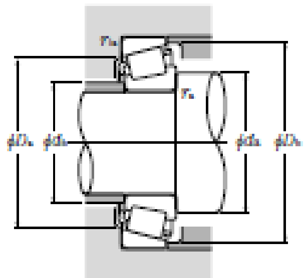

Equivalent radial load

dynamic

$P_r = XF_r + YF_a$

$\frac{F_a}{F_r} \le e$		$\frac{F_a}{F_r} > e$	
X	Y	X	Y
1	0	0.4	Y_1

static

$P_{or} = 0.5F_r + Y_o F_a$

When $P_{or} < F_r$ use $P_{or} = F_r$

For values of e, Y_1 and Y_o see the table below.

Bearing numbers	Abutment and fillet dimensions mm						Load center mm	Constant	Axial load factors		Mass kg
	d_a	d_b	D_a	D_b	r_{as} max	r_{1as} max	a	e	Y_1	Y_o	(approx.)
# 4T-JM207049/JM207010	64	62	85	91	1.5	2.5	7.6	0.33	1.79	0.99	0.82
4T-385/382A	65	61	89	92	2.3	0.8	3.1	0.35	1.69	0.93	0.616
# 4T-JH307749/JH307710	71	64	97	104	3	2.5	11.7	0.35	1.73	0.95	1.71
4T-28680/28622	68	62	88	92	3.5	0.8	3.3	0.40	1.49	0.82	0.774
4T-72218C/72487	80	67	102	116	3.5	3.3	−1.5[1]	0.74	0.81	0.45	1.99
4T-HM813840/HM813810	76	70	111	121	3.5	3.3	3.7	0.50	1.20	0.66	2.34
4T-389/382A	65	61	89	92	2.3	0.8	3.1	0.35	1.69	0.93	0.608
4T-387/382A	66	62	89	92	2.3	0.8	3.1	0.35	1.69	0.93	0.583
4T-387A/382A	69	62	89	92	3.5	0.8	3.1	0.35	1.69	0.93	0.581
4T-387AS/382A	72	62	89	92	5	0.8	3.1	0.35	1.69	0.93	0.576
4T-387S/382A	63	62	89	92	0.8	0.8	3.1	0.35	1.69	0.93	0.585
4T-28682/28622	70	63	88	92	3.5	0.8	3.3	0.40	1.49	0.82	0.747
4T-462/453X	67	63	92	98	2.3	3.3	7.1	0.34	1.79	0.98	1.06
4T-469/453X	70	63	92	98	3.5	3.3	7.1	0.34	1.79	0.98	1.06
4T-45289/45220	65	65	93	99	0.8	3.3	7.9	0.33	1.80	0.99	1.1
4T-469/453A	70	63	97	100	3.5	0.8	7.1	0.34	1.79	0.98	1.11
4T-390/394A	70	66	101	104	2.3	1.3	0.7	0.40	1.49	0.82	0.954
4T-469/454	70	63	96	100	3.5	2	7.1	0.34	1.79	0.98	1.24
4T-3979/3920	72	66	99	106	3.5	3.3	4.5	0.40	1.49	0.82	1.4
4T-39580/39520	72	66	101	107	3.5	3.3	6.6	0.34	1.77	0.97	1.41
4T-39581/39520	81	66	101	107	8	3.3	6.6	0.34	1.77	0.97	1.4
4T-33225/33462	74	68	104	112	3.5	3.3	2.6	0.44	1.38	0.76	1.58
4T-66225/66462	76	69	100	111	3.5	3.3	0.4	0.63	0.96	0.53	1.54
4T-623/612	72	66	105	110	3.5	3.3	14.4	0.31	1.91	1.05	2.12
4T-72225C/72487	81	67	102	116	3.5	3.3	−1.5[1]	0.74	0.81	0.45	1.96
4T-555S/552A	73	67	109	116	3.5	3.3	9.4	0.35	1.73	0.95	2.18
4T-78225/78551	83	77	117	132	3.5	2.3	−8.5[1]	0.87	0.69	0.38	2.69
4T-388A/382A	69	63	89	92	3.5	0.8	3.1	0.35	1.69	0.93	0.575
4T-66589/66520	74	73	105	116	0.8	3.3	−1.8[1]	0.67	0.90	0.50	1.66
4T-H913840†/H913810	88	82	124	138	3.5	3.3	−4.3[1]	0.78	0.77	0.42	3.22
# 4T-JLM508748/JLM508710	75	66	85	91	5	2.5	3.0	0.40	1.49	0.82	0.606
4T-29580/29520	75	68	96	103	3.5	3.3	0.6	0.46	1.31	0.72	0.992

Note: 3. Bearing numbers marked " # " designate **J-series** bearings. The tolerances of these bearings is listed in **Table 6.6** on **page A-42**.

1) " − " means that load center at outside of end of inner ring.

APPENDIX C4: CYLINDRICAL ROLLER BEARING

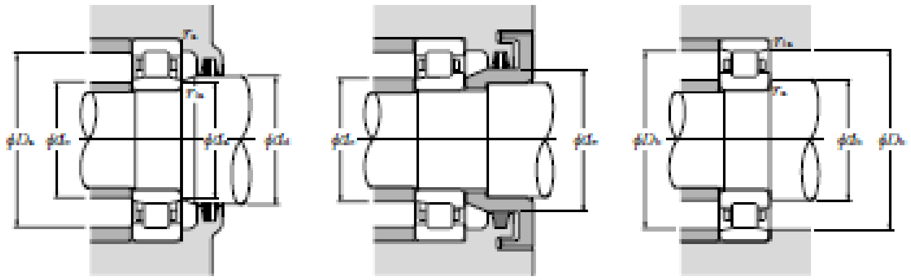

Dynamic equivalent radial load
$P_r = F_r$

Static equivalent radial load
$P_{or} = F_r$

	Dimensions			Abutment and fillet dimensions										Mass	
	mm			mm										kg	
type NF	F_w	E_w	J	d_a min	d_b min	d_c max	d_d min	d_e min	D_a max	D_b max	D_b min[4]	r_{as} max	r_{1as} max	type NU (approx.)	type N (approx.)
—	26.5	—	29.5	24	—	26	29	32	42	—	—	1	0.6	0.122	—
—	26.5	—	29.5	24	—	26	29	32	42	—	—	1	0.6	0.158	—
—	27.5	—	31.1	24	—	27	30	33	45.5	—	—	1	0.6	0.176	—
—	27.5	—	31.1	24	—	27	30	33	45.5	—	—	1	0.6	0.242	—
—	30.5	41.5	32.7	27	29	30	32	33	43	45	42.5	0.6	0.3	0.092	0.091
—	31.5	—	34.5	29	—	31	34	37	47	—	—	1	0.6	0.151	—
—	31.5	—	34.5	29	—	31	34	37	47	—	—	1	0.6	0.186	—
—	34	—	38	31.5	—	33	37	40	55.5	—	—	1	1	0.275	—
—	34	—	38	31.5	—	33	37	40	55.5	—	—	1	1	0.386	—
NF	38.8	62.8	43.6	33	33	38	41	46	72	72	64	1.5	1.5	0.55	0.536
—	36.5	48.5	38.9	34	35	35	38	39.5	50	51	49.5	1	0.6	0.13	0.128
—	37.5	—	41.1	34	—	37	40	44	57	—	—	1	0.6	0.226	—
—	37.5	—	41.1	34	—	37	40	44	57	—	—	1	0.6	0.297	—
—	40.5	—	44.9	36.5	—	40	44	48	65.5	—	—	1	1	0.398	—
—	40.5	—	44.9	36.5	—	40	44	48	65.5	—	—	1	1	0.58	—
NF	45	73	50.5	38	38	44	47	52	82	82	74	1.5	1.5	0.751	0.732
—	42	55	44.6	39	40	41	44	45	57	58	56	1	0.6	0.179	0.176
—	44	—	48	39	—	43	46	50	65.5	—	—	1	0.6	0.327	—
—	44	—	48	39	—	43	46	50	65.5	—	—	1	0.6	0.455	—
—	46.2	—	51	41.5	—	45	48	53	72	—	—	1.5	1	0.545	—
—	46.2	—	51	41.5	—	45	48	53	72	—	—	1.5	1	0.78	—
NF	53	83	59	43	43	52	55	61	92	92	84	1.5	1.5	0.99	0.965
—	47	61	49.8	44	45	46	49	50.5	63	64	62	1	0.6	0.22	0.217
NF	50	70	54.2	46.5	46.5	49	52	56	73.5	73.5	72	1	1	0.378	0.37
—	49.5	—	53.9	46.5	—	49	52	56	73.5	—	—	1	1	0.426	—
—	50	70	54.2	46.5	46.5	49	52	56	73.5	73.5	72	1	1	0.49	0.48
—	49.5	—	53.9	46.5	—	49	52	56	73.5	—	—	1	1	0.552	—
NF	53.5	77.5	58.4	48	48	51	55	60	82	82	80	1.5	1.5	0.658	0.643
—	52	—	57.6	48	—	51	55	60	82	—	—	1.5	1.5	0.754	—
—	53.5	77.5	58.4	48	48	51	55	60	82	82	80	1.5	1.5	0.951	0.932
—	52	—	57.6	48	—	51	55	60	82	—	—	1.5	1.5	1.06	—
NF	58	92	64.8	49	49	57	60	67	101	101	93	2	2	1.3	1.27

4) Does not apply to side of the outer ring rib of type **NF** bearings.

APPENDIX C5: SPHERICAL ROLLER THRUST BEARING

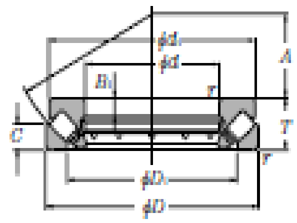

d 60 ~ 160mm

Boundary dimensions (mm)				Basic load ratings dynamic (kN)	static (kN)	dynamic (kgf)	static (kgf)	Limiting speeds (min⁻¹)	Bearing numbers	Dimensions (mm)				
d	D	T	$r_{s\,min}$ [1]	C_a	C_{0a}	C_a	C_{0a}	oil		D_1	d_1	B_1	C	A
60	130	42	1.5	283	805	28 900	82 000	2 600	29412	89	123	15	20	38
65	140	45	2	330	945	33 500	96 500	2 400	29413	96	133	16	21	42
70	150	48	2	365	1 040	37 000	106 000	2 200	29414	103	142	17	23	44
75	160	51	2	415	1 190	42 500	122 000	2 100	29415	109	152	18	24	47
80	170	54	2.1	460	1 380	47 000	141 000	1 900	29416	117	162	19	26	50
85	150	39	1.5	265	820	27 000	84 000	2 300	29317	114	143.5	13	19	50
	180	58	2.1	490	1 480	50 000	151 000	1 800	29417	125	170	21	28	54
90	155	39	1.5	285	915	29 100	93 500	2 300	29318	117	148.5	13	19	52
	190	60	2.1	545	1 680	56 000	172 000	1 700	29418	132	180	22	29	56
100	170	42	1.5	345	1 160	35 500	118 000	2 100	29320	129	163	14	20.8	58
	210	67	3	685	2 130	69 500	217 000	1 500	29420	146	200	24	32	62
110	190	48	2	445	1 500	45 000	152 000	1 800	29322	143	182	16	23	64
	230	73	3	845	2 620	86 500	267 000	1 400	29422	162	220	26	35	69
120	210	54	2.1	535	1 770	54 500	181 000	1 600	29324	159	200	18	26	70
	250	78	4	975	3 050	99 000	310 000	1 300	29424	174	236	29	37	74
130	225	58	2.1	615	2 100	62 500	215 000	1 500	29326	171	215	19	28	76
	270	85	4	1 080	3 550	110 000	360 000	1 200	29426	189	255	31	41	81
140	240	60	2.1	685	2 360	70 000	241 000	1 400	29328	183	230	20	29	82
	280	85	4	1 110	3 750	114 000	385 000	1 200	29428	199	268	31	41	86
150	215	39	1.5	340	1 340	34 500	136 000	1 800	29230	178	208	14	19	82
	250	60	2.1	675	2 390	68 500	243 000	1 400	29330	194	240	20	29	87
	300	90	4	1 280	4 350	131 000	445 000	1 100	29430	214	285	32	44	92
160	225	39	1.5	360	1 460	36 500	149 000	1 700	29232	188	219	14	19	86
	270	67	3	820	2 860	84 000	292 000	1 300	29332	208	260	24	32	92
	320	95	5	1 500	5 150	153 000	525 000	1 000	29432	229	306	34	45	99

APPENDIX A11: TAPERED ROLLER BEARING

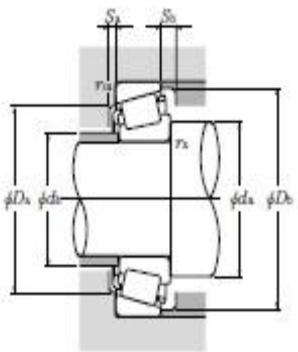

Equivalent radial load
dynamic

$P_r = XF_r + YF_a$

$\frac{F_a}{F_r} \leq e$		$\frac{F_a}{F_r} > e$	
X	Y	X	Y
1	0	0.4	Y_1

static

$P_{or} = 0.5F_r + Y_oF_a$

When $P_{or} < F_r$ use $P_{or} = F_r$

For values of e, Y_1 and Y_o see the table below.

Dimensions series to ISO	Abutment and fillet dimensions mm									Load center mm	Constant	Axial load factors		Mass kg
	d_a min	d_b max	D_a max	D_a min	D_b min	S_a min	S_b min	r_{as} max	r_{1as} max	a	e	Y_1	Y_o	(approx.)
	38.5	39.5	63.5	57	67	3	5.5	1.5	1.5	17.5	0.47	1.27	0.70	0.398
7FB	38.5	39	63.5	55	68	3	6.5	1.5	1.5	23.5	0.83	0.73	0.40	0.398
2FD	38.5	38	63.5	59	66	3	5.5	1.5	1.5	18.5	0.31	1.90	1.05	0.583
5FD	38.5	37	63.5	57	68	2	5.5	1.5	1.5	23	0.55	1.10	0.60	0.592
	38.5	37	63.5	57	67.5	2	5.5	1.5	1.5	23	0.61	0.99	0.54	0.594
4CC	37.5	38	52.5	50	55	3	4	1	1	14.5	0.45	1.32	0.73	0.181
2DE	37.5	38	59.5	55	62	5	5.5	1	1	17	0.35	1.73	0.95	0.395
5FD	40.5	39	66.5	61	71	3	6.5	1.5	1.5	23	0.55	1.10	0.60	0.659
2BD	39.5	40	50.5	48	52.5	2.5	2.5	0.6	0.6	10.5	0.29	2.06	1.13	0.121
4CC	40.5	40	56.5	54	59	4	4	1	1	15.5	0.45	1.32	0.73	0.224
2CE	40.5	40.5	56.5	52	59	3	4	1	1	14	0.31	1.97	1.08	0.263
3DB	43.5	44	63.5	62	67	3	3	1.5	1.5	15	0.37	1.60	0.88	0.344
3DC	43.5	43	63.5	61	67	3	5	1.5	1.5	17.5	0.37	1.60	0.88	0.457
5DC	43.5	42	63.5	59	68	3	6	1.5	1.5	21.5	0.58	1.03	0.57	0.461
	43.5	42	63.5	59	68	3	6	1.5	1.5	20.5	0.55	1.10	0.60	0.461
2DE	43.5	42	63.5	61	68	5	6	1.5	1.5	18.5	0.35	1.70	0.93	0.531
2FB	45	45	71.5	70	74	3	4.5	2	1.5	17	0.31	1.90	1.05	0.540
	45	44	71.5	63.5	75.5	3	5.5	2	1.5	20.5	0.55	1.10	0.60	0.517
7FB	45	44	71.5	62	76.5	3	7.5	2	1.5	26	0.83	0.73	0.40	0.530
2FE	45	43	71.5	66	74	3	7.5	2	1.5	20.5	0.31	1.90	1.05	0.787
5FE	45	43	71.5	66	76	3	7.5	2	1.5	25	0.55	1.10	0.60	0.797
2BC	44.5	45.5	57.5	54	58.5	3	3	0.6	0.6	11.5	0.29	2.07	1.14	0.161
3CD	45.5	46	62.5	60	65	4	4.5	1	1	15	0.38	1.58	0.87	0.273
2BE	45.5	46	62.5	60	64	2.5	4	1	1	15	0.28	2.12	1.17	0.312
2CE	48.5	47	66.5	65	71	4	5.5	1.5	1.5	18	0.36	1.69	0.93	0.494
3DB	48.5	49	71.5	69	75	3	3.5	1.5	1.5	16.5	0.37	1.60	0.88	0.435
3DC	48.5	48	71.5	68	75	3	5.5	1.5	1.5	19	0.37	1.60	0.88	0.558
2DE	48.5	47	71.5	67	76	5	7	1.5	1.5	21	0.36	1.68	0.92	0.728
2EE	52	48	75	70	80	5	5	2	2	22.5	0.34	1.74	0.96	0.907
2FB	50	52	81.5	77	82	3	5	2	1.5	19.5	0.35	1.74	0.96	0.769
	50	50	80	72	85.5	3.5	6	2	1.5	23	0.55	1.10	0.60	0.728
7FB	50	50	81.5	71	86.5	3	8	2	1.5	29.5	0.83	0.73	0.40	0.738
2FD	50	50	81.5	73	82	3	8	2	1.5	23	0.35	1.74	0.96	1.08
5FD	50	48	81.5	72	84	3	8	2	1.5	27.5	0.55	1.10	0.60	1.1

APPENDIX D: DRAWING

APPENDIX D1: SUPPORTING ARM DRAWING

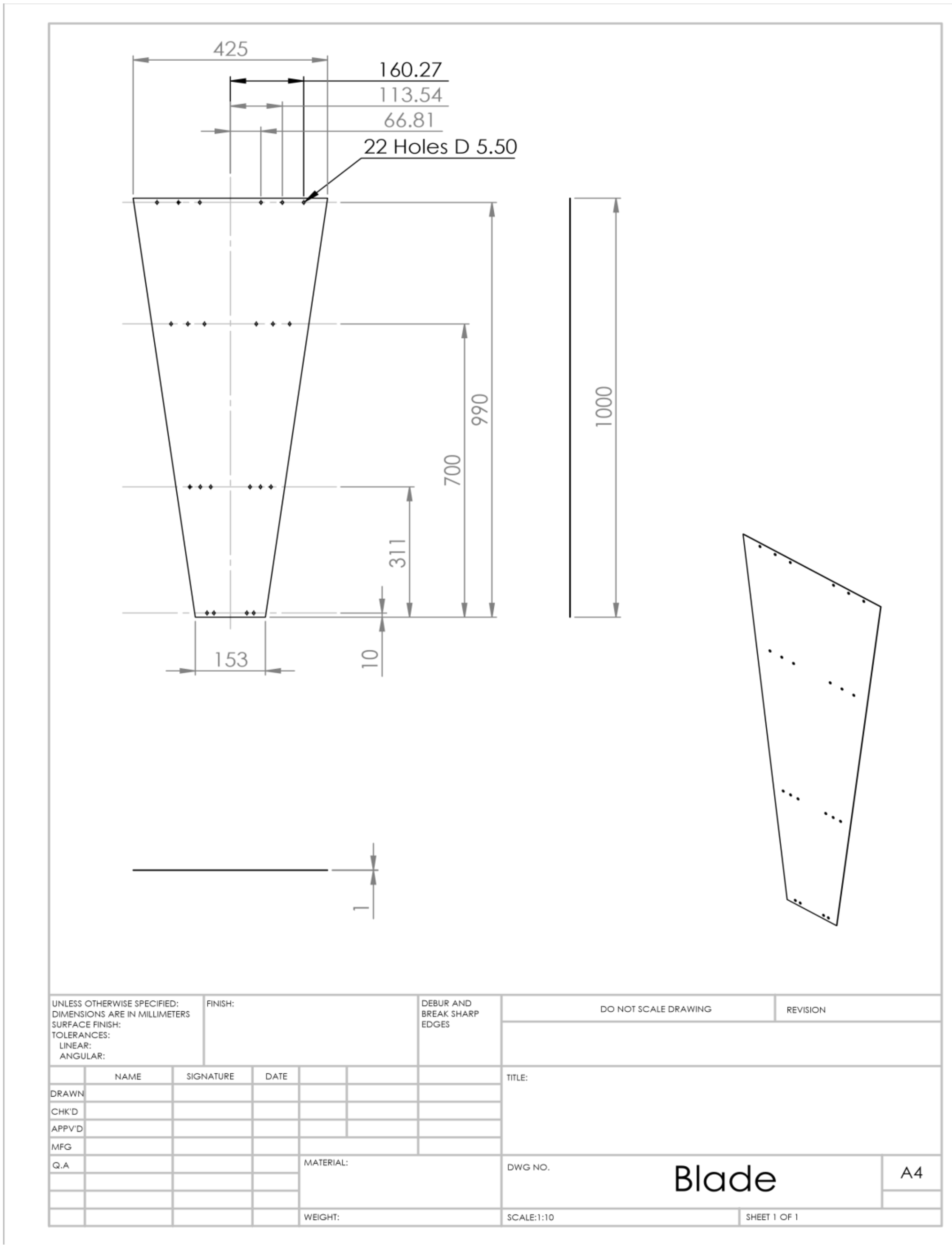

APPENDIX D2: SUPPORTING ARM DRAWING

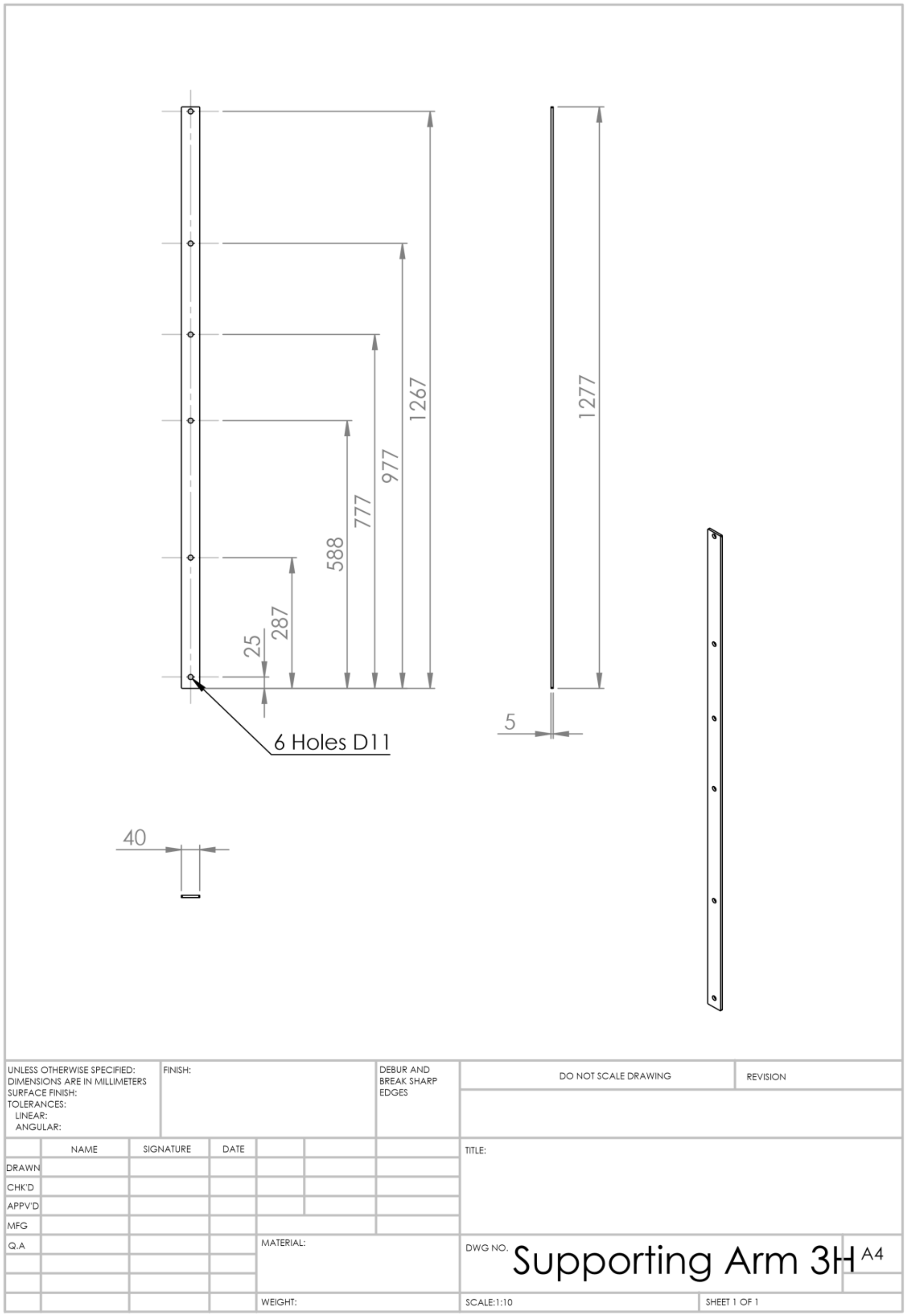

APPENDIX D3: BLADE FIX 1 DRAWING

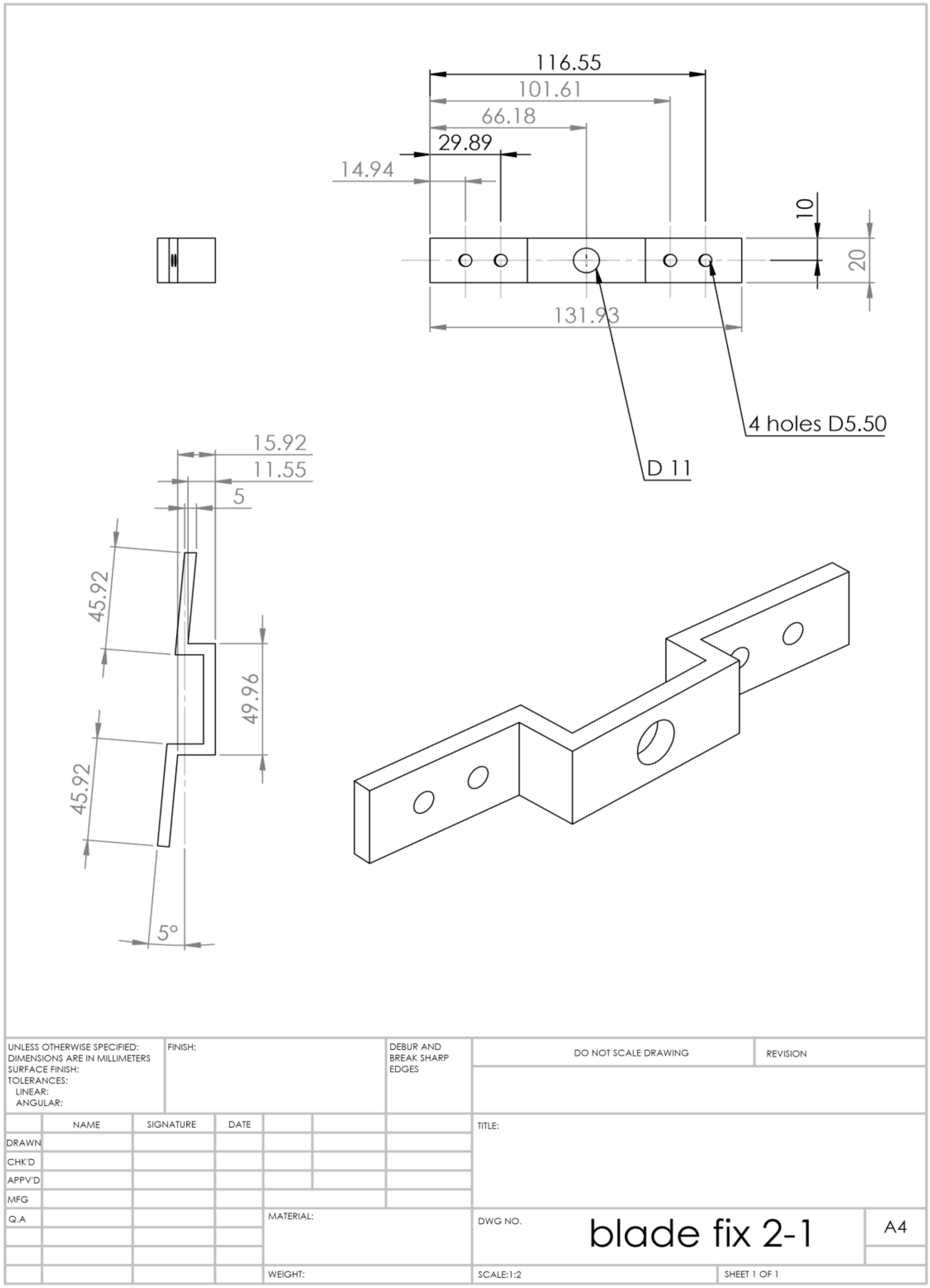

APPENDIX C4: BLADE FIX 2 DRAWING

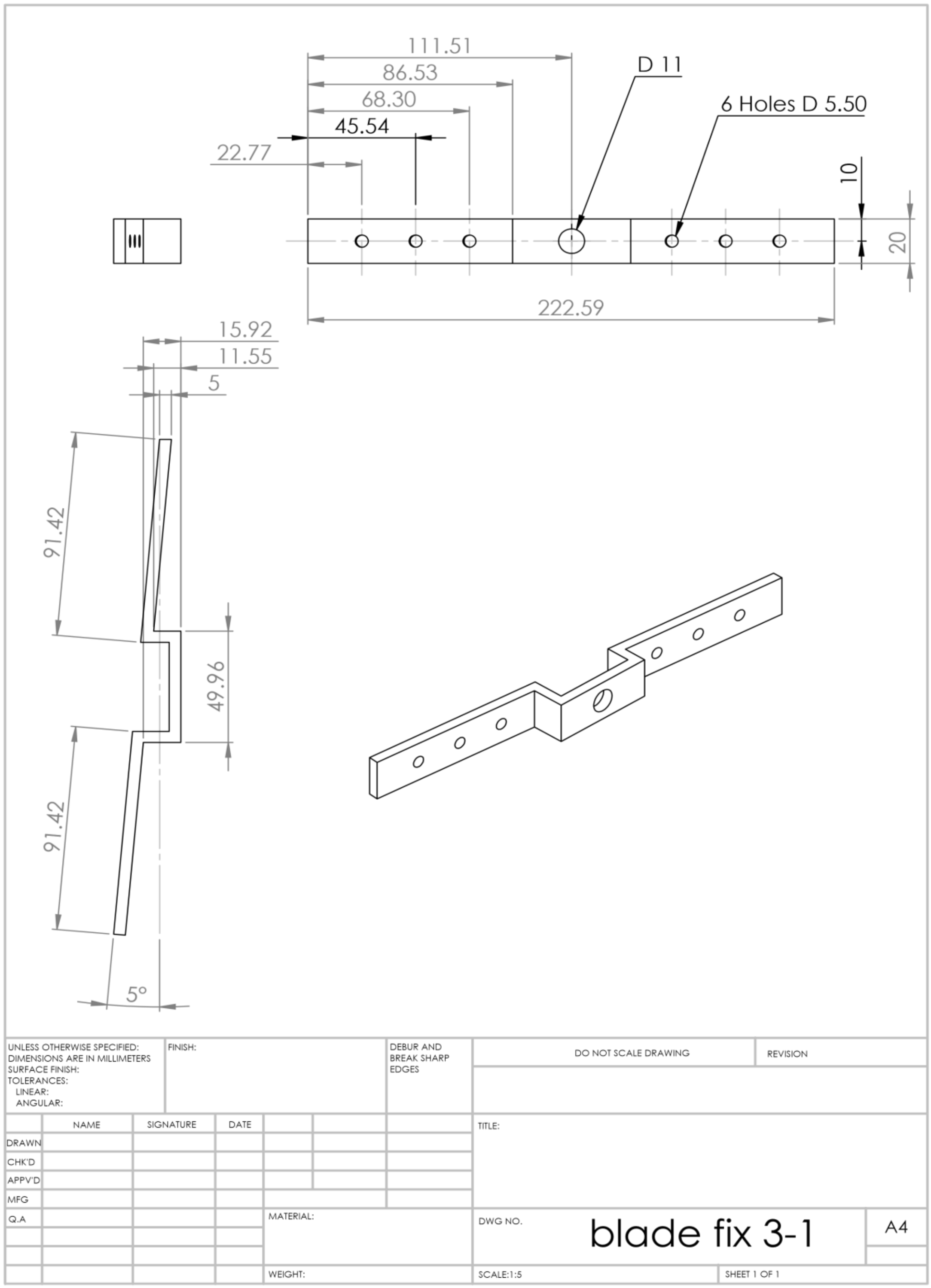

APPENDIX D5: BLADE FIX 3 DRAWING

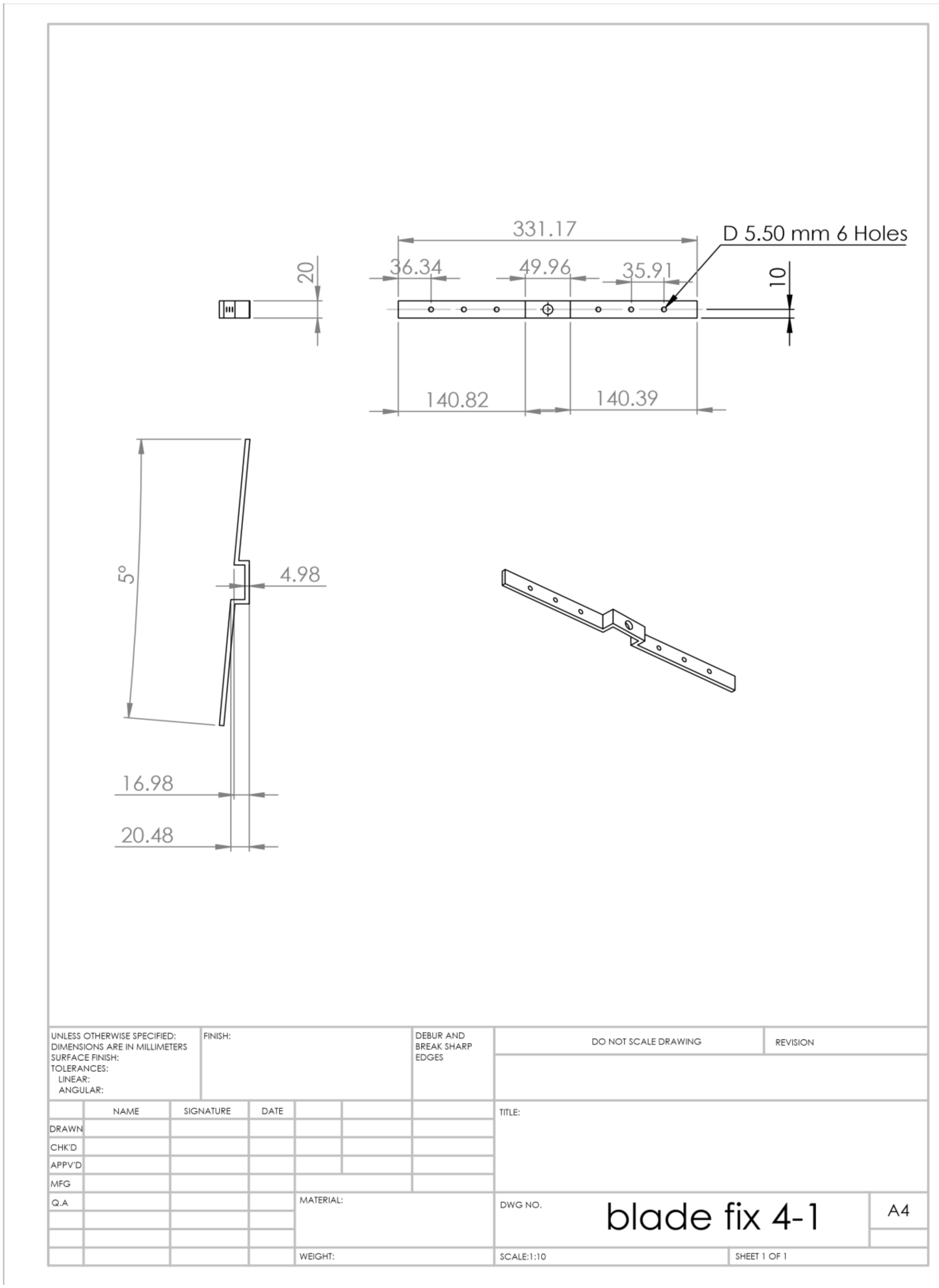

APPENDIX D6: BLADE FIX 4 DRAWING

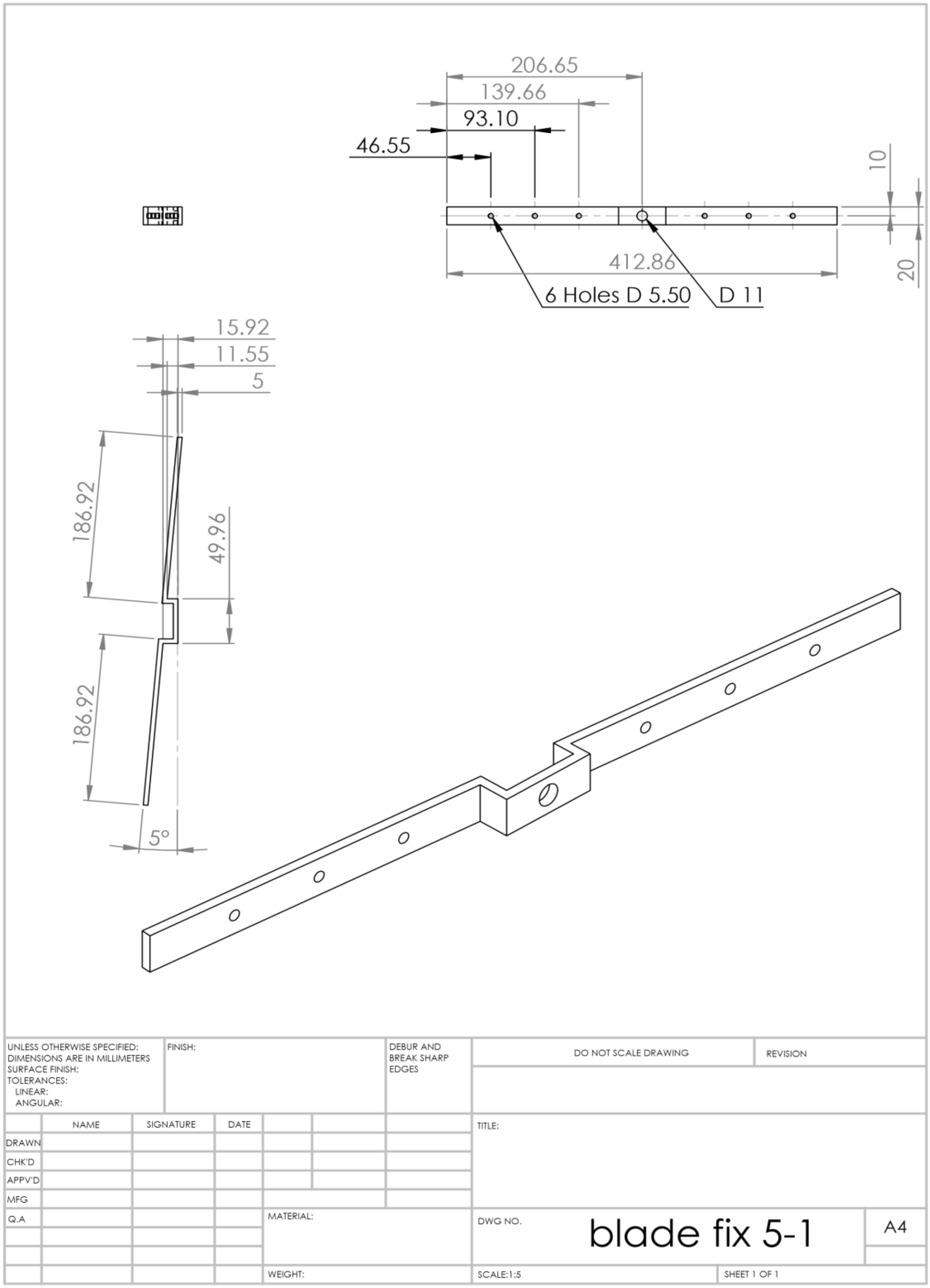

APPENDIX D7: SUPPORTING RIM DRAWING

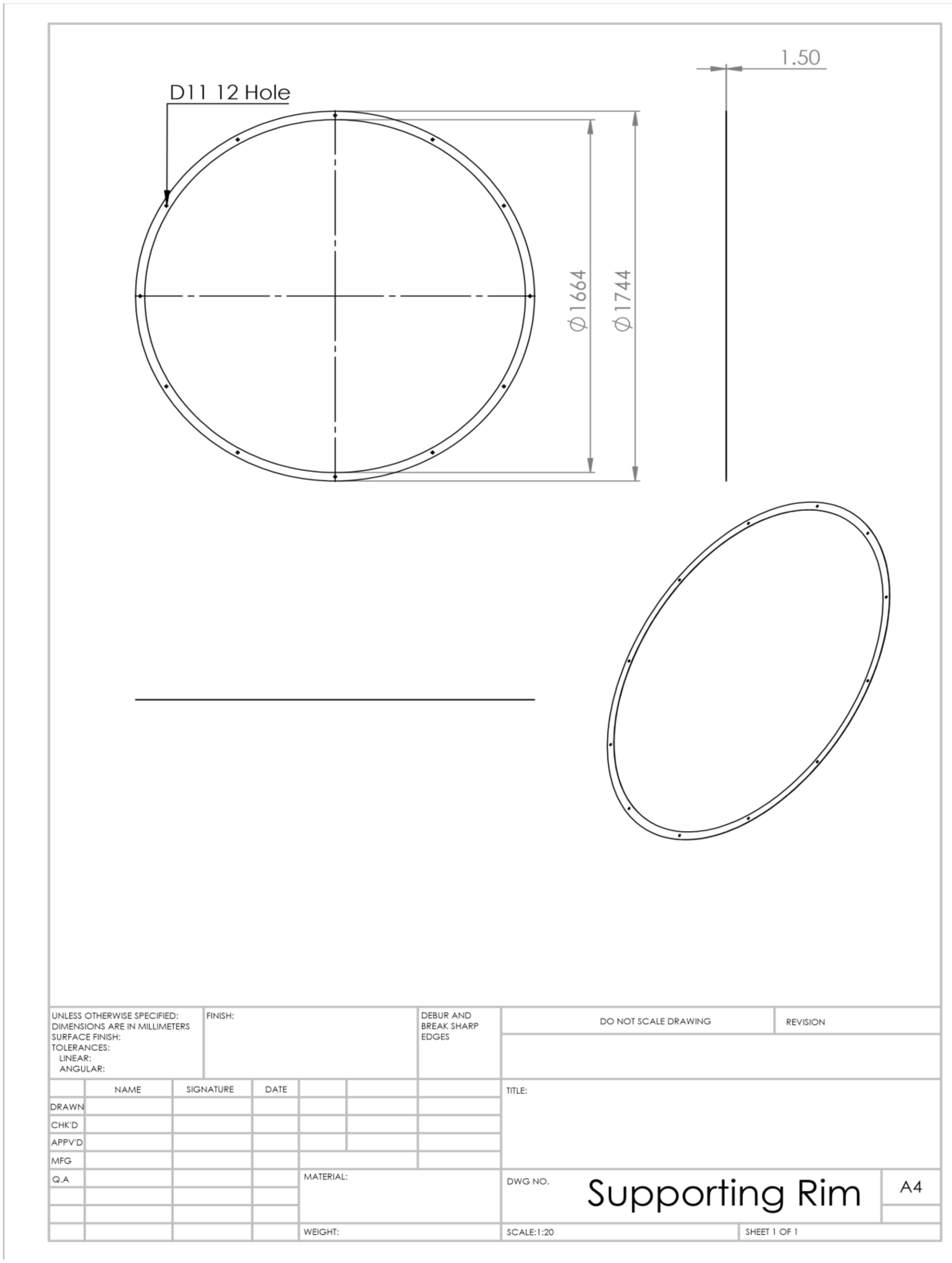

APPENDIX D8: BACK ARM DRAWING

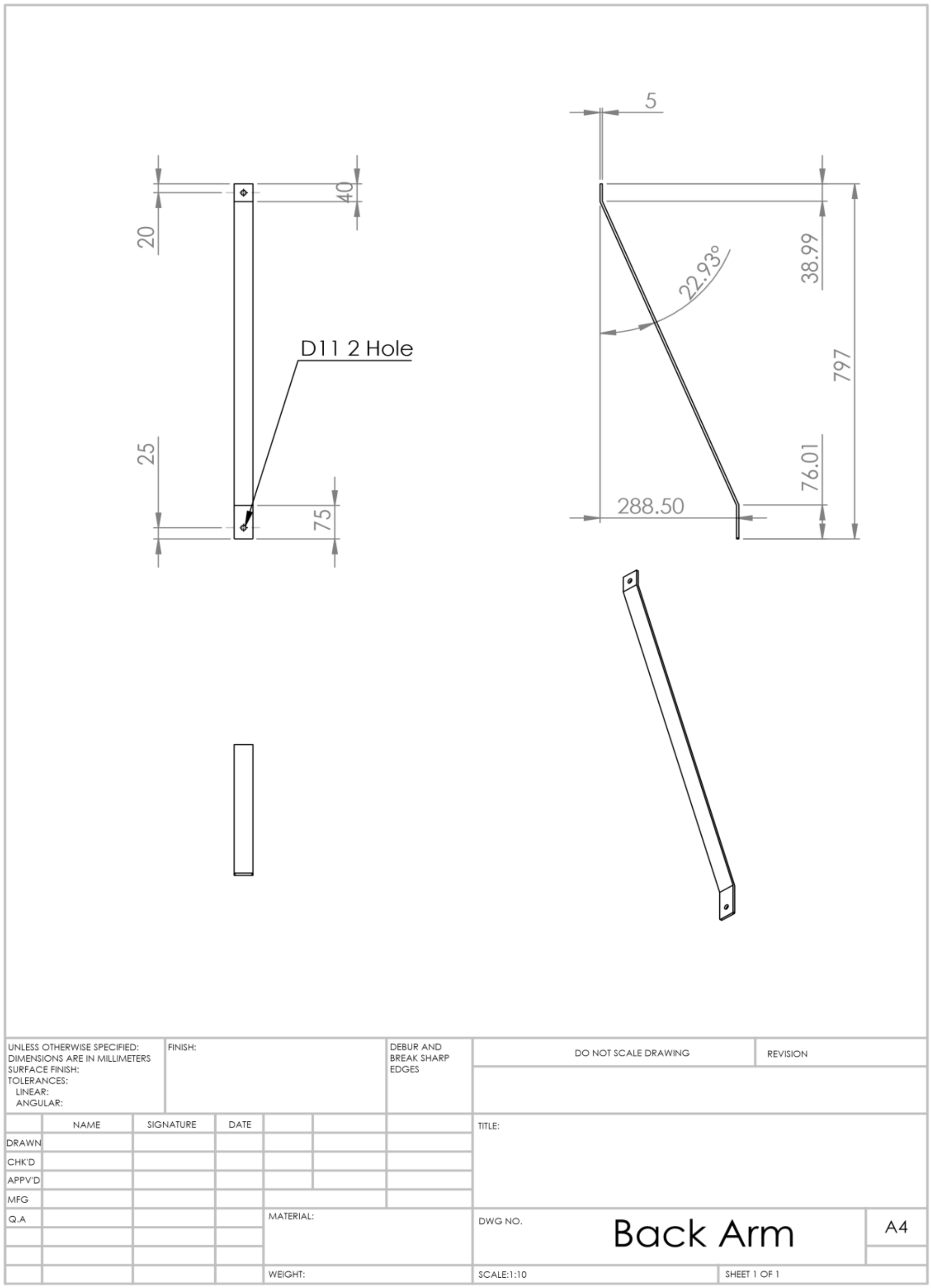

APPENDIX D9: HUB DRAWING

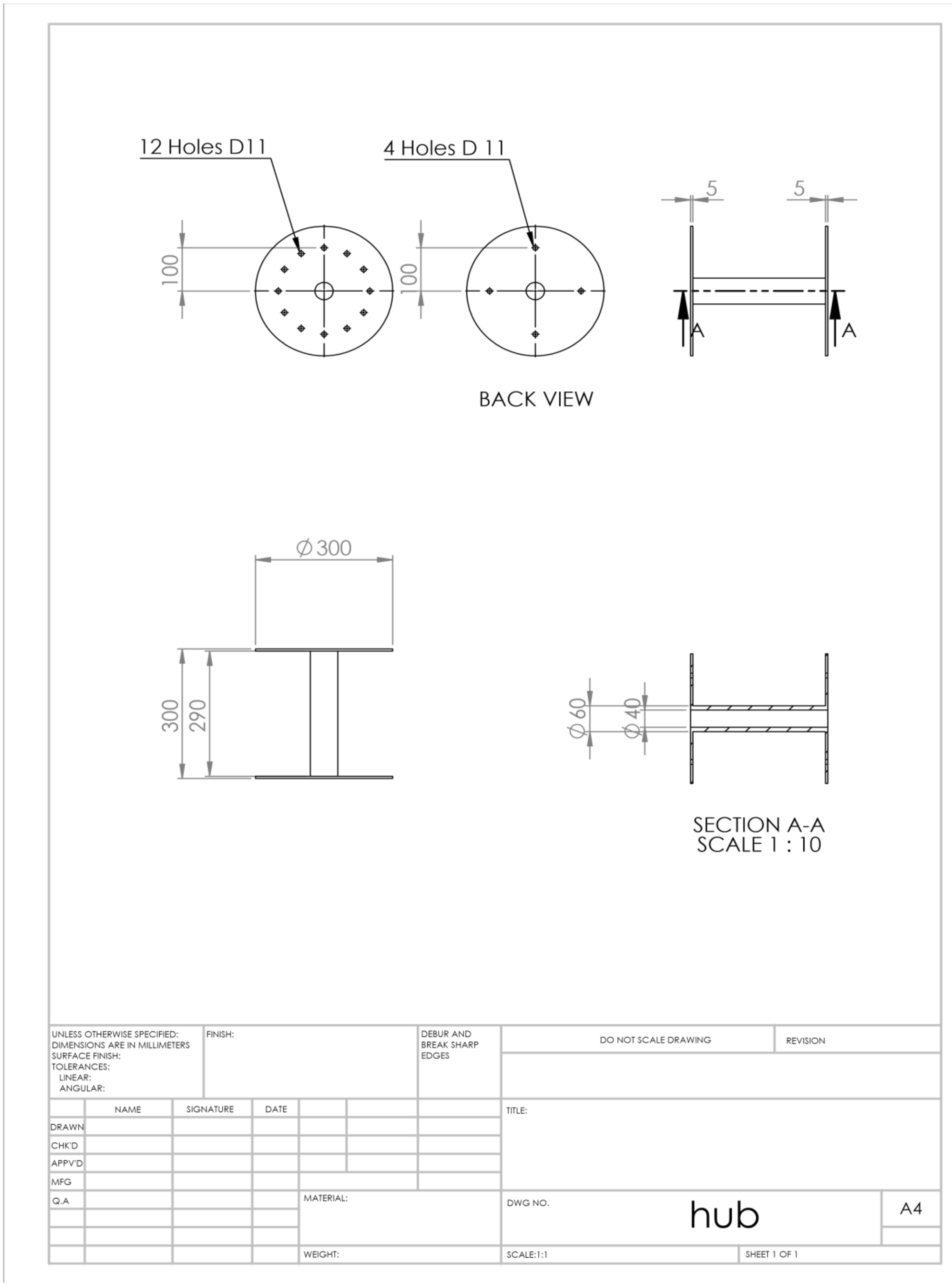

APPENDIX D10: SHAFT LEFT ROD DRAWING

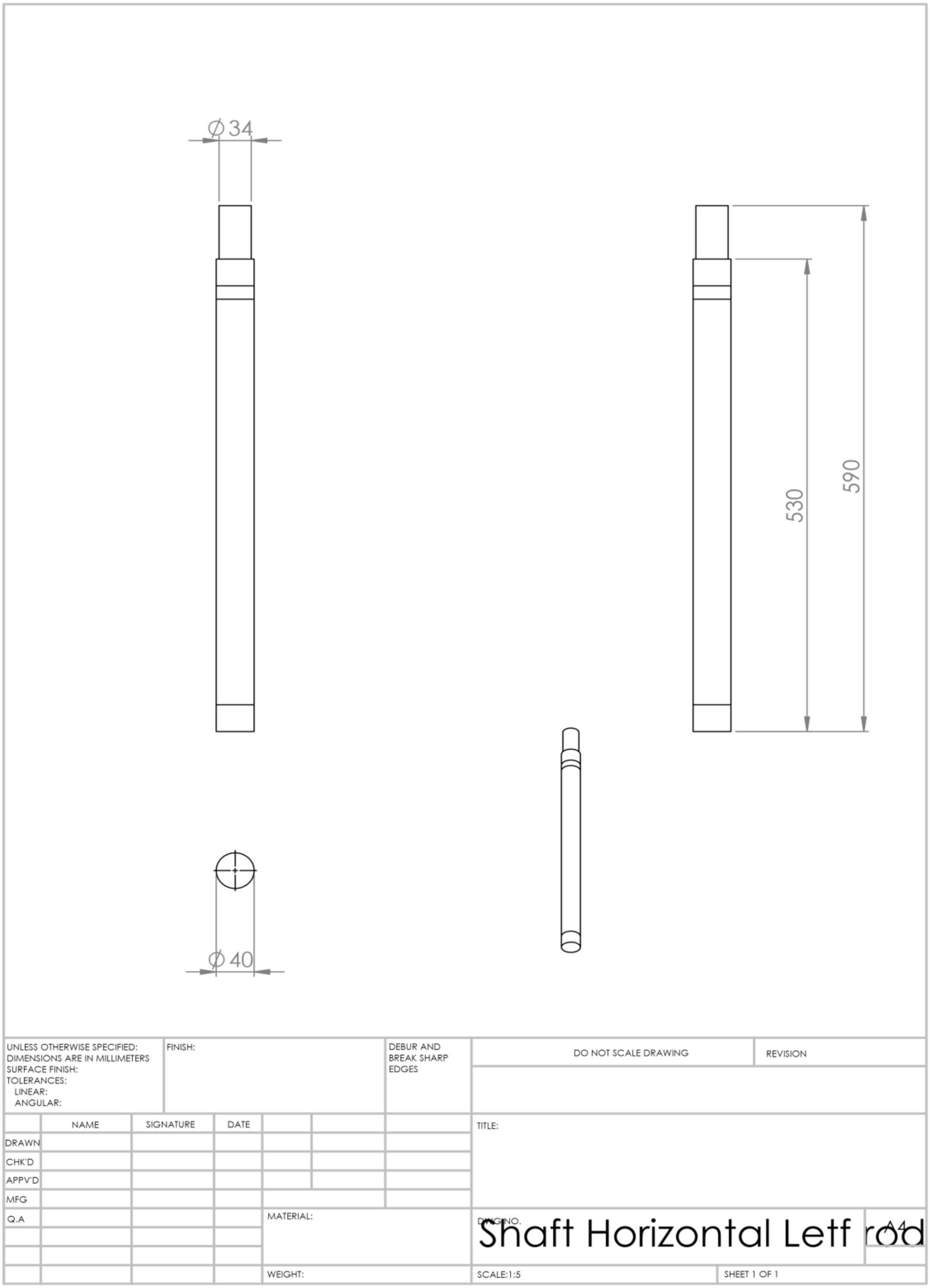

APPENDIX D11: SHAFT MIDDLE ROD DRAWING

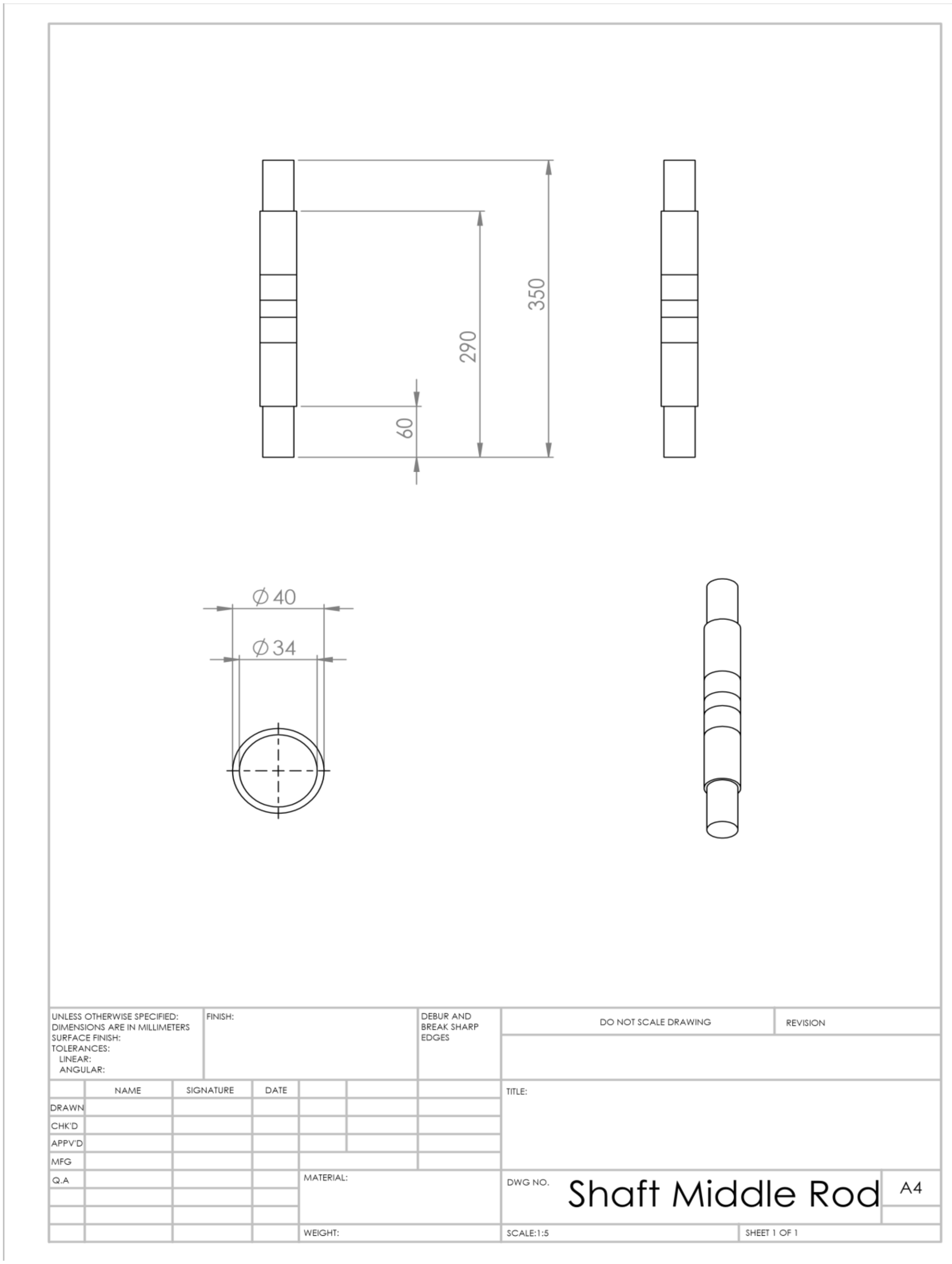

APPENDIX D12: SHAFT RIGHT ROD DRAWING

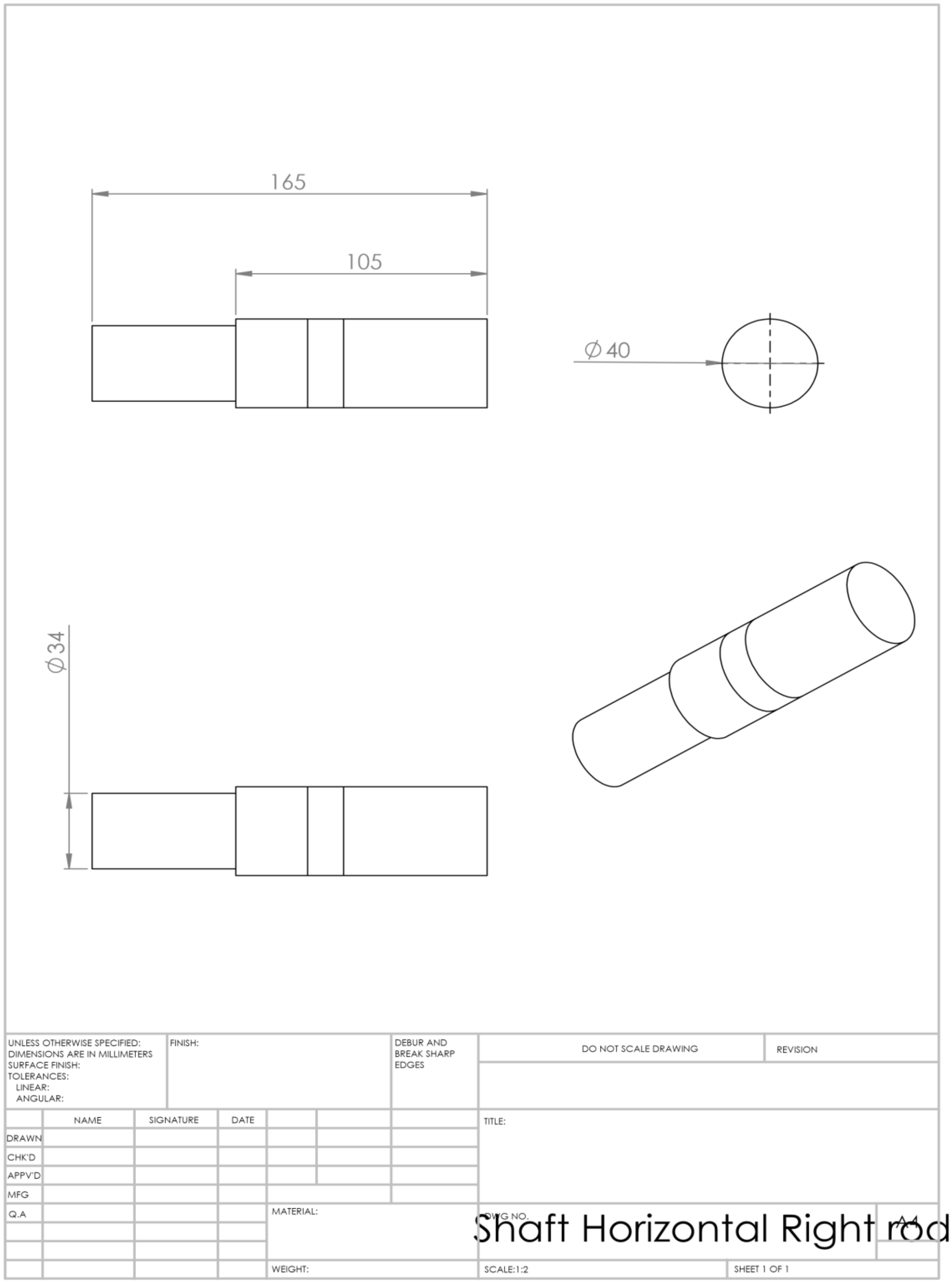

APPENDIX D13: SHAFT VERTICAL ARM DRAWING

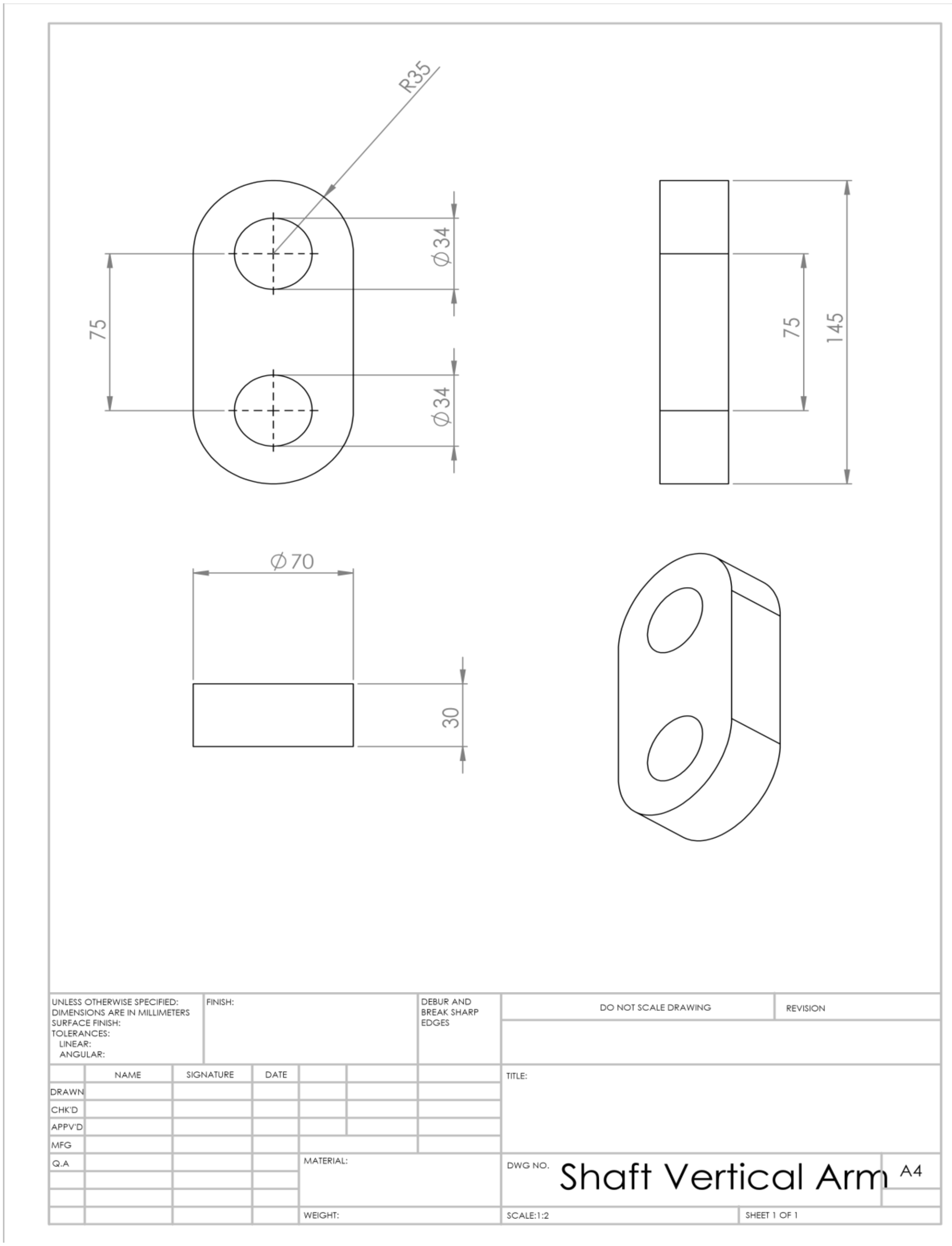

APPENDIX D14: VAIN S BAR DRAWING

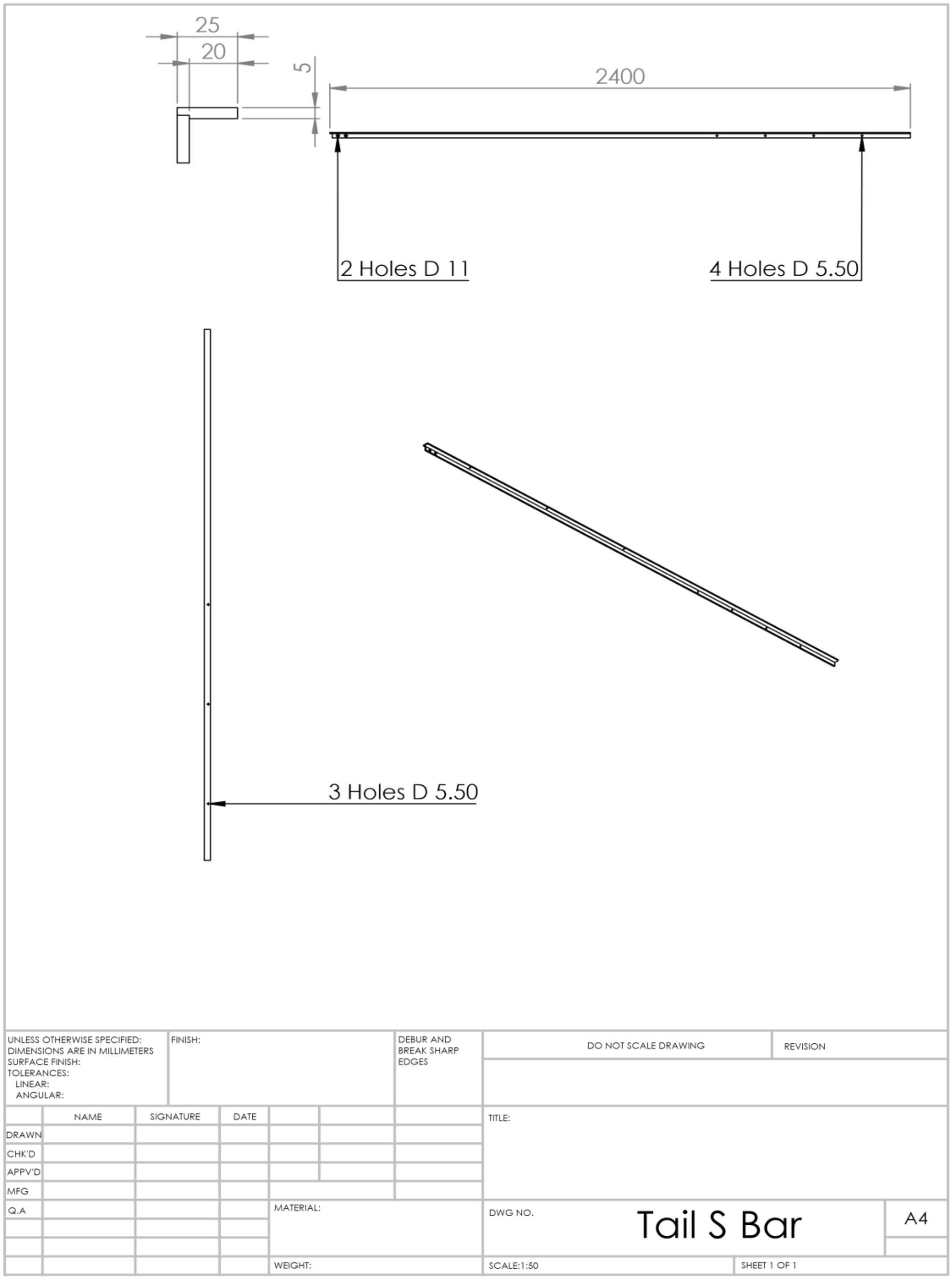

APPENDIX D15: VAIN S BAR 2 DRAWING

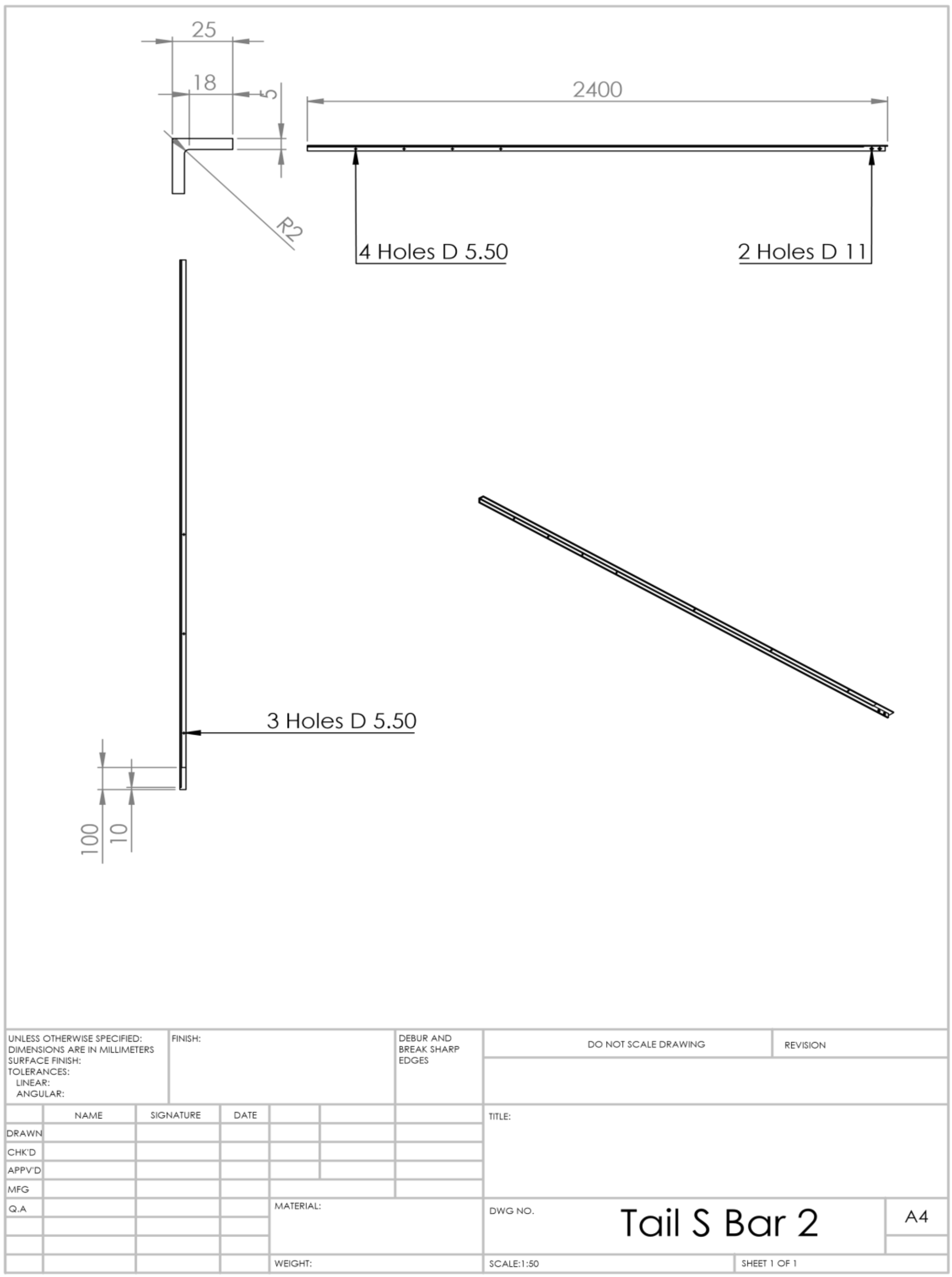

APPENDIX D16: TAIL FIX DRAWING

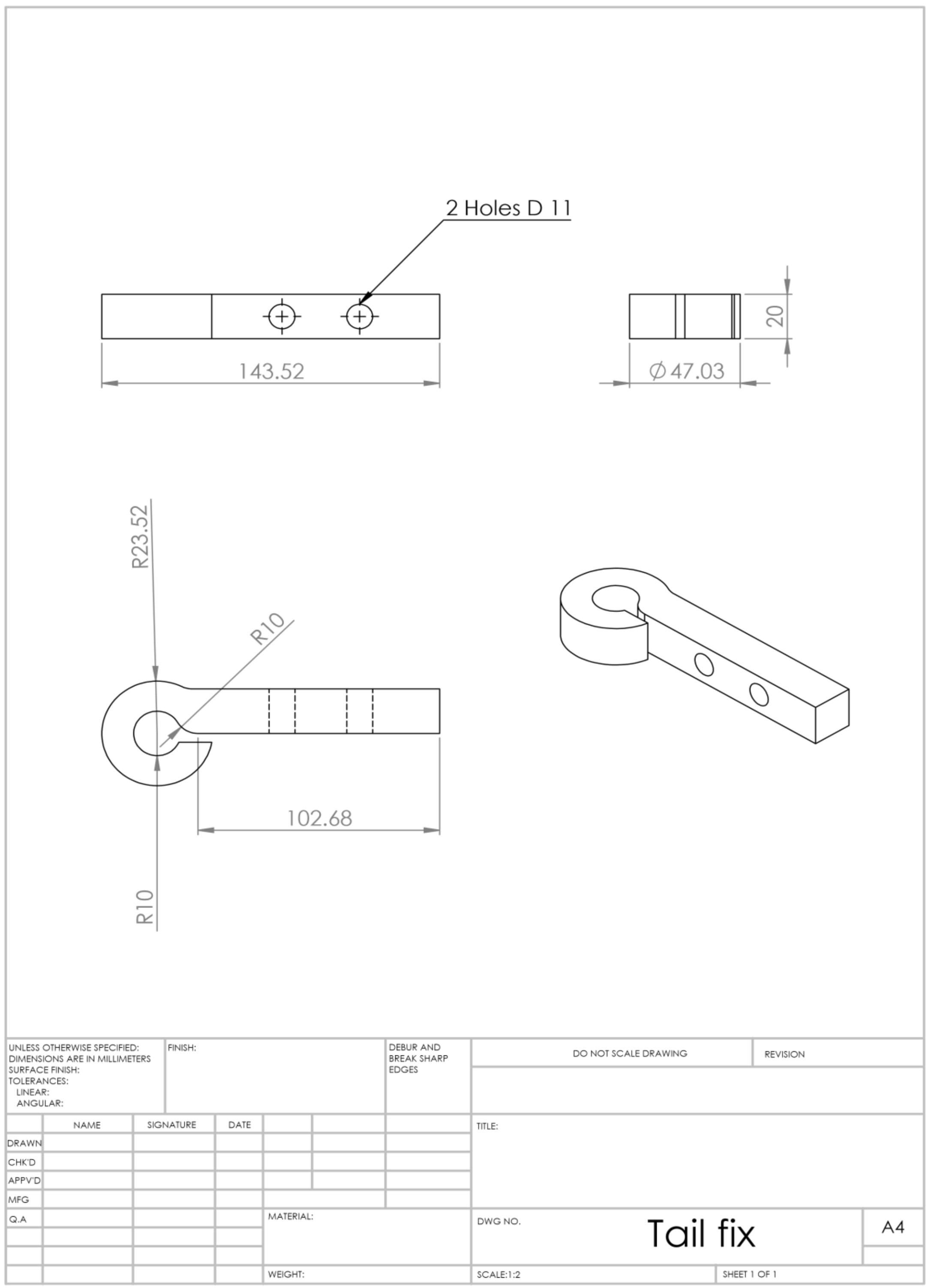

APPENDIX D17: TAIL ROD DRAWING

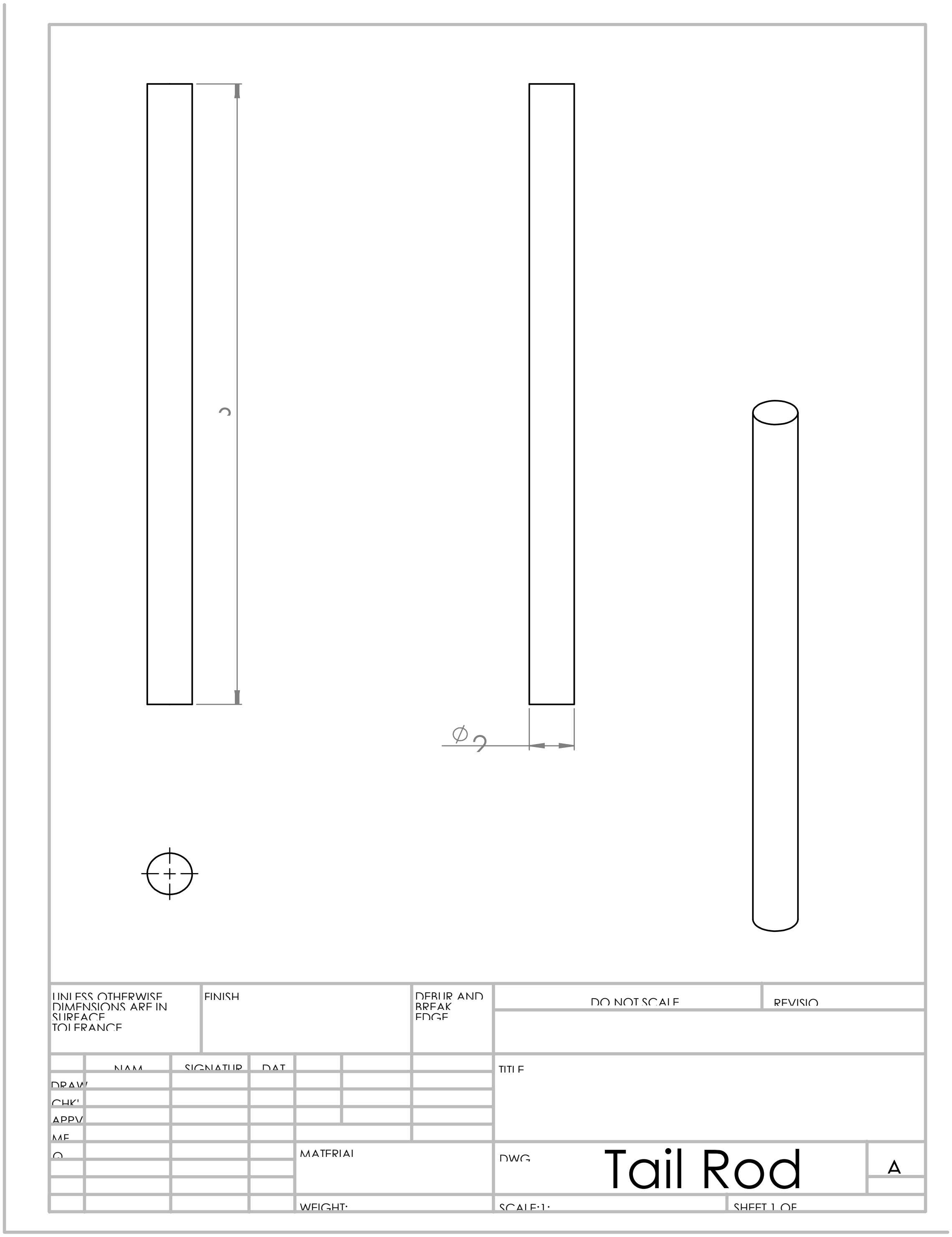

APPENDIX D18: TAIL STRUCTURE DRAWING

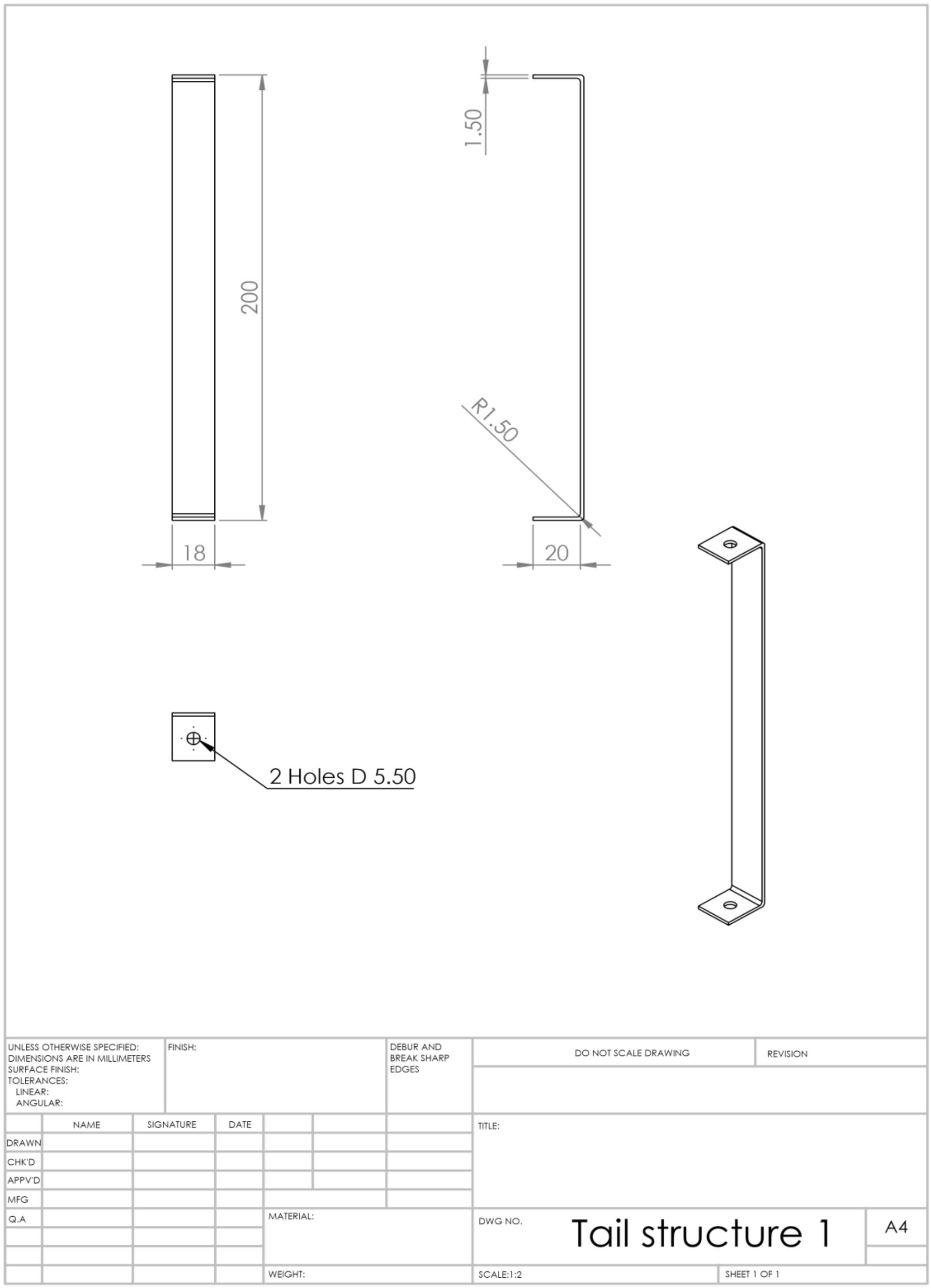

APPENDIX D19: TAIL VAIN DRAWING

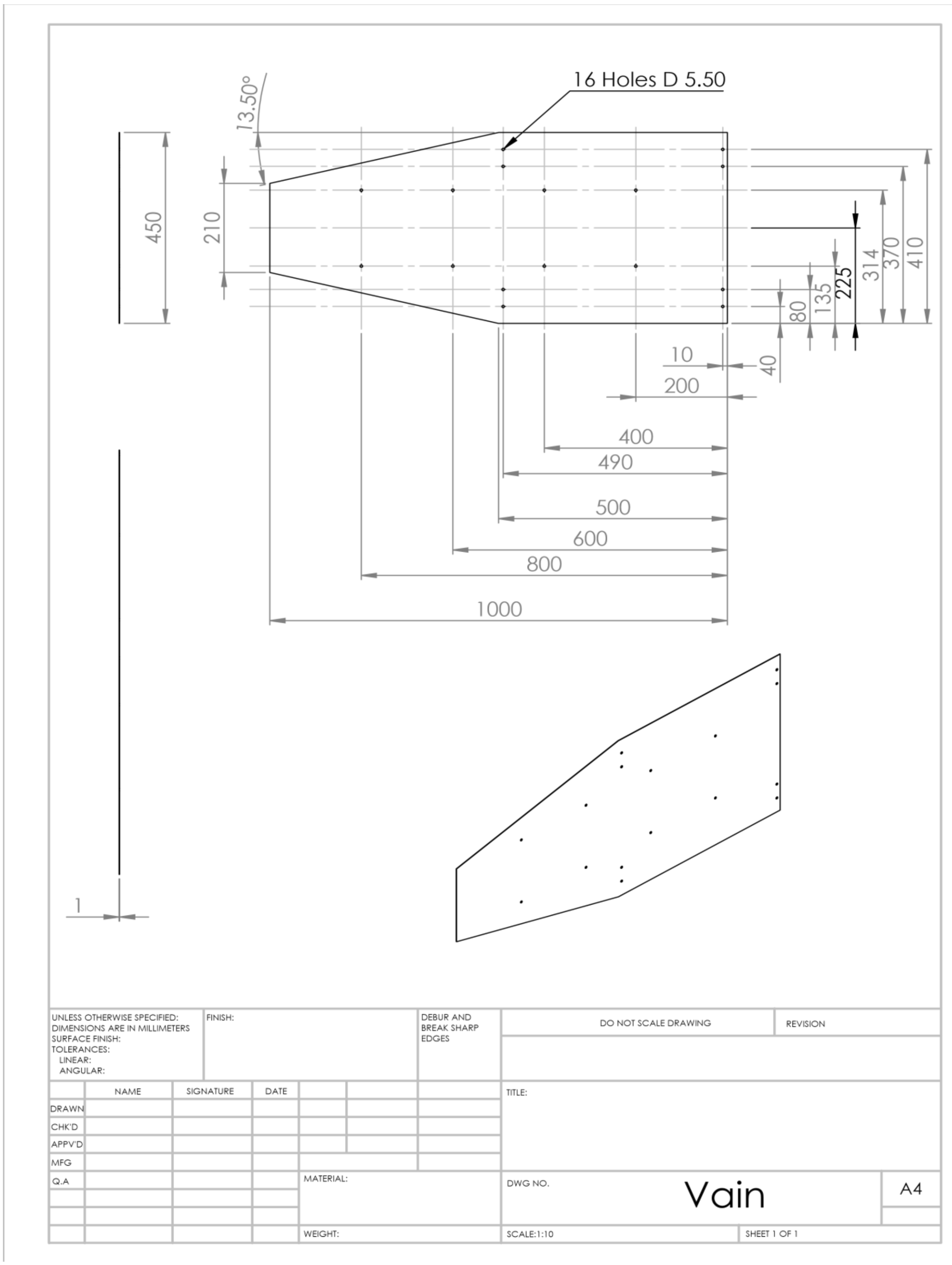

APPENDIX D20: TAIL VAIN STRUCTURE DRAWING

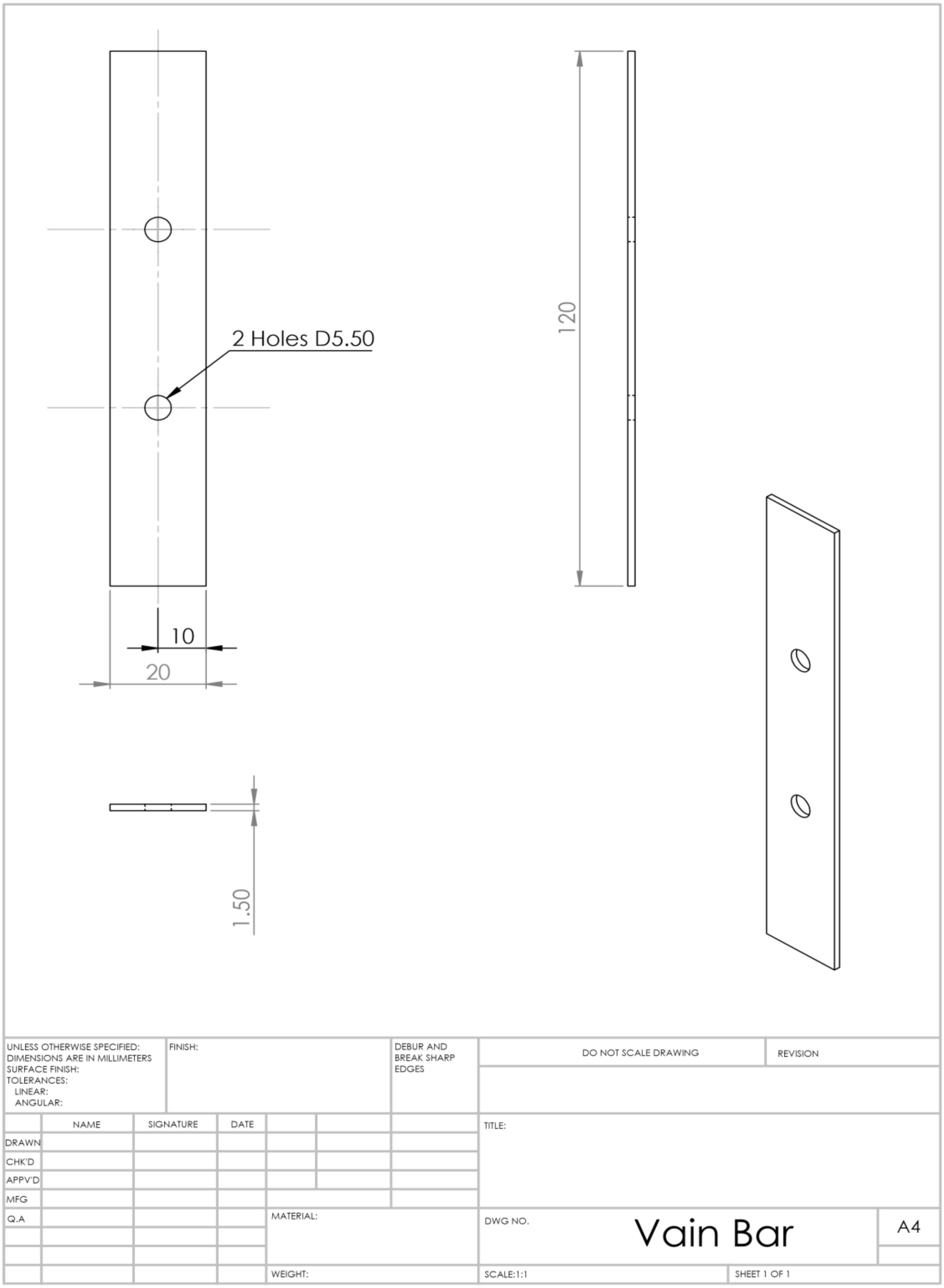

APPENDIX D21: BASE LEFT STAND DRAWING

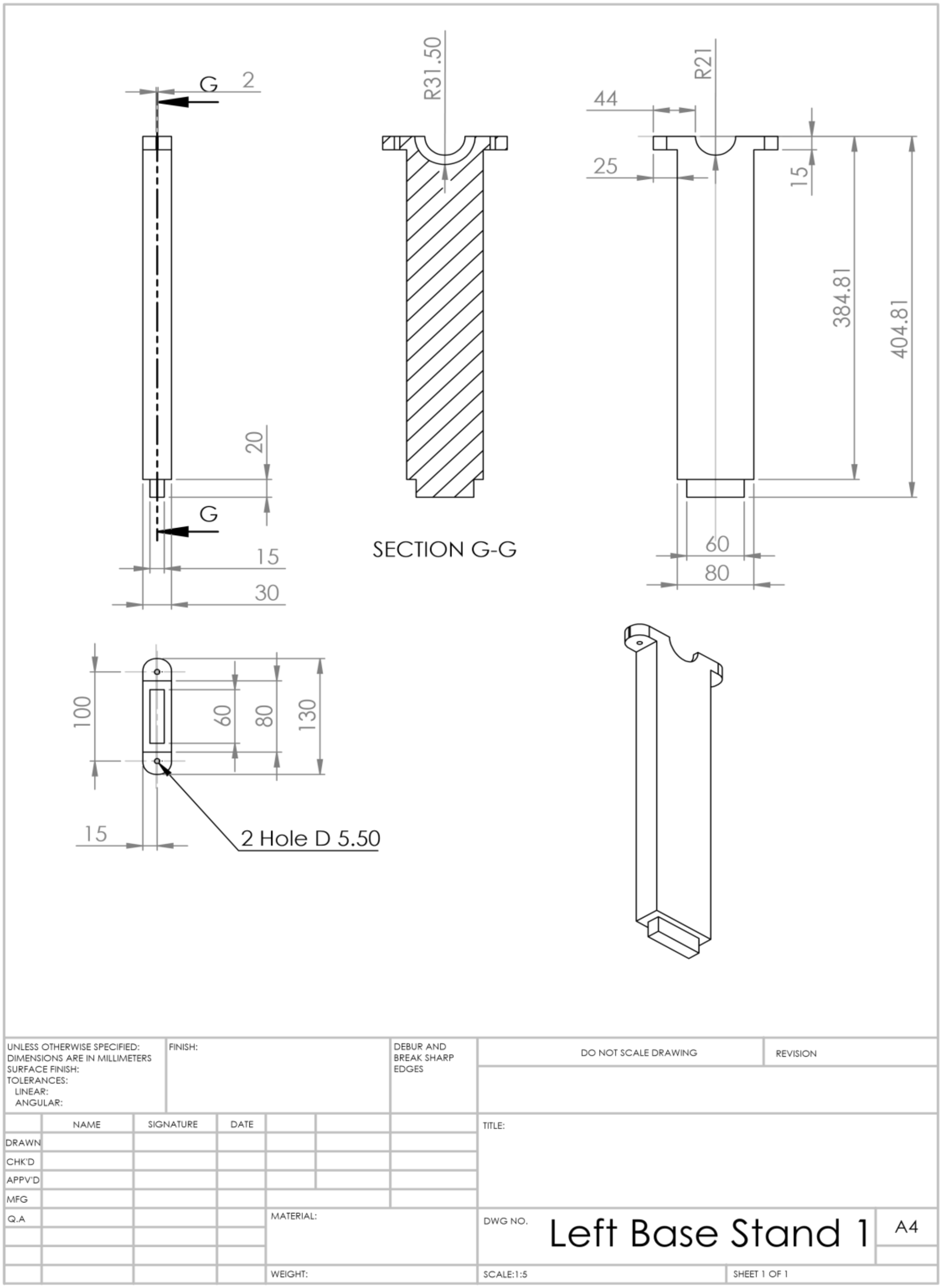

APPENDIX D22: BASE RIGHT STAND DRAWING

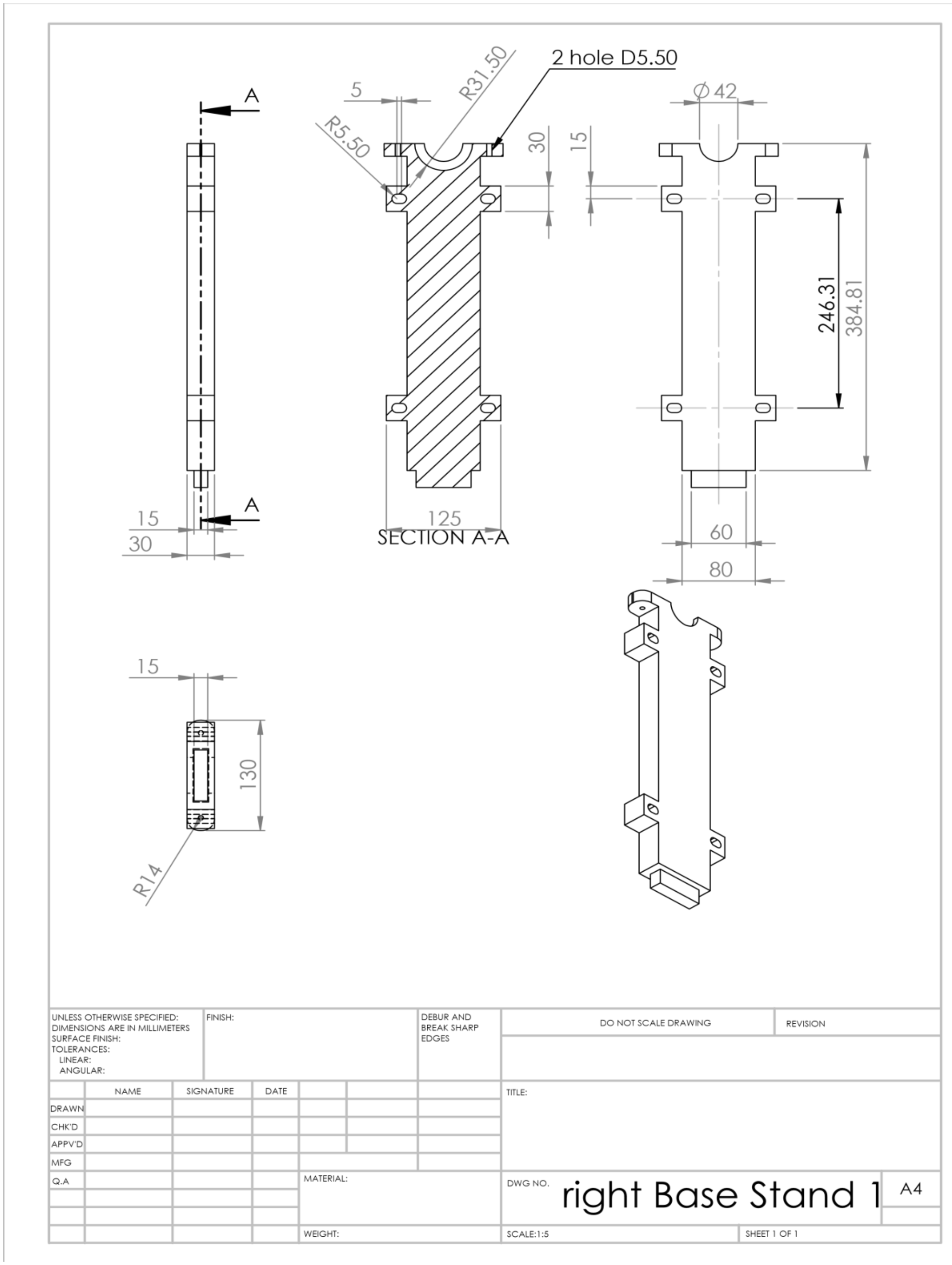

APPENDIX D23: STAND CAB DRAWING

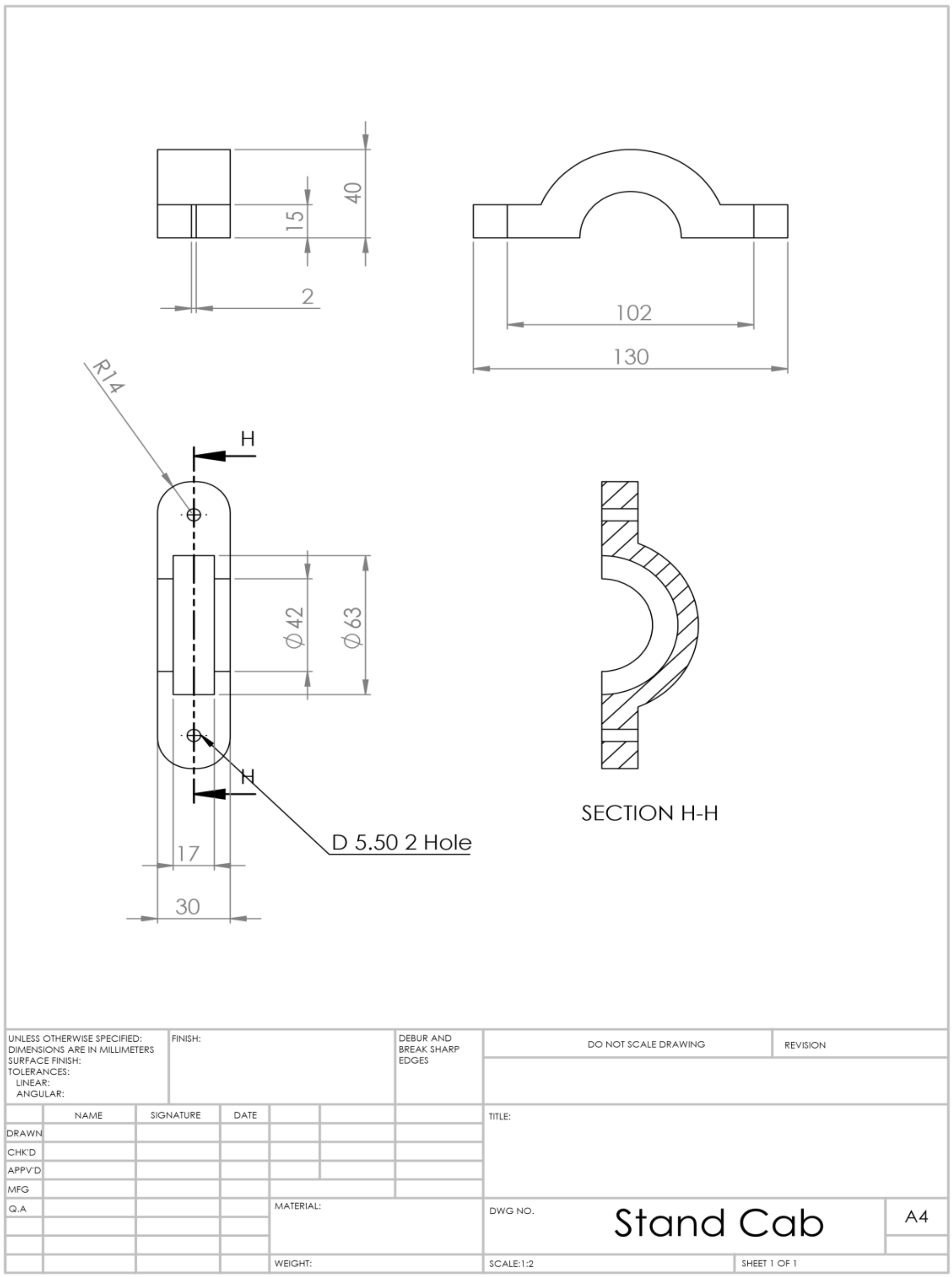

APPENDIX D24: BASE DRAWING

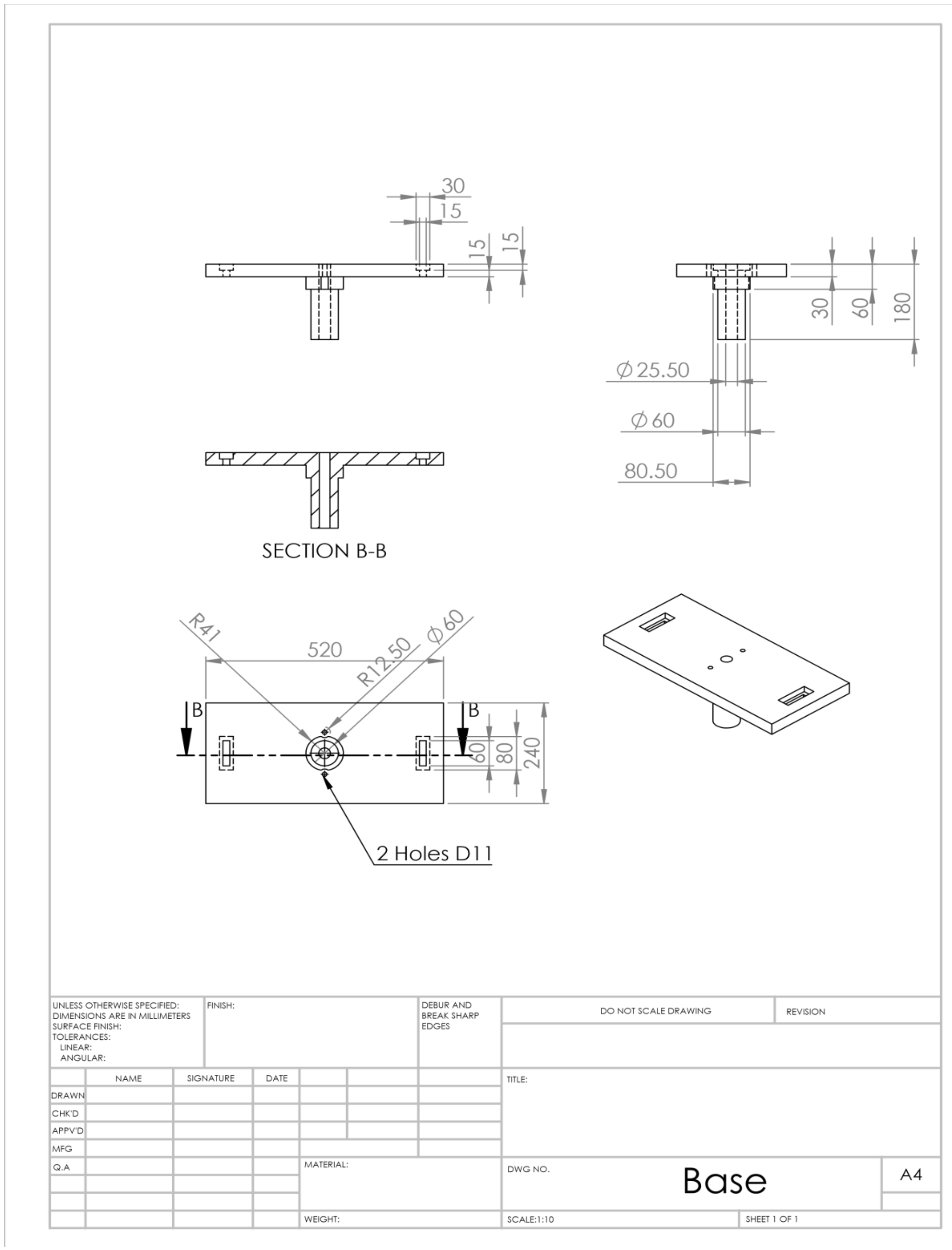

APPENDIX D25: GUIDE PIN DRAWING

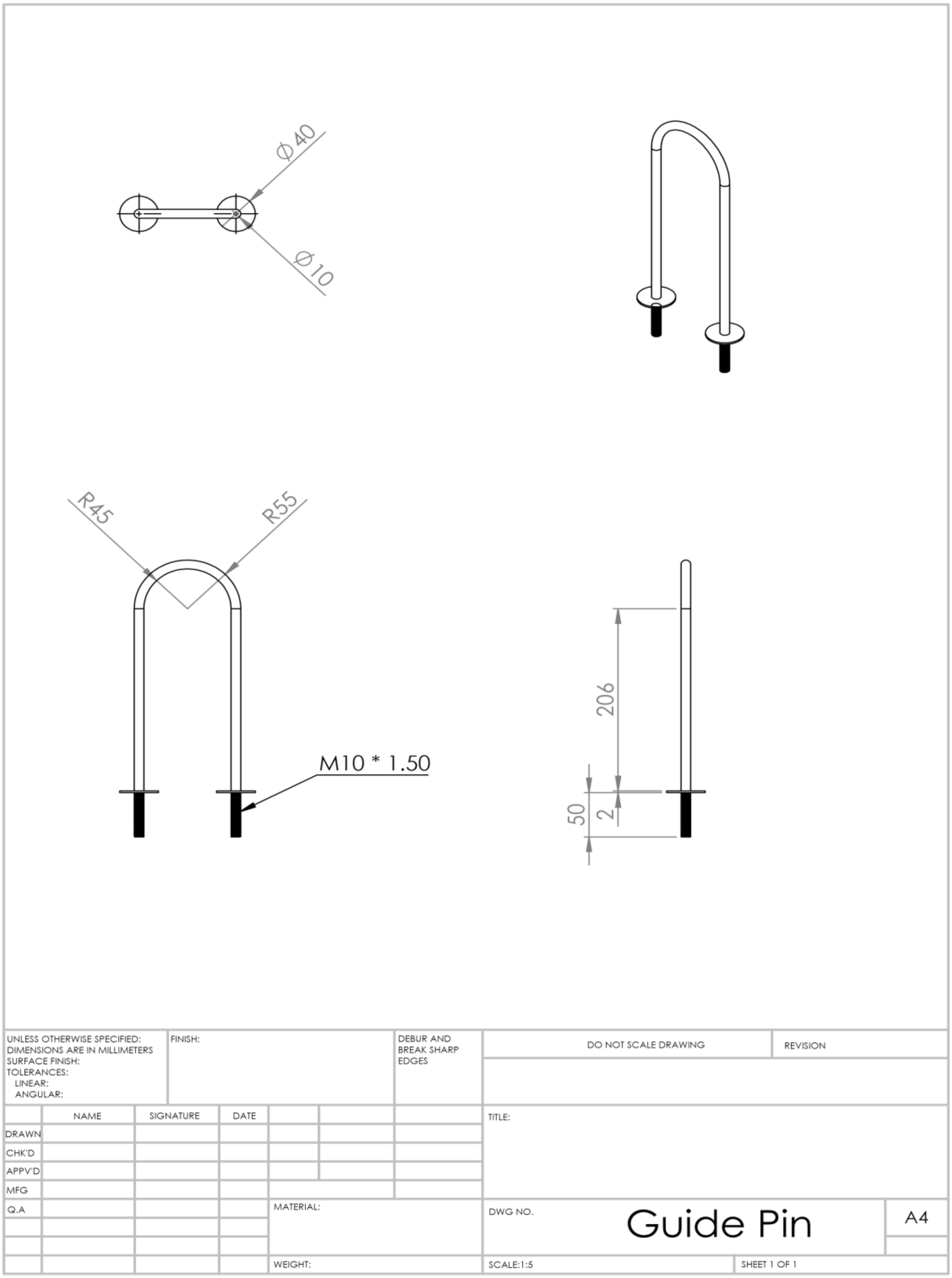

APPENDIX D26: LIFTING BULLY DRAWING

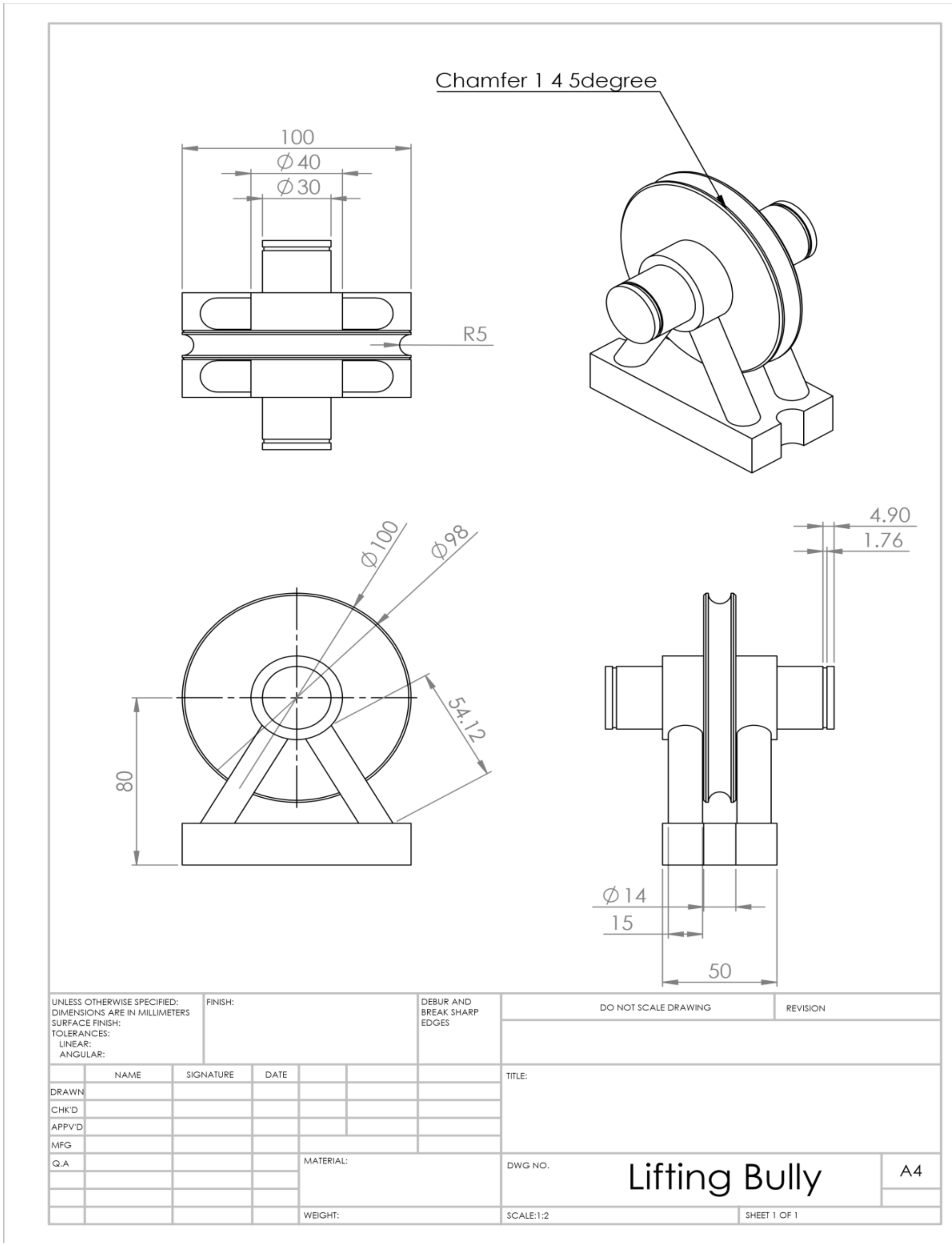

APPENDIX D27: SHAFT-BULLY LINK DRAWING

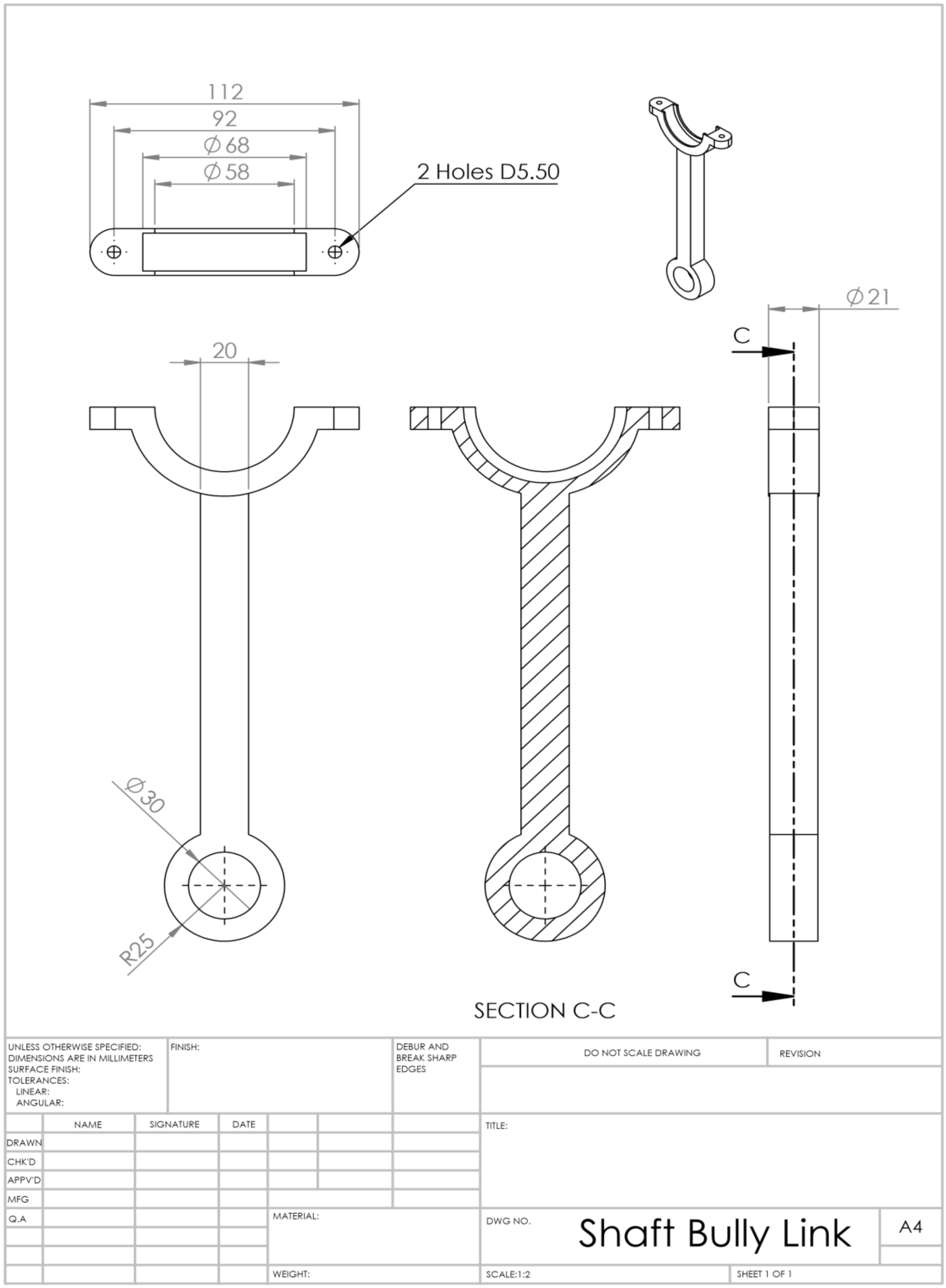

APPENDIX D28: SHAFT-BULLY LINK FIX DRAWING

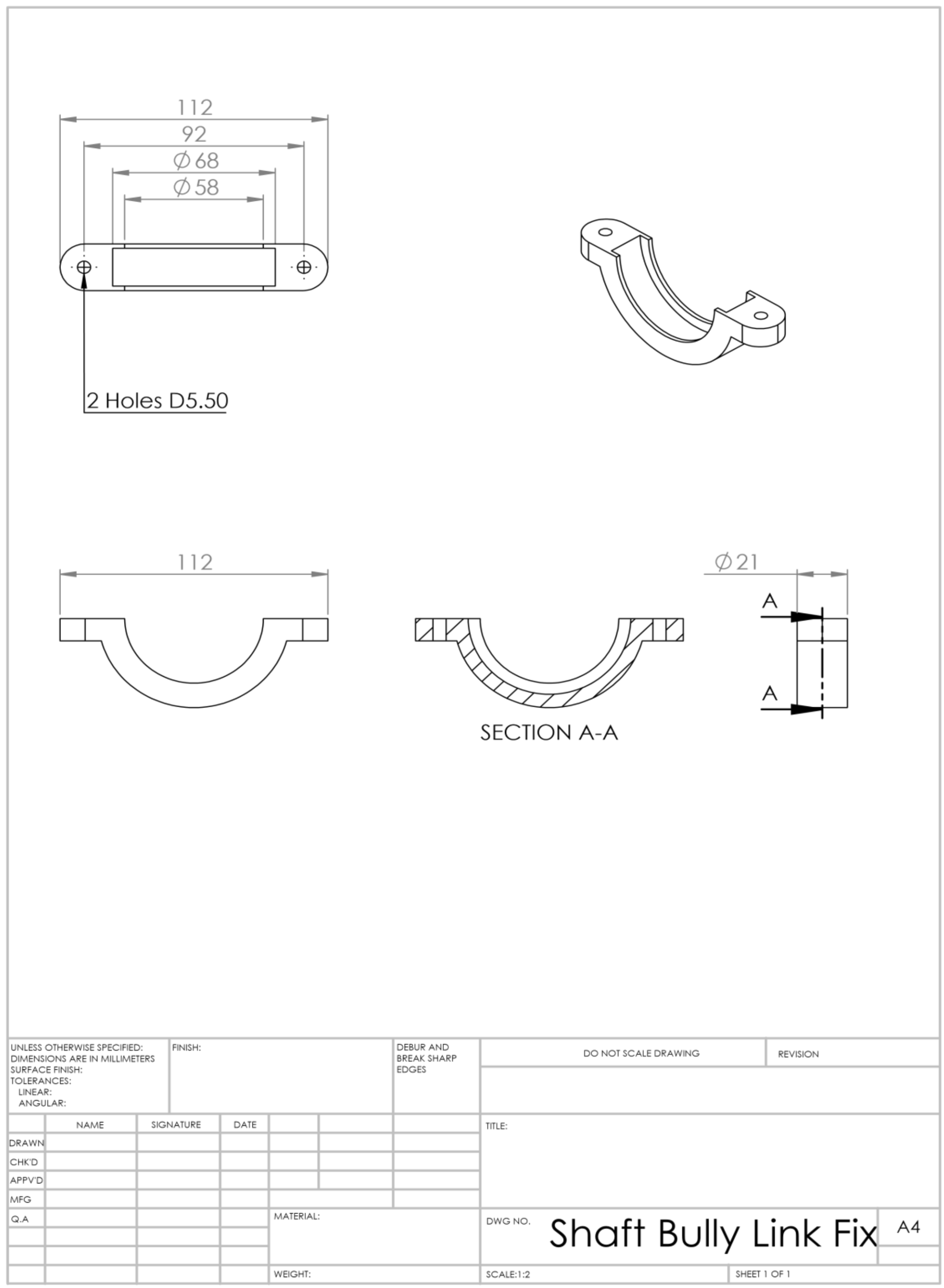

APPENDIX D29: TOP TOWER BASE DRAWING